UNIVERSITY OF CALIFORNIA,
IRVINE

Beyond Standard Modeling: Modular Symmetries and Non-Perturbative Methods

DISSERTATION

submitted in partial satisfaction of the requirements
for the degree of

DOCTOR OF PHILOSOPHY

in Physics

by

Shreya Shukla

Dissertation Committee:
Professor Michael Ratz, Co-Chair
Professor Yuri Shirman, Co-Chair
Professor Mu-Chun Chen
Professor Tim Tait

2024

DEDICATION

To my aunt Seema Mishra, thank you for encouraging my passion for physics and mathematics and for all the love and support you showed me, until the very end.

TABLE OF CONTENTS

LIST OF FIGURES

LIST OF TABLES

ACKNOWLEDGMENTS

I want to express my heartfelt gratitude to my parents, Neerja Shukla and Shashank Shukla, for their unwavering love, and encouragement to study physics to get my PhD. Whether financial or emotional, their support has meant the world to me. Their boundless compassion has been my guiding light, and I am forever grateful for their belief in me. Also thanks to my brother, Varun Shukla, for his constant companionship in my life, and for being my friend. His passion and tenacity for life have been very inspiring to me.

To my partner, Pratik Sathe, I owe a debt of gratitude for his unwavering support, understanding, patience, and insights into life and physics. His love and encouragement have been a constant source of motivation, enriching my life in countless ways. I hope we will collaborate on some physics papers one day!

A special thank you to my dear friends Amy, Ishita, Isha, Laurie, Mark, Nishi, Abhijit, Shivali, Shrawani and Urvashi for their invaluable friendship, invaluable support, and countless moments of laughter and joy. Their presence in my life has been a blessing, and I am grateful for our shared memories. Their support through times of hardship has been one of the biggest sources of strength for me, and I am grateful for every shared moment.

Another thank you to my friends and colleagues Yahya Almumin, Victoria Knapp-Perez, Anne-Katherine Burns, Max Fieg, Adreja Mondol, Rutvij, Abu, Aditya, Varun, Uddipan, Vidul and Michael Waterbury for their exceptional collaboration and unwavering support throughout this research journey. Their dedication, insights, and encouragement were invaluable, especially during challenging moments. I am grateful for their collaborations, their friendship, and camaraderie which greatly enriched this work.

I cannot begin to express how deeply indebted to my advisors, Yuri Shirman, Michael Ratz, and my mentor Mu-Chun Chen I am. Not just for their exceptional guidance, mentorship, and encouragement but also their patience and unwavering support which have been instrumental in shaping my research and academic growth. I remember how stressed I felt in my first year regarding my abilities, and their words of encouragement, belief in my abilities, and advice in those moments are something I have always kept with me, and it is the reason that I have been able to continue on this journey at all. I would not have been able to enjoy my PhD experience and the amazing summer schools without their support, and I am forever indebted for showing their trust and confidence in my abilities from the start. Thank you for being on my team.

Thank you to Danniel and Emily, and my most beloved Tuco, for being the most supportive, cool and wonderful roommates ever.

Finally, I want to mention Domino and Aria, my beloved cats, who have been the joy and comfort of my life. Their playful antics, their persistence towards destroying every single piece of furniture, and above all, their unconditional love have brought endless happiness into my days.

Thank you to the UCI Department of Physics, especially My Banh, for all the help and for the dissertation fellowships in my last year. This work received was supported by the National Science Foundation, under Grant No. PHY-1915005 and by UC-MEXUS CONACyT grant No. CN-20-3.

Chapter 1 of this dissertation is a reprint of the material as it appears in [111], used with permission from the Journal of High Energy Physics (JHEP). The co-authors listed in this publication are Yuri Shirman and Michael Waterbury. Chapter 2 and appendix A of this dissertation is a reprint of the material as it appears in [106], used with permission from the Journal of High Energy Physics (JHEP). The co-authors listed in this publication are Saul Ramos-Sanchez, Michael Ratz, Yuri Shirman and Michael Waterbury. Chapter 3 and appendix B is a reprint of the material as it appears in [5], used with permission from the Journal of High Energy Physics (JHEP). The co-authors listed in this publication are Yahya Almumin, Mu-Chun Chen, Michael Ratz, Saul Ramos-Sanchez, and Victor Knapp-Perez [5]. Finally, Chapter 4 and appendix C is a reprint of the material as it appears in [24], used with permission from the Journal Physics letters B. The co-authors listed in this publication are Mu-Chun Chen, Victor Knapp-Perez, Mario Ramos-Hamud, Saul Ramos-Sanchez, and Michael Ratz. I am thankful for the collaborations with them, the interesting physics discussions, their valuable insights, and the research and writing that led to these publications.

VITA

Shreya Shukla

EDUCATION

Doctor of Philosophy in Physics **2024**
University of California, Irvine *Irvine, CA*

Masters in Theoretical and Mathematical Physics **2018**
University of Edinburgh *Edinburgh, UK*

Bachelors in Physics **2017**
Indian Institute of Technology, Kanpur *Kanpur, India*

RESEARCH EXPERIENCE

Graduate Student **2019–2024**
University of California, Irvine *Irvine, California*

Masters Student **2017–2018**
The Higgs Centre for Theoretical Physics, University of Edinburgh *Edinburgh, UK*

TEACHING EXPERIENCE

Teaching Assistant **2019–2024**
University of California, Irvine *Irvine, CA*

REFEREED JOURNAL PUBLICATIONS

Chirality Changing RG Flows **2023**
Journal of High Energy Physics (JHEP)

Authors: Yuri Shirman, Shreya Shukla, Michael Waterbury

Flavor Model Building and the Origins of Flavor and CP Violation **2023**
Universe 2023

Authors: Yahya Almumin, Mu-Chun Chen, Murong Cheng, Víctor Knapp-Pérez, Yulun Li, Adreja Mondol, Saúl Ramos–Sánchez, Michael Ratz, Shreya Shukla

Quasi-Eclectic Modular Flavor Symmetries **2022**
Physics Letters B

Authors: Mu–Chun Chen, Víctor Knapp–Pérez, Mario Ramos–Hamud, Saúl Ramos–Sánchez, Michael Ratz, Shreya Shukla

Generation flow in field theory and strings **2021**
Journal of High Energy Physics (JHEP)

Authors: Saúl Ramos-Sánchez, Michael Ratz, Yuri Shirman, Shreya Shukla, Michael Waterbury

Metaplectic Flavor Symmetries from Magnetized Tori **2021**
Journal of High Energy Physics (JHEP)

Authors: Yahya Almumin, Mu-Chun Chen, Víctor Knapp-Pérez, Saúl Ramos-Sánchez, Michael Ratz, Shreya Shukla

ABSTRACT OF THE DISSERTATION

Beyond Standard Modeling: Modular Symmetries and Non-Perturbative Methods

By

Shreya Shukla

Doctor of Philosophy in Physics

University of California, Irvine, 2024

Professor Michael Ratz, Co-Chair
Professor Yuri Shirman, Co-Chair

In this thesis, we investigate the fundamental aspects of particle physics, specifically in the context of physics beyond the Standard Model. We focus on addressing two of the problems in this context: the flavor problem and the dynamical evolution of chiral symmetries.

We explore the flavor problem, specifically concerning the mystery behind the number of generations in the Standard Model (SM) by using the tools in supersymmetric theories to challenge notions of 'generations' as an invariant through RG flows from UV to IR. To achieve this, we perform a detailed analysis of non-perturbative field theoretic dynamics in supersymmetric models. This study not only offers profound insights into the peculiarities of QFTs but also helps navigate the string landscape of viable models. Furthermore, we also develop model-building tools to achieve mass gaps in chiral models, a crucial ingredient in generation flows, in full generality for various gauge groups.

In the second part of this thesis, we explore the flavor problem using the lens of modular symmetries. Focusing on a torus-based approach, the underlying physical parameters in this methodology are derived by adding flux to the two compactified extra dimensions. In chapter 4, we wade through the strengths and challenges of this method. We can understand the flavor parameters by examining the modular-form Yukawas, and the overall symmetry

group in terms of the flux parameters. Expanding on the strengths of the modular approach, in chapter 5, we also propose an eclectic scheme, where we draw from the union of modular and traditional discrete flavor groups in string theory, to provide a unified framework for understanding flavor physics.

Using mathematical analysis in various settings, be it stringy models, or supersymmetric theories, we present this thesis as a minor contribution to the search for an understanding of the puzzles of the Standard Model. It offers several model-building tools and frameworks that provide non-standard insights beyond the Standard Model. I would like to conclude this abstract with the following poem:

We work beyond the Standard Model,
On things unheard of and popular,
We used some supersymmetry and strings,
And explored everything modular.

The generations are explored,
Are they three or more?
Some fluxes on donuts we find,
As never seen before!

There's still a long way to go,
The history of physics is colossal!
And while we want to know much more,
We'll respect the Standard Model.

Chapter 1

Introduction

Quantum Mechanics and Relativity are two successful frameworks that explain several mind-boggling experiments and puzzles at the smallest and largest scales, respectively. However, a new framework emerged when Quantum Mechanics was combined with Relativity - Quantum Field Theories (QFT). The uncertainty relations of Quantum Mechanics and the ambiguity of time ordering between space-like events in Relativity imply that in QFTs particles can be created out of and annihilated into the vacuum. This gives rise to various intermediate dynamics that can be studied for any scattering process in the framework of Quantum Field Theories. Quantum Electrodynamics (QED), has been a remarkably successful framework, with experimental results being verified up to various orders of magnitude. The Standard Model, framed in a QFT language, encapsulates our current understanding of quantum phenomena at the level of what constitutes matter (fermions) and force carriers (bosons).

While the Standard Model remains one of the most successful theoretical frameworks of our understanding of particle physics, various aspects remain unanswered. Why are there so many unknown parameters? How can one incorporate gravity into this structure? Why is Higgs mass the value it is? Current-day particle physics lies at a crossroads: we can

simultaneously access various advanced mathematical tools towards an understanding of the UV completion of the Standard Model and what it might look like, and String Theory remains one of the most consistent frameworks incorporating gravity and quantum theories into a unified framework, yet it remains experimentally inaccessible.

However, one can start at a much simpler level - Why is the number of generations in the SM just three? Is it possible to get three-generation models from string-inspired setups? Is it possible for the number of generations to change from UV to IR? In our thesis, we explore these questions, and if the answer is yes, we show what the possible models could look like.

1.1 Chiral Symmetries and Generation Flows

The chiral nature of the Standard Model is well known: the left-handed and right-handed particles are charged differently, and right-handed neutrinos have not been observed yet, and may not exist. The chiral symmetries and their origin present an intriguing question in particle physics, and possible mechanisms govern the dynamics of particle interactions of various models. However, in traditional QFT models, one finds that mass terms break chiral symmetries, and thus introducing a mass term without breaking chiral symmetry is not possible.

Can the chiral structure of a theory change under RG flow? For supersymmetric theories, one can show that the answer is yes. The question would be harder to answer in ordinary QFTs since we lose theoretical control over such theories at certain energy scales. In the case of supersymmetry, however, we have certain tools at our disposal: holomorphicity and non-renormalization theorems. In particular, a phenomenon known as s-confinement means that in certain supersymmetric theories, the underlying structure is nice and smooth enough that there is no order parameter between the Higgs regime and the confining regime, and

there is a chirality-preserving vacuum at the origin of the field space. This means that remarkably, concerning this vacuum, chiral symmetries are preserved even with the addition of mass terms.

However, the fact that chiral structure can change from UV to IR is well known. Recently, however, a paper [107, 117] explored specific examples where fermions can be gapped in the IR. These thus opened up avenues for studying chirality changing flows from UV to IR in a more general setting, as well as the consequences of such phenomena in studying the string landscape.

In what follows, the analysis of chiral theories that we perform in Chapters 1 and 2 will be based on a supersymmetric setup. As discussed earlier, the value of Higgs mass being finite compared to the GUT scale has presented itself as the 'hierarchy problem'. In non-supersymmetric QFTs, such scalar masses receive large contributions, as large as the UV cutoff. Not only are these mass corrections divergent, but they are also quadratically divergent. Supersymmetry emerged as a framework that addressed this problem: since every fermion has a bosonic superpartner and vice-versa, their contributions cancel out, giving rise to finite scalar masses. Supersymmetric theories also follow powerful non-renormalization theorems, which when compounded by the fact that the interaction term is holomorphic, implies that the behavior of such terms is controlled and easier to study.

Despite its successful application in various domains, we have not been able to verify SUSY experimentally. This raises questions regarding the reliability of such theories in studying realistic phenomena, especially since the superpartners predicted by SUSY have not been found. However, by using SUSY breaking methods like dynamical SUSY breaking, we can still benefit from the strengths of SUSY in theories whose IR limits are non-supersymmetric. We also note that supersymmetry has emerged as a crucial tool for understanding non-perturbative physics, as opposed to QFTs, where it is harder to retain theoretical control over strongly coupled sectors of the theory. In this sense, SUSY remains an important tool

for furthering our understanding of QFTs. Before proceeding further, let us review some important ideas of supersymmetry and models that exhibit s-confinement, as opposed to those that do not.

1.1.1 A Review of Supersymmetric Methods

In this section, we review various exact results in SUSY [108, 109]. The key difference between the supersymmetric and non-supersymmetric theories is the restriction over the precise functional form of the interaction terms in the Lagrangean, due to the co-variance under a bigger symmetry group. To be more precise, any 4D $\mathcal{N} = 1$ SUSY Lagrangian can be written as a sum of three terms [115]

$$\mathcal{L}_{SUSY} = \int d^2\theta d^2\overline{\theta}\, \mathscr{K} + \int d^2\theta \mathscr{W} + \int d^2\overline{\theta} \mathscr{W}^\dagger \,, \tag{1.1}$$

where $\mathscr{K}$ is the Kähler potential governing the kinetic terms and $\mathscr{W}$ is the superpotential, governing the interaction terms. While the Kähler potential is a real function of all the fields in the theory, the superpotential is necessarily a holomorphic function of the chiral superfields Φ. This heavily constrains the terms which are allowed in $\mathscr{W}$. Couplings in the superpotential can also be regarded as background fields, and so superpotentials are also holomorphic functions of coupling constants. This can be used to prove powerful non-renormalization theorems, and we can use these to find out exact superpotentials after taking non-perturbative effects into account. Specifically, consider the case of pure SUSY Yang-Mills with gauge group SU(N). In this case, the U$(1)_R$ symmetry is anomalous, and broken by instantons to a discrete $\mathbb{Z}_{2N}$ subgroup. The gaugino condensate further breaks the symmetry down to $\mathbb{Z}_2$, and contributes to the superpotential,

$$\langle \lambda^a \lambda^a \rangle = -32\pi^2\, \mathrm{e}^{2\pi \mathrm{i} k/N} \Lambda^3 \,, \tag{1.2}$$

where $k = 1, 2 \cdots N$ and Λ is the holomorphic scale of the theory, $\Lambda = |\Lambda| e^{i\theta_{YM}/b}$.

For SYM with matter content, let us mention gauge-singlet composite operators which may characterize the theory at low energies. These are scalar "meson" and "baryon" fields and their superpartners (The baryons and anti-baryons only exist for $F \geq N$):

$$M_i^j = \bar{\Phi}^{jn}\Phi_{ni}, \tag{1.3}$$

$$B_{i_1,\ldots,i_N} = \Phi_{n_1 i_1} \ldots \Phi_{n_N i_N}\epsilon^{n_1,\ldots,n_N}, \tag{1.4}$$

$$\overline{B}^{i_1,\ldots,i_N} = \bar{\Phi}^{n_1 i_1} \ldots \bar{\Phi}^{n_N i_N}\epsilon_{n_1,\ldots,n_N}, \tag{1.5}$$

where we note that the baryon fields are only valid for cases where $F \geq N$. For now, consider Supersymmetric-QCD (SQCD) with $F \leq N$ flavors. At the classical level, the theory has no superpotential.

	SU(N)	SU(F)	SU(F)	U(1)	U(1)$_R$
Φ, Q	$\square$	$\square$	$\mathbf{1}$	1	$\frac{F-N}{F}$
$\bar{\Phi}, \bar{Q}$	$\square$	$\mathbf{1}$	$\bar{\square}$	-1	$\frac{F-N}{F}$

Table 1.1: Matter content of SQCD for $F \leq N$ flavors

For non-zero flavors, $F \neq 0$, we note that there is a non-anomalous combination of U(1)$_A$ and U(1)$_R$, and this is the U(1)$_R$ in the table table 1.1.

We recall that the auxiliary fields are given by

$$D^a = g\big(\Phi^{*jn}(T^a)_n^m\Phi_{mj} - \bar{\Phi}^{jn}(T^a)_n^m\bar{\Phi}^*_{mj}\big)\ , \tag{1.6}$$

where j is a flavor index that runs from 1 to F, m and n are color indices that run from 1 to N, and the index a labels an element of the adjoint representation. The D-term potential is given by:

$$V = \frac{1}{2}D^a D^a\ . \tag{1.7}$$

This form of the potential assigns itself to a D-flat moduli space, i.e. a field space where the potential is zero, given by

$$\left\langle \bar{\Phi}^* \right\rangle = \langle \Phi \rangle = \begin{pmatrix} v_1 & & & \\ & \ddots & & \\ & & & v_F \\ 0 & \dots & 0 & \\ \vdots & & \vdots & \\ 0 & \dots & 0 & \end{pmatrix} . \tag{1.8}$$

At a generic point in the moduli space the SU(N) gauge symmetry is broken to SU($N-F$). The $2NF-F^2$ degrees of freedom are eaten by the SuperHiggs Mechanism, and the remaining F^2 light degrees of freedom in a gauge invariant way by an $F \times F$ matrix field or the 'meson' field,

$$M_i^j = \overline{\Phi}^{jn} \Phi_{ni} \, . \tag{1.9}$$

By using holomorphy and the non-renormalization theorem, one can derive the Affleck-Dine-Seiberg superpotential [4]:

$$\mathscr{W}_{\rm ADS} = (N-F) \left(\frac{\Lambda^{3N-F}}{\det M} \right)^{1/(N-F)} . \tag{1.10}$$

For $F = N-1$ this can be verified by an explicit instanton calculation.

Now consider the case of $F = N$ flavors. In this case, the baryons are flavor singlets. They also satisfy a classical constraint

$$\det M = B\overline{B} \, . \tag{1.11}$$

Using holomorphy and the symmetries of the theory, one can (after some analysis) find out that the classical constraint will be modified at the quantum level due to instanton effects

$$\det M - B\overline{B} = \Lambda^{2N} \ . \tag{1.12}$$

Now note that we cannot take $M = B = \overline{B} = 0$, i.e. we cannot go to the origin of moduli space anymore. This means that the global symmetries are at least partially broken everywhere in the quantum moduli space.

For $F = N + 1$, baryons are flavor anti-fundamentals (and the anti-baryons are flavor fundamentals) since they are antisymmetrized in $N = F - 1$ colors. In this case, the classical constraints are

$$\left(M^{-1}\right)^i_j \det M = B^i \overline{B}_j \ , \tag{1.13}$$

$$M^j_i B^i = M^j_i \overline{B}_j = 0 \ . \tag{1.14}$$

From here, one can write the most general superpotential in terms of the baryon and meson fields and find the correct values of the unknown parameters by integrating out one flavor and matching the superpotential to $F = N$ case. The correct superpotential turns out to be

$$\mathscr{W}_{F=N+1} = \frac{1}{\Lambda^{2N-1}} \left[B^i M^j_i \overline{B}_j - \det M \right] \ . \tag{1.15}$$

This equation can also be obtained by an explicit instanton calculation. Now, since the point $M = B = \overline{B} = 0$ lies on the quantum moduli space, one can worry about the singular behavior that might occur there. One might expect that gluons and gluinos become massless, but it turns out that only the components of $M, B, \overline{B}$ become massless. That is, we simply have confinement without chiral symmetry breaking, a phenomenon we call s-confinement.

1.2 An Introduction to Modular Symmetries and the Flavor Problem

As previously discussed, the Standard Model is only a low-energy effective theory and its UV completion remains unknown. Despite being a rather successful framework, the model contains several free parameters whose top-down origin is unclear, and float as free parameters. In particular, these problems plague the flavor sector, where mixing angles, fermion masses, and phases need to be dialed manually to match experiments. Whether in a top-down or bottom-up framework, modular symmetries have emerged as a possible solution to this flavor puzzle.

Modular symmetries and the theory of modular forms have also been instrumental in various areas of physics, such as String Theory. In stringy contexts, they naturally arise at the two-loop torus contribution of closed strings, as well as at the level of extra dimensions [54, 55], which may be a product of tori. They have also played a major role in mathematics, where such symmetries played an important role in the landmark paper outlining the proof of Fermat's theorem [122] and have currently been used to understand the packing efficiency of spheres in higher dimensions [119]. These symmetries manifest as transformations under the modular group $\mathrm{SL}(2,\mathbb{Z})$ or its variants, such as metaplectic groups, and are closely linked to the geometry and topology of compactified dimensions. In the context of particle physics where we will be most interested, modular symmetries have garnered attention for their potential to explain various phenomena, including the hierarchies observed in fermion masses and mixing angles. They also provide a rather simple top-down approach for deriving the full symmetry group of various D-brane models with fluxes in the extra dimensions compactified on tori [30]. In particular, such constructions have been able to provide chiral models with three generations, as observed in the Standard Model. In bottom-up approaches, modular symmetries have proven especially useful, for example in the neutrino sector [49],

where a small number of parameters can be used to predict nine neutrino mass parameters. These symmetries therefore provide powerful tools for exploring beyond the Standard Model physics. Further into this section, we review some mathematical aspects of modular symmetries and the underlying structures behind them, before we go into how these can be used to tackle the flavor problem, in chapters 4 and 5.

1.2.1 A Review of Modular Groups and Modular Forms

Definition 1: The modular group is the group of 2-by-2 matrices with integer entries and determinant 1 and given by [37]

$$\mathrm{SL}(2,\mathbb{Z}) = \left\{ \begin{pmatrix} a & b \\ c & d \end{pmatrix} : a,b,c,d \in \mathbb{Z}, ad-bc=1 \right\} . \tag{1.16}$$

This group acts on the complex parameter τ on the upper half plane $\mathcal{H}$, defined as

$$\mathcal{H} = \{\tau \in \mathbf{C} : \mathrm{Im}(\tau) > 0\} . \tag{1.17}$$

To make the notation more coherent, we will denote the $\mathrm{SL}(2,\mathbb{Z})$ transformation by γ, such that the action of γ on the parameter τ is given by

$$\tau \overset{\gamma}{\mapsto} \frac{a\tau+b}{c\tau+d} \qquad \gamma \in \mathrm{SL}(2,\mathbb{Z}) . \tag{1.18}$$

The parameter τ is also called the half-period ratio and is given by $\tau := \omega_2/\omega_1$. Here ω_2 and ω_1 are the generators of the periodic lattice tessellating the complex plane (see figure 1.1). These generators also define a torus by identifying the opposite sides of each lattice. However, all tori related by so-called "modular transformations" are equivalent. The true group of these transformations is the group $\mathrm{PSL}(2,\mathbb{Z}) := \mathrm{SL}(2,\mathbb{Z})/\mathbb{Z}_2$. We divide by a $\mathbb{Z}_2$ group since an overall minus sign still results in the same modular transformation. Modular transformations

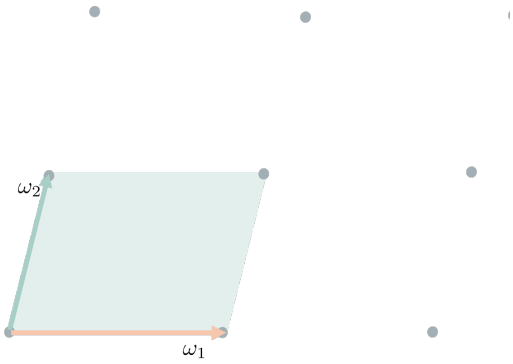

Figure 1.1: The generators ω_1 and ω_2 of the lattice. If the opposite sides are identified, we obtain a torus characterized by $\tau = \omega_2/\omega_1$.

play a central role in the theory of modular forms, as they encode the symmetry properties of modular forms under the action of congruence subgroups of $\mathrm{SL}(2,\mathbb{Z})$. The modular group $\Gamma = \mathrm{SL}(2,\mathbb{Z})$ can be defined by the presentation relations

$$S^4 = (S\,T)^3 = \mathbb{1} \quad \text{and} \quad S^2\,T = T\,S^2\,, \tag{1.19}$$

where the generators S and T are usually chosen as

$$S = \begin{pmatrix} 0 & 1 \\ -1 & 0 \end{pmatrix} \quad \text{and} \quad T = \begin{pmatrix} 1 & 1 \\ 0 & 1 \end{pmatrix}\,. \tag{1.20}$$

These generators act on the modulus τ according to

$$\tau \xmapsto{S} -\frac{1}{\tau} \quad \text{and} \quad \tau \xmapsto{T} \tau + 1\,. \tag{1.21}$$

Moreover, since modular transformations define an equivalence relation, various values of τ on the upper half plane are equivalent to others. This means that there is a fundamental domain on $\mathcal{H} \in \mathbb{C}$ which contains all the unique values of the parameter τ. Of course, this

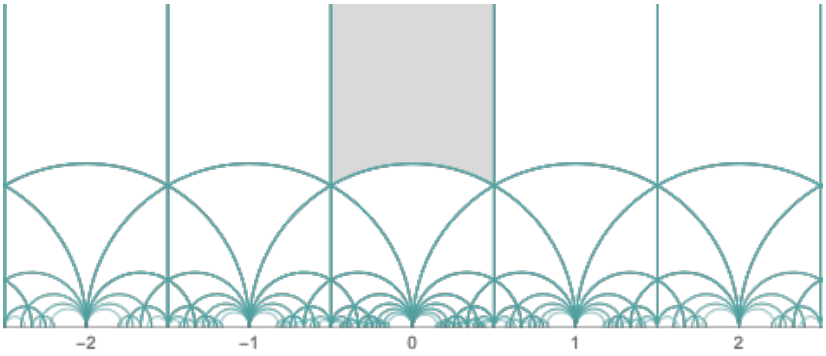

Figure 1.2: The gray region shows one of the fundamental domains in the upper-half complex plane $\mathcal{H}$.

fundamental domain is not unique, but it is customary to define it in the following way,

$$D = \{\tau \in \mathcal{H} |\ |\tau| \geq 1, |\,\mathrm{Re}(\tau)| \leq 1/2\}\ . \tag{1.22}$$

Thus, For every $\tau \in \mathcal{H}$ there exists $\gamma \in \Gamma$ such that $\gamma \in D$. We show the fundamental group in figure 1.2 generated on `Mathematica` [62] for completeness.

Definition 2: The principal congruence subgroup of level N, given by $\Gamma(N)$ is [29, 37]

$$\Gamma(N) := \left\{ \begin{pmatrix} a & b \\ c & d \end{pmatrix} \in \mathrm{SL}(2,\mathbb{Z}) \ :\ \begin{pmatrix} a & b \\ c & d \end{pmatrix} = \begin{pmatrix} 1 & 0 \\ 0 & 1 \end{pmatrix} \bmod N \right\}. \tag{1.23}$$

Definition 3: A subgroup Γ of $SL(2,\mathbb{Z})$ is a congruence subgroup if $\Gamma(N) \subset \Gamma$ for some $N \in \mathbb{Z}^+$, in which case Γ is said to be a congruence subgroup of level N.

Definition 4: A modular form is a complex-analytic function defined on the upper half-plane $\mathcal{H}$ satisfying the following transformation properties under the action of a congruence subgroup Γ of $\mathrm{SL}(2,\mathbb{Z})$, where $\gamma \in \Gamma$ [82]:

$$f_a(\gamma\,\tau) \ = \ (c\,\tau + d)^k\, \rho_{\boldsymbol{r}}(\gamma)_{ab}\, f_b(\tau)\,, \tag{1.24}$$

where τ is a complex number in the upper half-plane, and k is an integer representing the weight of the modular form. In this context, a and b are regarded simply as integer counters, while $(c\tau + d)^k$ is frequently termed the automorphy factor. Additionally, $\rho_{\boldsymbol{r}}(\gamma)$ represents an r-dimensional (irreducible) representation matrix of γ under the finite modular group $\Gamma'_N \cong \mathrm{SL}(2, \mathbb{Z}_N)$. These finite groups are defined by the relations:

$$S^4 = (S\,T)^3 = \mathbb{1}\,, \quad S^2\,T = T\,S^2\,, \quad T^N = \mathbb{1}\,. \tag{1.25}$$

Note that these relations are not enough to ensure finiteness for $N > 5$, and additional relations are needed.

In anticipation of future chapters, let's examine the modular symmetries associated with modular forms with half-integral modular weights [84]. Analogously to the groups SU(2) and SO(3), we need to consider the double cover of $\mathrm{SL}(2, \mathbb{Z})$, known as the metaplectic group $\widetilde{\Gamma} = \mathrm{Mp}(2, \mathbb{Z})$. This is the usual modular group, in conjunction with an additional phase factor that one needs to keep track of.

Definition 5: The unique double cover of the group $\mathrm{SL}(2, \mathbb{Z})$, or the metaplectic group $\mathrm{Mp}(2, \mathbb{Z})$ is defined as

$$\widetilde{\Gamma} = \left\{\widetilde{\gamma} = (\gamma, \varphi(\gamma, \tau)) \mid \gamma \in \Gamma,\ \varphi(\gamma, \tau) = \pm(c\,\tau + d)^{1/2}\right\}\,, \tag{1.26}$$

where the group operation acts as follows:

$$(\gamma_1,\, \varphi(\gamma_1, \tau))(\gamma_2,\, \varphi(\gamma_2, \tau)) = (\gamma_1\gamma_2,\, \varphi(\gamma_1, \gamma_2\,\tau)\varphi(\gamma_2, \tau))\,. \tag{1.27}$$

The metaplectic generators $\widetilde{S}$ and $\widetilde{T}$ of the group $\widetilde{\Gamma}$ satisfy the relations:

$$\widetilde{S}^8 = (\widetilde{S}\,\widetilde{T})^3 = \mathbb{1} \quad \text{and} \quad \widetilde{S}^2\widetilde{T} = \widetilde{T}\,\widetilde{S}^2\,, \tag{1.28}$$

which may be represented by the choice

$$\widetilde{S} = (S, -\sqrt{-\tau}) \quad \text{and} \quad \widetilde{T} = (T, +1) \ , \qquad S, T \in \Gamma \ . \tag{1.29}$$

We note that the presentation relation for $\widetilde{S}$ is $\widetilde{S}^8 = \mathbb{1}$ instead of $S^4 = \mathbb{1}$, and the double cover nature of the metaplectic group is manifest. To infer the sign of $\varphi(\gamma, \tau)$ for any element $\widetilde{\gamma} \in \widetilde{\Gamma}$ unambiguously, one needs to express $\widetilde{\gamma}$ as a product of the metaplectic generators (1.29) and then utilize the multiplication rule (1.27).

The modular transformations $\widetilde{\gamma}$ act on the modulus identical to γ. Let us now generalize the notion of 'half-integer' weights to modular forms as well.

Defintion 6: Metaplectic modular forms are functions on the congruence subgroups of the metaplectic group $\widetilde{\Gamma}_{4N}$, with modular weight $k/2$ and level $4N$, where $k, N \in \mathbb{N}$, are defined by

$$f_a(\tau) \ \stackrel{\widetilde{\gamma}}{\longmapsto} \ f_a(\widetilde{\gamma}\,\tau) \ := \ \varphi(\gamma, \tau)^k \, \rho_{\boldsymbol{r}}(\widetilde{\gamma})_{ab} \, f_b(\tau) \ . \tag{1.30}$$

Here $\varphi(\gamma, \tau)^k$ is now the automorphy factor, and $\rho_{\boldsymbol{r}}(\widetilde{\gamma})$ is an (irreducible) representation matrix of $\widetilde{\gamma}$ in the finite metaplectic modular group $\widetilde{\Gamma}_{4N}$. The generators $\widetilde{S}$ and $\widetilde{T}$ of this discrete group satisfy

$$\widetilde{S}^8 = (\widetilde{S}\,\widetilde{T})^3 = \mathbb{1} \ , \quad \widetilde{S}^2\widetilde{T} = \widetilde{T}\,\widetilde{S}^2 \ , \quad \widetilde{T}^{4N} = \mathbf{1} \ . \tag{1.31}$$

As before, these relations are insufficient to ensure finiteness for $N > 1$, and additional relations are needed. We thus need to identify the correct combinations of $\widetilde{S}$ and $\widetilde{T}$ that result in $\mathbb{1}_2 \mod 4N$. We thus need to ensure that this combination yields identity in the

finite group. For the case of $N = 2$, we adopt the selection proposed in [84, equation (21)]:

$$\widetilde{S}^5\widetilde{T}^6\widetilde{S}\widetilde{T}^4\widetilde{S}\widetilde{T}^2\widetilde{S}\widetilde{T}^4 = \mathbf{1}\ . \tag{1.32}$$

We also note that our choice for $N = 3$ is

$$\widetilde{S}\widetilde{T}^3\widetilde{S}\widetilde{T}^{-2}\widetilde{S}^{-1}\widetilde{T}\widetilde{S}\widetilde{T}^{-3}\widetilde{S}^{-1}\widetilde{T}^2\widetilde{S}^{-1}\widetilde{T}^{-1} = \mathbf{1}\ . \tag{1.33}$$

This concludes our review of modular groups and modular forms, and we describe the outline of the thesis below.

Outline of the thesis

In chapter 2, we outline a general method-building tool to introduce the phenomenon of chirality-changing RG flows. Starting with supersymmetric models, particularly focusing on how the presence or absence of *true* s-confinement can significantly change the chirally symmetric vacuum at the origin and lead to flows where chiral structure changes between the UV and the IR. In particular, we show that in the absence of true, stable s-confinement, the naive expectation of the efficacy of this mechanism does not hold.

In chapter 3, we focus on the applications of chirality changing RG flows specifically in string setups. We build various string models where the number of generations of the models changes from UV to IR, which means that common model searches in the string landscape need to perform more systematic analyses. In particular, a model that appears unviable due to the 'wrong' number of generations in the UV may be a close fit to the SM in the IR.

In chapter 4, we explore the flavor sector of the SM from a modular symmetric standpoint. In particular, we show that Yukawa couplings in specific tori-based approaches may have simple

structures behind complicated expressions, by using various properties of theta functions. Furthermore, we show that these approaches follow the appropriate boundary conditions exactly and that these symmetries offer a predictive model-building approach.

In chapter 5, we show how modular symmetries in conjunction with traditional discrete flavor groups combine the strengths of both approaches in an 'eclectic' scheme. We show how this scheme offers an approach where one can control the Kähler corrections, and motivate the vacuum expectation values which offer a promising fit to the neutrino masses data, displaying the strengths of modular symmetries in bottom-up approaches. And finally, in chapter 6, we conclude the thesis.

Chapter 2

Chirality Changing RG Flows: Dynamics and Models

(This section is heavily based on the publication with Yuri Shirman and Michael Waterbury) [111]

2.1 Chiral Symmetries and gapping fermions

As discussed in section 1.1 of the introduction, one of the many puzzles of the Standard Model is regarding the number of generations. In this chapter and next, we will discuss how the notion of generations of a theory is not invariant across RG Flows, and how one can change the chiral structure of theories with various gauge groups by generating mass gaps.

Chiral symmetries have proven indispensable for the study of the dynamics of quantum field theory (QFT). Since mass terms break chiral symmetries, they are only allowed for fermions in vector-like representations, while fermions in theories with chiral matter content must remain massless unless chiral symmetries are broken spontaneously. While it seems obvious that these statements are renormalization group (RG) invariant, examples of RG flows alter-

ing the chiral structure of QFT have been known for quite some time. [90,107,114,117]. The underlying physics relies on the existence of models exhibiting confinement without chiral symmetry breaking [108] referred to as s-confinement *. Generically, the elementary and low–energy degrees of freedom of s-confining theories transform in different representations of the global symmetries. Thus the chiral structure of the matter sector may differ between ultraviolet (UV) and IR. The early models of this type [90, 114] were motivated by a search for realistic supersymmetry (SUSY) extensions of the SM and contained composite massless SM generations in the IR. More recently, the possibility of developing a mass gap in theories with apparently chiral matter content attracted some attention. References [107, 117] explored the deformation class of QFT by constructing flows in theory space from anomaly-free chiral theories to the trivial theory with no massless fermions. The ideas introduced in [90, 107, 114, 117] were used in [105] to argue that string compactifications may lead to realistic low energy physics even if the number of chiral generations in the UV differs from 3. The authors of [105] also began a careful analysis of dynamics underlying the chirality changing RG flows. The goal of this chapter is to complete the systematic analysis of this phenomenon and elucidate a unifying picture of chirality changing RG flows. While we will concentrate on the generation of mass gap, our analysis will also cover models where additional composite chiral multiplets appear in the IR as well as more general cases where the chiral matter content in IR differs from that in UV.

The model-building prescription for generating a mass gap is quite simple: one deforms an s-confining gauge theory [33] by introducing the superpotential couplings to a set of spectators superfields, transforming under the chiral symmetry in representations conjugate to the representations of the composites of the strong dynamics. The most general superpotential allowed by such a deformation of the s-confining model lifts all classical flat directions of the s-confining sector ensuring that in the ground state the strong s-confining group is unbroken and confines. One must then verify that the classical flat directions associated with the

*See [33] for a complete classification of s-confining theories.

spectator superfields are also lifted, which will generically be the case. If the spectator flat directions are indeed lifted, the global symmetry group of the s-confining sector is unbroken and a chiral subgroup of the global symmetry may be gauged thus leading us to the desired result. On the other hand, we will also see examples where the flat directions associated with the spectator fields are destabilized by the non-perturbative dynamics. Since the spectators are charged under the chiral sector the chiral symmetry is broken in this class of models. Finally, if one is interested in the appearance of chiral composite generations, one chooses different representations for the spectators so that in the IR some or all of the composites do not have partners to generate mass terms.

2.1.1 Generic Construction

To construct models of chirality changing RG flows we will adopt the model-building approach of [107, 117] taking a product group theory $H \times G$ as a starting point. Here G is the chiral symmetry group of interest which may be either a weakly-coupled gauge group or an anomaly-free global symmetry, while H is the gauge group of an s-confining sector whose dynamics is responsible for the chirality flows. For now, assume that G is unbroken by the confining dynamics of H, such that it is sensible to study the chiral properties of G in both the UV and IR. Fields charged under both G and H confine into composites which generically transform under tensor representations of G and have different chiral properties than the elementary representations of G. We call these flows from the UV to IR chirality changing flows on G induced by H. We are particularly interested in deformations of s-confining models where some or all of the composite fields pair up with the spectators of the strong dynamics in vector-like representations. When this is the case, the vector-like representations can be decoupled with the addition of superpotential interactions that may be marginal or irrelevant in the UV but behave as mass terms in the IR. As we will show, the fact that the IR mass terms originate from the dimension $d > 2$ operators in the UV

implies that dynamical effects of these superpotential terms are quite non-trivial and may disrupt the confining dynamics of H. We will draw special attention to these scenarios.

Here, we restrict our attention to $H \times G$ models with $\mathcal{N} = 1$ SUSY. In our analysis we will be able to employ familiar tools often used in the study of dynamical supersymmetry breaking [110] even though the models we consider will possess supersymmetric ground states.

Let us discuss the construction in a bit more detail. We will start with s-confining models based on gauge group H and matter fields Q_i transforming in a chiral representation of $H \times \widetilde{G}$, where $\widetilde{G}$ is a possibly anomalous chiral symmetry of the theory. We will limit our attention to an anomaly-free subgroup G of this global symmetry and thus will study $H \times G$. As long as G is only a global symmetry, the anomaly freedom means that mixed H^2G anomalies cancel. The anomaly cancellation condition is automatically satisfied whenever G is non-Abelian, continuous, and only imposes nontrivial constraints on the model when G contains U(1) factors. Aside from these weak constraints, G could be identified with any subgroup of $\widetilde{G}$. Generically G will have cubic anomalies. These are harmless as long as G is a global symmetry, however, we will imagine weakly gauging G. This is only possible if we add a set of spectators charged under G whose contribution to cubic anomaly cancels the contribution of Q_i's. The dynamics of our s-confining model can be described in terms of the gauge invariant composites $\mathcal{M}_f$. In the UV these composites scale as $\mathcal{M}_f \sim Q_i^{d_f}$ and thus have engineering mass dimension d_f.[†] In the IR the composite moduli $\mathcal{M}_f$ are weakly coupled and have mass dimension one. Generically, $\mathcal{M}_f$ will transform in chiral representations of G and will contribute to cubic anomalies of G. The 't Hooft anomaly matching condition ensures that the $\mathcal{M}_f$ saturate the anomalies of the microscopic theory. To be able to gauge G we must introduce a set of spectator fields that cancel G^3 anomalies. The choice of spectators

[†]Here our notation for the composites derives from the simplest case of a bilinear composite, a meson, $\mathcal{M} \sim Q^2$. We stress that in this general discussion, $\mathcal{M}_f$ represent all moduli of the theory regardless of their engineering dimension.

is not unique. For example, one can choose spectators $\bar{q}_i$ to transform in representations conjugate to those of elementary fields, Q_i, or a different set of spectators $\overline{M}_f$ transforming in representations conjugate to the composites $\mathcal{M}_f$. As we shall soon see, the former choice may lead to an appearance of massless chiral composites of G in the IR while the latter choice may allow an RG flow to a gapped vacuum.

For the moment we choose the spectators transforming as $\overline{M}_f$ so that an IR mass term is allowed in the superpotential

$$\mathscr{W} = \sum_f \mathcal{M}_f \overline{M}_f \,. \tag{2.1}$$

We must remember that H is s-confining, thus the full non-perturbative superpotential takes the form

$$\mathscr{W} = f(\mathcal{M}_f, \Lambda) + \sum_f \mathcal{M}_f \overline{M}_f \,, \tag{2.2}$$

where $f(\mathcal{M}_f, \Lambda)$ is a dynamical superpotential generated by the s-confining dynamics of H.

By construction the full $H \times G$ symmetry is chiral and the mass terms are not allowed. Moreover, even the G sector alone is chiral in the UV. In the IR the strongly coupled H sector confines while the low energy matter content is vector-like under G. As long as the deformation (2.1) of the s-confining model does not lift the chirally symmetric vacuum at the origin of the moduli space, the dynamics of the deformed s-confining theory results in development of the mass gap in the IR.

For chiral symmetry to be unbroken in the IR, the VEVs of both the composite moduli $\mathcal{M}_f$ and the spectators $\overline{M}_f$ must vanish in the ground state. This is indeed true for the moduli $\mathcal{M}_f$ since the deformation (2.1) lifts all classical flat directions of H as long as it contains mass terms for all H moduli. However, while the deformation (2.1), when written in terms

of the IR degrees of freedom, looks like a simple set of mass terms for all the spectators, the interplay between the non-perturbative dynamics of the s-confining sector and the tree level superpotential is quite non-trivial and may result in the spontaneous breaking of G. Indeed, while (2.1) lifts all the classical flat directions of H, it introduces new classical flat directions parameterized by $\overline{M}_f$. To see that one simply needs to look at the deformation in terms of elementary degrees of freedom

$$\mathscr{W} = \sum_f (Q_i)^{d_f} \overline{M}_f \,. \tag{2.3}$$

The extrema of this superpotential with respect to $\overline{M}_f$ are found at $\mathcal{M}_f = 0$ or, equivalently at $Q_i = 0$. On the other hand, the extrema with respect to Q_i are given by

$$\sum_f \frac{\partial \mathcal{M}_f}{\partial Q_i} \overline{M}_f = 0 \,, \tag{2.4}$$

which is satisfied for all values of $\overline{M}_f$ since in the UV the composites M_f are simply monomials of Q_i's with dimensions greater than or equal to two.

As we will see in the following sections the interplay between the strong dynamics and the deformation (2.1) generates a non-perturbative superpotential for the spectators. This is most easily seen by considering physics along classical flat directions for spectators that couple to mesons of strong dynamics. Along such flat directions the spectator VEVs generate large masses for all the quarks Q_i and the low energy physics is described in terms of a pure super-Yang–Mills (SYM) theory with dynamical superpotential generated by gaugino condensation:

$$\mathscr{W} = \Lambda_L^3 = \left(\overline{M}^F \Lambda^b \right)^{3/b_L} , \tag{2.5}$$

where Λ_L is the dynamical scale of the low energy SYM theory, b and b_L are one-loop beta-

function coefficients of the UV and IR theories respectively, F is the effective number of flavors in our s-confining UV model and in the second equality we used the scale matching relation $\Lambda_L^{b_L} = \overline{M}^F \Lambda^b$. As long as $3F/b_L > 1$ the dynamical superpotential stabilizes the spectators near the origin, the analysis of the ground state in terms of the IR degrees of freedom is valid and the mass gap is generated. This is the case, for example, in models satisfying the s-confinement conditions [33, 108]. On the other hand, whenever $3F/b_L < 1$ the dynamical superpotential destabilizes the chirally symmetric vacuum near the origin and the models of this type cannot lead to a mass gap. Before looking at the examples outlined in Chapter2, let us make a connection to Razamat–Tong (RT) [107] language. The discussion of [107] takes the model with chiral symmetry group G as a starting point, then assigns some, but not all, chiral superfields charges under the strongly coupled H sector. In this language, the spectators $\overline{M}$ represent the basic chiral matter of the UV description. This is in contrast to our construction where $\overline{M}$ fields are spectators needed to generate a mass gap in an s-confining model. Nevertheless, once a model is fully specified we achieve the same result as in [107] — a chiral theory with a mass gap in the IR.

2.2 Chirality flows and $\mathrm{SP}(2N)$ dynamics

In this section we consider the simplest class of models exhibiting chirality flows. These models are based on the s-confining models with $\mathrm{SP}(2N)$ gauge group with $F = N + 2$ chiral matter fields in the fundamental representation. We will identify the chiral symmetry group G with a subgroup of $\mathrm{SU}(2F)$, the maximal chiral symmetry of the $\mathrm{SP}(2N)$ dynamics. In section 2.2.1 we consider an example of a dynamically generated mass gap [107], while studying a closely related example of a composite massless generation [90] in section 2.2.2. In section 2.2.3 we briefly discuss additional chirality flow models that can be obtained by considering different embeddings of G into the maximal global symmetry of the s-confining

sector.

2.2.1 Dynamically generated mass gap

Following [107] we consider SP($2N$) models where the chiral symmetry group G is identified with the maximal global symmetry of the s-confining sector, $G = \mathrm{SU}(2F) = \mathrm{SU}(2N+4)$. To analyze the non-perturbative dynamics of this class of models we recall that an SP($2N$) theory with F flavors has an SU($2F$) global symmetry and possesses a set of classical flat directions [63] which, up to gauge and global symmetry transformations, can be parameterized by[‡]

$$Q = \begin{pmatrix} q_1 & & & \\ & q_2 & & \\ & & \cdots & \\ & & & q_F \\ & & & \\ & & & \end{pmatrix} \otimes \mathbb{1}_2 \,. \tag{2.6}$$

Alternatively, the space of classical vacua can be parameterized in terms of mesons, $\mathcal{A}_{ij} \sim Q_i Q_j$ transforming in an antisymmetric representation of the global SU($2F$) symmetry. At a generic point on the moduli space $\mathrm{rank}(\mathcal{A}) = \min(2N, 2F)$. This means that for $F > N$ the mesons must satisfy a set of constraints. Specifically in the case of interest, $F = N+2$, the meson VEVs satisfy classical constraints

$$\epsilon^{i_1 \ldots i_{2N+2}} \mathcal{A}_{i_1 i_2} \mathcal{A}_{i_3 i_4} \ldots \mathcal{A}_{i_{2N+1} i_{2N}} = 0 \,. \tag{2.7}$$

[‡]Here we have restricted our attention to the $F > N$ case.

These constraints may be compactly written as

$$\frac{\partial}{\partial \mathcal{A}}(\mathrm{Pf}\,\mathcal{A}) = 0\,. \tag{2.8}$$

Following Seiberg's analysis [108] of s-confinement in SU(N), Intriligator and Pouliot argued that the quantum and classical space coincide in $F = N+2$ SP($2N$) models. Since the origin belongs to the quantum moduli space, the model posseses a supersymmetric vacuum with unbroken chiral symmetry. The low energy physics is described in terms of mesons with a non-perturbative superpotential [§]

$$\mathscr{W}_{\rm dyn} = \frac{1}{\Lambda^{2N+2}}\mathrm{Pf}\mathcal{A}\ . \tag{2.9}$$

To generate the mass gap [107] we deform the theory by including a set of spectator superfields $\overline{A}$ transforming in the conjugate antisymmetric representation of the chiral SU($2F$) = SU($2N+4$) symmetry with the tree superpotential

$$\mathscr{W}_{\rm tree} = \overline{A}Q^2 \sim \Lambda\overline{A}\mathcal{A}\,, \tag{2.10}$$

where the second expression is written in terms of mesons $\mathcal{A}$. The UV and IR matter content of the model is presented in the top and bottom parts of table 2.1 respectively:

	SP($2N$)	SU($2N+4$)	U(1)$_R$
Q	$\square$	$\square$	$\frac{1}{N+2}$
$\overline{A}$	$\mathbf{1}$	$\overline{\begin{smallmatrix}\square\\\square\end{smallmatrix}}$	$\frac{2N+2}{N+2}$
$\mathcal{A}\sim Q^2$	$\mathbf{1}$	$\begin{smallmatrix}\square\\\square\end{smallmatrix}$	$\frac{2}{N+2}$
$\overline{A}$	$\mathbf{1}$	$\overline{\begin{smallmatrix}\square\\\square\end{smallmatrix}}$	$\frac{2N+2}{N+2}$

Table 2.1: Field content of the SP($2N$) model with $F = N+2$ flavors.

[§]The equations of motion following from this superpotential enforce classical constraints on mesons $\mathcal{A}$.

The IR form of the superpotential (2.10) suggests that all the fields in the low energy effective theory become massive and the model possesses a unique vacuum at the origin with an unbroken chiral symmetry. While ultimately correct in this model, the conclusion requires a more careful analysis of the non-perturbative dynamics. Indeed, while the tree level superpotential lifts all flat directions associated with $\mathrm{SP}(2N)$ gauge group, the deformed theory has a new set of classical flat directions parameterized by spectators $\overline{A}$. Far enough along this new branch of classical vacua, $\overline{A} \gg \Lambda$, the theory is weakly coupled and the analysis of dynamics is most easily performed in terms of quark superfields since their Kähler potential is nearly canonical in this regime. The spectator VEVs generate mass terms for quark superfields which can be integrated out. The low energy physics is then described as a pure SYM theory whose coupling constant is field dependent:

$$\Lambda_L^{3(N+1)} = \mathrm{Pf}\,\overline{A}\Lambda^{2N+1}\,. \tag{2.11}$$

In the IR pure SYM dynamics generates the gaugino condensate superpotential, which can also be interpreted as a superpotential for the spectators

$$\mathscr{W} = \Lambda_L^3 = \big(\mathrm{Pf}\big(\overline{A}\big)\Lambda^{2N+1}\big)^{\frac{1}{N+1}} \sim \overline{A}^{1+\frac{1}{N+1}}\Lambda^{2-\frac{1}{N+1}}\,. \tag{2.12}$$

It is easy to see that $\overline{A}$ is stabilized near the origin of the moduli space thus justifying the naive analysis based on the tree level superpotential in terms of IR degrees of freedom. Of course, in this model one does not have to rely on the semiclassical analysis we just performed. Indeed, the description of the theory in terms of IR degrees of freedom is valid everywhere on the moduli space of the deformed theory, and analysis of the full superpotential (given by the sum of (2.9) and (2.10)) would yield the same result [¶]. However, the semiclassical analysis is often more intuitive and, as we shall see in section 2.3, in some models it is the

[¶]One must remember that while the Kähler potential of mesons is, in principle, calculable it is far from canonical at large $\bar{A}$.

only tool at our disposal.

So far we have illustrated dynamical generation of the mass gap in models where the chiral symmetry group is SU(M) with $M = 2F = 2N + 4$ even. This restriction is a consequence of the fact that the fundamental of SP($2N$) has an even dimension. However, it is easy to generalize this construction to models with odd M [107]. Indeed, one can simply start with the same s-confining SP($2N$) sector but choose the chiral group $G = \mathrm{SU}(M) = \mathrm{SU}(2F - 1)$ to be a subgroup of the maximal chiral symmetry. Under SU(M) the meson $\mathcal{A}$ decomposes into an antisymmetric $\mathcal{A}$ and a fundamental $\mathcal{Q}$. Given this choice of chiral symmetry the IR matter content of the model is given in Table 2.2. Since our mass gap analysis did not rely

	SP($2N$)	SU($2N+3$)	U(1)$_R$
$\mathcal{A}$	$\mathbf{1}$	$\begin{array}{|c|}\hline\ \\ \hline\ \\ \hline\end{array}$	$\frac{2}{N+2}$
$\mathcal{Q}$	$\mathbf{1}$	$\begin{array}{|c|}\hline\ \\ \hline\end{array}$	$\frac{2}{N+2}$
$\overline{A}$	$\mathbf{1}$	$\begin{array}{|c|}\hline\ \\ \hline\ \\ \hline\end{array}$	$\frac{2N+2}{N+2}$
$\overline{Q}$	$\mathbf{1}$	$\begin{array}{|c|}\hline\ \\ \hline\end{array}$	$\frac{2N+2}{N+2}$

Table 2.2: IR content of the odd M model, $M = 2N + 3$.

on the dynamics of the SU($2N + 4$) sector [‖], the chirally symmetric vacuum with mass gap will exist as long as we include the tree level superpotential (2.10), now written in terms of SU($2N + 3$) degrees of freedom. Note that while the tree level superpotential must result in a maximal rank mass matrix in the IR it does not have to respect the maximal global SU($2N + 4$) symmetry.

2.2.2 A Massless Composite Generation

In the previous subsection, we have mentioned that the choice of spectators is not unique. Rather than choosing them in representations of SU($2N + 4$) conjugate to those of mesons,

[‖]Recall that aside from requiring a cancellation of cubic anomalies we treat G sector of the model as a global symmetry.

we could choose, for example, the spectators transforming in representations conjugate to those of quark superfields Q. In this case, while the full theory is chiral, the UV matter content from the point of view of the $\mathrm{SU}(2N+4)$ sector is non-chiral. Once the theory confines, the low energy degrees of freedom contain $\mathrm{SP}(2N)$ composites which transform in an antisymmetric representation of the $\mathrm{SU}(2N+4)$ symmetry. Thus a non-chiral $\mathrm{SU}(2N+4)$ sector acquires in the IR a massles chiral generation containing an antisymmetric tensor and $2N$ antifundamentals. This theory may further be complemented by superpotential interactions between the $\mathrm{SP}(N)$ moduli and spectators. Consider for example an $\mathrm{SP}(2) \times \mathrm{SU}(6)$ model with matter given in (2.1). If we choose $G = \mathrm{SU}(3) \times \mathrm{SU}(2) \times \mathrm{U}(1) \subset \mathrm{SU}(5) \subset \mathrm{SU}(6)$ with a standard decomposition of GUT fields under the SM, add two more spectator generations charged under the SM and include all the superpotential terms allowed by symmetries we will arrive at the composite supersymmetric model of Nelson and Strassler [90].

2.2.3 Different Embeddings of G

We conclude the discussion of chirality flows in s-confining $\mathrm{SP}(2N)$ models by noting that one can construct new models by simply choosing different embeddings of the chiral symmetry group G into the maximal global symmetry of the s-confining sector. Let's briefly look at some examples. For our first example, we consider the model studied in [107] with $H = \mathrm{SP}(2)$ and $G = \mathrm{SU}(3) \times \mathrm{SU}(2) \times \mathrm{U}(1) \subset \mathrm{SU}(5) \subset \mathrm{SU}(6)$. Once again, the tree level superpotential must be the most general one consistent with G but does not need to respect the full SU(6) global symmetry of the s-confining sector. A somewhat more elaborate example can be found by considering $N = 3$ case, i.e. an s-confining SP(6) model with 5 flavors and SU(10) global symmetry. We will take $G = \mathrm{SU}(5)$ and embed it into SU(10) global symmetry so that 10 quark superfields transform in an antisymmetric representation of SU(5). The mesons $M \sim Q^2$ then transform as $\mathbf{45}$ of SU(5). We now add the spectators in the $\overline{\mathbf{45}}$ representation of SU(5). The analysis of strong SP(6) dynamics remains unchanged and the model develops

a mass gap in the IR. In our final example we start with the same SP(6) s-confining sector and choose $G = \mathrm{SU}(3)$ embedding it into SU(10) in such a way that 10 quark superfields transform in a 3-index symmetric representation of SU(3). The SP(6) mesons decompose as $\mathbf{10} \oplus \mathbf{35}$ of SU(3). Adding spectators in $\overline{\mathbf{10}} \oplus \overline{\mathbf{35}}$ representations as well as the most general superpotential results in a mass gap appearing in the IR. Our discussion so far suggests that, in addition to generating mass gaps or composite chiral matter, chirality flows may lead to more general results. Indeed, in the following sections, we will see examples of models where both UV and IR physics is chiral yet the chiral structure of the theory changes in the course of RG flow. Our examples will include models based on different s-confining sectors but even within specific s-confining dynamics we will have the freedom to construct different models of chirality flow by using two different tools: an ability to choose different representations of spectators introduced to cancel anomalies and use of different embeddings of G into the maximal global symmetry of the s-confining sector.

2.3 The Role of s-confinement: An $\mathrm{SO}(N)$ example

In the previous section, we analyzed the dynamics of models where mass gap is generated in the IR despite the matter content being chiral in the UV. Following [107] our examples were based on s-confining SP($2N$) theories and the choices of chiral matter representations were dictated by embedding of the chiral symmetry in the maximal global symmetry of the s-confining model. The simplest and most illuminating embedding generated a mass gap in models with matter transforming in an antisymmetric representation of the chiral SU(N) symmetry. This was a consequence of the fact that the composites of SP($2N$) models transform as antisymmetrics of global symmetries. It is then natural to expect that chiral matter may be gapped in models where the composites of the confining sector transform in symmetric representations of the global symmetry. To that end, the authors of [117] argued

that a mass gap in theories with symmetric chiral matter can be generated by deformations of confining SO(N) sector with $F = N - 4$ chiral superfields in a vector representation. It is known [64] that this class of models exhibits two phases: a phase with dynamically generated runaway superpotential and a no-superpotential phase where quantum moduli space coincides with the classical one and extends to the origin. It was argued in [117] that an appropriate deformation of these models generates a mass gap in the no-superpotential phase. Unfortunately, this class of SO(N) models is not s-confining [33] and the phase with chirally symmetric vacuum is quite fragile. We will argue here that the deformations necessary to generate the gap destroy the chirally symmetric vacuum. Fortunately, as we will show in section 2.4 constructions of gapped symmetric fermion models are still possible albeit they are more cumbersome than hoped for in [117].

2.3.1 An SU(F) × SO($F + 4$) model

We begin the analysis by reviewing the dynamics of SO(N) theories with $F = N - 4$ flavors [64]. The quantum numbers of the matter fields under the gauge SO(N) and global SU($N - 4$) symmetries are given in Table Table 2.3.

	SO(N)	SU(F)	U(1)$_R$
Q	$\square$	$\square$	$\frac{F-N+2}{F}$
$\mathcal{S}$	**1**	$\square\square$	$\frac{2(F-N+2)}{F}$
$\overline{S}$	**1**	$\overline{\square\square}$	$\frac{2(N-2)}{F}$

Table 2.3: Field content of the SO(N) model with F flavors.

The one-loop beta function of SO(N) theory, for $N > 4$ is

$$b = 3(N - 2) - F \ . \tag{2.13}$$

The classical moduli space can be parameterized in terms of quark VEVs or gauge invariant mesons $\mathcal{S}_{ij} = Q_i Q_j$. At a generic point on this moduli space the gauge group is broken to a pure SYM SO(4) $\sim$ SU(2)$_L \times$ SU(2)$_R$. Further, in the IR SU(2)$_L \times$ SU(2)$_R$ group confines, generating the gaugino condensate superpotential. Since the dynamical scale of the low energy physics depends on the moduli, this results in the superpotential for SO(N) fields which, in terms of mesons, takes the form

$$\mathscr{W}_{\rm dyn} = 2\langle\lambda\lambda\rangle_L + 2\langle\lambda\lambda\rangle_R \tag{2.14}$$

$$= \frac{1}{2}(\epsilon_L + \epsilon_R)\left(\frac{16\Lambda^{2(N-1)}}{\det\mathcal{S}}\right)^{1/2}, \tag{2.15}$$

where $\epsilon_{L,R} = \pm 1$. As explained in [64] the theory has two phases. When $\epsilon_L\epsilon_R = 1$ the two contributions to the superpotential add up constructively and the classical moduli space is lifted, resulting in a phase without a stable ground state. When $\epsilon_L\epsilon_R = -1$ the two contributions to the superpotential cancel[**], resulting in a smooth quantum moduli space with an unbroken SO(N) chiral global symmetry at the origin.

Let us now deform the theory by including superfields $\overline{S}$ transforming in conjugate symmetric reprsentation of the chiral SU(F) = SU($N-4$) symmetry[††]. Since the low energy matter content is vector-like we can include a tree level superpotential which appears as a mass term in the IR. The full low energy superpotential takes the form

$$\mathscr{W} = \frac{1}{2}(\epsilon_L + \epsilon_R)\left(\frac{16\Lambda^{2(N-1)}}{\det\mathcal{S}}\right)^{1/2} + \Lambda\mathcal{S}\overline{S}\,. \tag{2.16}$$

A naive analysis of the no-superpotential branch suggests that our deformation generates a mass gap. However, the absence of s-confinement and the presence of a second, runaway,

[**]A pure SYM SO(4) theory is described by two dynamical scales, Λ_L and Λ_R which need not be equal. However, in our case the dynamical scales of the low energy gauge groups are determined uniquely (up to a sign) by the dynamical scale of UV physics and mesons VEV, thus ensuring the cancellation of the two terms in the superpotential.

[††]It is easy to see that the matter content is anomaly free under the full SO(N) $\times$ SU($N-4$) symmetry.

phase in SO(N) models implies that, in contrast to the theories we discussed earlier, the chirally symmetric vacuum is unstable under any deformation. For example, an explicit mass term, mQ^2, lifts the classical moduli space while remaining consistent with an existence of the chirally symmetric vacuum at the origin. Yet, as argued in [64], at the quantum level the full no-superpotential branch, including the chirally symmetric vacuum, is lifted.

To better understand the fate of the chirally symmetric phase we will study the non-perturbative dynamics in a weakly coupled regime. We note that the deformed theory possesses a new classical flat direction parameterized by $\overline{S}$. When $\overline{S} \gg \Lambda_{\mathrm{SO}(N)}$ the physics is weakly coupled and the Kähler potential is nearly canonical in terms of the quark superfields. Furthermore, along this flat direction the quarks become massive, suggesting that argument of [64] for the disappearance of the chirally symmetric vacuum should apply. The dynamical nature of $\overline{S}$ allows us to perform a more detailed analysis. At large $\overline{S}$ the quarks must be integrated out, and the low energy physics is described by a pure SO(N) SYM theory with the dynamical scale given by

$$\Lambda_L^{3(N-2)} = \det \overline{S} \Lambda^{2N-2} \,. \tag{2.17}$$

The low energy physics then generates the dynamical superpotential

$$\mathscr{W} = \Lambda_L^3 = \left(\det \overline{S}\right)^{\frac{1}{N-2}} \Lambda^{2+\frac{2}{N-2}} \,. \tag{2.18}$$

One can see that this superpotential leads to runaway behavior for $\overline{S}$. While our derivation is only valid at large values of $\overline{S}$, holomorphy suggests that in the absence of a singularity in the Kähler potential the SUSY vacuum at the origin must be lifted.

2.4 Chirality Flows and SU(N) Dynamics

2.4.1 s-confining SQCD

We begin by briefly reviewing an s-confining SQCD model with $F = N + 1$ flavors. The theory has an $\mathrm{SU}(N+1)_{\mathrm{L}} \times \mathrm{SU}(N+1)_{\mathrm{R}} \times \mathrm{U}(1)_B \times \mathrm{U}(1)_R$ anomaly-free global symmetry and the matter charges under gauge and global symmetries are given in the top part of Table 2.4. The existence of a large chiral symmetry will allow us to construct a variety of

	SU(N)	SU(F)$_{\mathrm{L}}$	SU(F)$_{\mathrm{R}}$	U(1)$_B$	U(1)$_R$
Q	$\square$	$\square$	$\mathbf{1}$	1	$\frac{1}{N+1}$
$\overline{Q}$	$\overline{\square}$	$\mathbf{1}$	$\overline{\square}$	-1	$\frac{1}{N+1}$
$\mathcal{M}$	$\mathbf{1}$	$\square$	$\overline{\square}$	0	$\frac{2}{N+1}$
$\mathcal{B}$	$\mathbf{1}$	$\overline{\square}$	$\mathbf{1}$	N	$\frac{N}{N+1}$
$\overline{\mathcal{B}}$	$\mathbf{1}$	$\mathbf{1}$	$\square$	N	$\frac{N}{N+1}$
S	$\mathbf{1}$	$\overline{\square}$	$\square$	0	$\frac{2N}{N+1}$
$\overline{B}$	$\mathbf{1}$	$\square$	$\mathbf{1}$	$-N$	$\frac{N+2}{N+1}$
B	$\mathbf{1}$	$\mathbf{1}$	$\overline{\square}$	$-N$	$\frac{N+2}{N+1}$

Table 2.4: Field content of s-confining SQCD model with $F = N + 1$ flavors. The top portion of the table shows the elementary SU(N) charged fields. The middle section of the table shows the confined degrees of freedom that are weakly coupled in the IR and near the origin of the moduli space. The bottom portion of the table shows the quantum numbers of the spectator fields needed to cancel flavor symmetry anomalies and generate mass gap for chiral fermions in the IR.

models exhibiting chirality changing RG flows by considering different embeddings of G in the maximal global symmetry group of the s-confining sector.

In the absence of the superpotential, the model possesses a large moduli space of classical flat directions. These flat directions can be parameterized in terms of gauge invariant composites, $\mathcal{M} \sim Q\overline{Q}$, $\mathcal{B} \sim Q^N$, and $\overline{\mathcal{B}} \sim \overline{Q}^N$, whose quantum numbers are presented in the middle

section of Table 2.4. Classically the moduli VEVs satisfy a set of identities

$$\mathcal{M}_{ij}\overline{\mathcal{B}}_j = \mathcal{B}_j M_{ji} = \mathcal{B}_j\overline{\mathcal{B}}_i = 0\,. \tag{2.19}$$

It is well known that this model s-confines and the low energy physics is described in terms of mesons, baryons, and anti-baryons with dynamically generated superpotential which implements the classical constraints at the quantum level

$$\mathscr{W} = \frac{1}{\Lambda^{2N-1}}\left(\mathcal{B}\mathcal{M}\overline{\mathcal{B}} - \det\mathcal{M}\right). \tag{2.20}$$

In the IR, mesons and baryons are weakly coupled and have a nearly canonical Kähler potential. Thus it is convenient to rescale the moduli by absorbing appropriate powers of the dynamical scale into the definition of the moduli so that $\mathcal{M}$, $\mathcal{B}$, and $\overline{\mathcal{B}}$ have mass dimension one.

In the following subsections, we will consider several illustrative embeddings of a chiral group G in the maximal global symmetry of the s-confining sQCD where a chirally symmetric vacuum is preserved while a mass gap is developed.

2.4.2 $G = \mathrm{SU}(N+1)_\mathrm{L} \times \mathrm{SU}(N+1)_\mathrm{R}$

As our first example, we choose[‡‡] $G = \mathrm{SU}(N+1)_L \times \mathrm{SU}(N+1)_R$. As discussed earlier, the low energy content of G is given by mesons $\mathcal{M}$, baryons $\mathcal{B}$, and anti-baryons $\overline{\mathcal{B}}$ transforming as $(\square, \overline{\square})$, $(\overline{\square}, 1)$, and $(1, \square)$, respectively. Since our goal is to deform this model in such a way that G^3 anomalies vanish while the low energy matter content is vector-like, we introduce a set of spectators, $\overline{M}$, B, and $\overline{B}$ in representations conjugate to those of $\mathcal{M}$, $\mathcal{B}$, and $\overline{\mathcal{B}}$. For completeness, the quantum numbers of the spectator fields are displayed in the bottom

[‡‡]The following analysis remains unchanged if we include a $\mathrm{U}(1)_B$ factor in the definition of G.

portion of Table 2.4.

The inclusion of the spectator fields in the theory allows a tree-level superpotential consistent with the full $H \times G$ symmetry,

$$\mathscr{W}_{\text{tree}} = \overline{M}\mathcal{M} + \overline{B}Q^N + B\overline{Q}^N \sim \overline{M}\mathcal{M} + \overline{B}\mathcal{B} + B\overline{\mathcal{B}}\,. \tag{2.21}$$

Repeating the analysis of section 2.2 far along the meson branch of the moduli space we obtain the low energy superpotential for mesons

$$\mathscr{W} = \Lambda_L^3 = \left(\det \overline{M}\Lambda^{2N-1}\right)^{1/N}, \tag{2.22}$$

where we used the scale matching relation

$$\Lambda_L^{3N} = \det \overline{M}\Lambda^{2N-1}\,. \tag{2.23}$$

We see that this superpotential stabilizes the spectator mesons at the origin of the moduli space. The analysis of baryonic directions is more complicated due to the non-renormalizability of the superpotential terms involving the baryons in the IR. Nevertheless, an analysis of the full superpotential shows that the baryons are also stabilized at the origin. Having established the absence of runaway directions on the moduli space we conclude that this model develops a mass gap.

2.4.3 $G = \mathrm{SU}(N+1)_D$ with Symmetric and Antisymmetric

Our next example involves the identification of G with an $\mathrm{SU}(N+1)_D$ diagonal subgroup of $\mathrm{SU}(N+1)_L \times \mathrm{SU}(N+1)_R$. However, if this diagonal subgroup is generated by $T_D = T_L + T_R$ the matter fields transform in non-chiral representations of $\mathrm{SU}(N+1)_D$ and thus this case

is not of interest to us. Instead, we will consider $\mathrm{SU}(N)_D$ generated by $T_D = T_L - T_R$. The easiest way to do so is to assign $\overline{Q}$ to a fundamental rather than antifundamental representation of $\mathrm{SU}(N+1)_R$. With this charge assignment, the mesons $\mathcal{M}$ transform as a sum of symmetric and antisymmetric representations of G while both baryons and anti-baryons transform in anti-fundamental representation. This implies that the spectator field $\overline{M}$ decomposes as $\overline{A}$ and $\overline{S}$, while both B and $\overline{B}$ transform as fundamentals of $\mathrm{SU}(N+1)_D$. The matter content of this model is given in Table 2.5. The deformation superpotential (2.21) takes the form

$$\mathscr{W} = \bar{A}\mathcal{A} + \overline{S}\mathcal{S} + \overline{B}\mathcal{B} + B\overline{\mathcal{B}} \tag{2.24}$$

The non-perturbative dynamics of the model remains unchanged and vacuum is found at the origin of the moduli space.

	$\mathrm{SU}(N)$	$\mathrm{SU}(N+1)_D$	$U(1)_B$
Q_i	$\square$	$\square$	1
$\overline{Q}_i$	$\overline{\square}$	$\square$	-1
$\mathcal{M} = \mathcal{A} + \mathcal{S}$	$\mathbf{1}$	$\square\square \oplus \begin{smallmatrix}\square\\\square\end{smallmatrix}$	0
$\mathcal{B}$	$\mathbf{1}$	$\overline{\square}$	N
$\overline{\mathcal{B}}$	$\mathbf{1}$	$\overline{\square}$	$-N$
$\overline{M} = \overline{A} + \overline{S}$	$\mathbf{1}$	$\overline{\square\square} \oplus \begin{smallmatrix}\overline{\square}\\\overline{\square}\end{smallmatrix}$	0
$\overline{B}$	$\mathbf{1}$	$\square$	$-N$
B	$\mathbf{1}$	$\square$	N

Table 2.5: Field content of the $\mathrm{SU}(N)$ model with $\mathrm{SU}(F)_D$ flavor symmetry

Simply by choosing a different chiral symmetry group G and selecting a desirable embedding of this group in the maximal global symmetry of s-confining $\mathrm{SU}(N)$ we have constructed a model with one chiral symmetric and one chiral antisymmetric representation in the UV which is fully gapped in the IR.

2.4.4 Antisymmetric $\leftrightarrow$ Symmetric Flows

The early studies of the chirality flows [90, 114] aimed at generating composite chiral matter in the IR while the recent work [107, 116] was driven by an interest in generating mass gaps in chirally symmetric vacua. In this section, we will illustrate that these two types of models are simply extreme examples of a more general class of chiral theories where the chirality structure changes under the RG flow. Indeed, we have already used the fact that the choice of spectators necessary to cancel G^3 anomalies is not unique. To generate the mass gap we chose the spectators in representations of G conjugate to the representations of the composites of the strong dynamics. On the other hand, to generate composite chiral matter in the IR we chose the spectators in the representations of G conjugate to representations of the elementary superfields. But one can mix and match. For example, in the model of section 2.4.3 we can replace $\overline{A}$ with $N-4$ spectators $\bar{q}$ transforming as antifundamentals of $\mathrm{SU}(N+1)_D$. In this case, the UV model contains a chiral symmetric representation of $\mathrm{SU}(N+1)_D$ and $N-4$ vector-like flavors (with all antiquarks of $\mathrm{SU}(N+1)_D$ being spectators and all quarks charged under $\mathrm{SU}(N)$). With this choice of G and the spectator fields the most general tree level superpotential is

$$\mathscr{W} = y\mathcal{A}q\bar{q} + \overline{S}\mathcal{S} + \overline{B}\mathcal{B} + B\overline{\mathcal{B}}\,, \tag{2.25}$$

where we have explicitly included the Yukawa coupling y in the first term. We note in passing that y is naturally small since it arises from a non-renormalizable term in the UV description. Analyzing the non-perturbative dynamics of this model we find that in the IR the composite $\mathcal{S}$ and the spectator $\overline{S}$ pick up a mass and decouple from the low energy physics while the massless matter content contains a single antisymmetric generation. Thus we constructed a more general model of chirality flow where non-perturbative dynamics modifies the chiral structure of the theory in IR instead of simply adding or removing a chiral generation. A reverse flow, from an antisymmetric generation in the UV to a symmetric generation in the

IR, is equally easy to achieve.

2.4.5 Gapping Symmetric Matter

The results of Section 2.4.4 suggest a model-building trick that allows one to gap the symmetric S of the chiral $G = \mathrm{SU}(F)$ symmetry, even if the required model is somewhat baroque. To that end, one needs two s-confining sectors, both with fields charged under G. The first s-confining sector is based on an $\mathrm{SU}(N)$, $N = F - 1$, gauge group whose composites transform as $\mathcal{A}$ and $\mathcal{S}$ of G, while the second sector is based on $\mathrm{SP}(2M)$, $2M = F - 4$, group whose composites transform as $\overline{\mathcal{A}}$. The matter content is given in Table 2.6.

	$\mathrm{SU}(N)$	$\mathrm{SU}(F)_D$	$\mathrm{SP}(2M)$
Q_i	$\square$	$\overline{\square}$	$\mathbf{1}$
$\overline{Q}_i$	$\overline{\square}$	$\overline{\square}$	$\mathbf{1}$
q	$\mathbf{1}$	$\square$	$\square$
$\overline{\mathcal{S}} \oplus \overline{\mathcal{A}}$	$\mathbf{1}$	$\overline{\square\square} \oplus \begin{smallmatrix}\overline{\square}\\ \square\end{smallmatrix}$	$\mathbf{1}$
$\mathcal{B}$	$\mathbf{1}$	$\square$	$\mathbf{1}$
$\overline{\mathcal{B}}$	$\mathbf{1}$	$\square$	$\mathbf{1}$
$\mathcal{A}$	$\mathbf{1}$	$\begin{smallmatrix}\square\\ \square\end{smallmatrix}$	$\mathbf{1}$
S	$\mathbf{1}$	$\square\square$	$\mathbf{1}$
B	$\mathbf{1}$	$\overline{\square}$	$\mathbf{1}$
$\overline{B}$	$\mathbf{1}$	$\overline{\square}$	$\mathbf{1}$

Table 2.6: Field content of the gapped symmetric model. The top section shows elementary fields of the model charged under one of the s-confining sectors, the middle section shows the composites of strong dynamics, and the bottom section shows the spectators charged only under the chiral $G = \mathrm{SU}(F)$ symmetry

The tree level superpotential in terms of composites and the spectators is given by

$$\mathscr{W}_{\text{tree}} = \overline{\mathcal{S}} S + \overline{\mathcal{A}}\mathcal{A} + B\overline{\mathcal{B}} + \overline{B}\mathcal{B}\,. \tag{2.26}$$

A careful analysis of dynamics in regions where either $\mathcal{A}$ or $\overline{\mathcal{A}}$ is large establishes that the model develops a mass gap in the IR.

2.5 A Concluding Poem

I wrote this poem about the general mechanisms of gapping fermions, told from the fermion's perspective:

I was alone, people told me I was destined to be,
Pauli excluded me from the principle, saddened me,
They told me I was light and my state was ground,
Into darkness, with no companion to be found!

Chiral symmetries cursed me to be single,
I'm starting to age, my skin is in wrinkles!
But SUSY saved me! I am at the origin, a deposit
I can confine with a partner and form a composite!

Now the messengers brought a long-awaited,
Mechanism for me, highly rated!
I was no longer on ground, no longer trapped,
I had a mass-partner, and I was gapped.

Chapter 3

Generation flow in field theory and strings

(This section is heavily based on the publication with Saúl Ramos–Sánchez, Michael Ratz, Yuri Shirman and Michael Waterbury) [106]

3.1 Chirality flows from UV to IR

In chapter 2, we outlined a procedure for altering the chiral structure of theories by generating mass gaps without breaking chiral symmetry. However, changing the chiral structure can also result in *increasing* the number of generations: This happens when one or more composite generations appear in the IR. We demonstrate how the evolution from UV to IR can either increase or decrease the generations using the techniques from the previous chapter. We emphasize that the non-perturbative dynamics play a crucial role in modifying the effective number of generations during the process of Renormalization Group (RG) flow. This has significant implications for string model searches, particularly when determining the number of generations in candidate UV completions of the Standard Model (SM).

As in the last chapter, we will concentrate on supersymmetric models both because it is convenient in the context of string model building and because the relevant non-perturbative dynamics are under qualitative and often quantitative control in such theories. As shown by Seiberg [108], non-perturbative effects can have a dramatic impact on gauge theories. In particular, due to confinement and duality, the degrees of freedom appropriate for describing IR physics often differ considerably from the UV degrees of freedom. Throughout this chapter, aiming at preserving the chirality of the SM (or its Grand Unified Theory (GUT) completion), we consider confinement without chiral symmetry breaking (so-called s-confinement [32,33]). Since the low-energy degrees of freedom in these models are composites of the elementary fields, they usually transform in different representations of the unbroken global symmetry. When a subgroup of such global symmetry is identified with a GUT or the SM gauge group, a new, composite, chiral generation may emerge in the IR or, alternatively, an existing chiral generation may become massive. The first of these phenomena was initially used in [90,114] to construct realistic extensions of the minimal supersymmetric Standard Model with some of the third generation quarks and Higgs bosons arising as composites of strong dynamics.

In this approach, which we will refer to as the Nelson–Strassler (NS) mechanism, the RG flow leads to the appearance of light chiral composites in the IR thus increasing the effective number of chiral generations. The NS mechanism may be modified in several fairly obvious ways. For example, some of the composites may acquire masses by mixing with elementary chiral fields, modifying the spectrum of light fields in the IR in nontrivial ways. When all of the composites acquire mass, the model is in the second regime which attracted attention more recently [107]. We will refer to the second phenomenon as the RT mechanism. Here all of the composites of strong dynamics acquire masses by partnering with elementary degrees of freedom and thus reduce the number of effective generations in the IR. As we will argue, these two mechanisms can be continuously connected by introducing mass terms for vector-like elementary fields, which are allowed to mix with the composites. When masses of vector-like fields are small while the mixing between elementary fields and composites is

of order one, the theory flows to the RT limit where all the light fields are elementary. On the other hand, in the limit of large mass the vector-like elementary fields decouple, leaving massless composites behind. In this case, the theory flows to the NS limit where some light fields are composites. By varying the mass terms, one can interpolate between the two limits, and for intermediate values of the mass term some IR degrees of freedom will be partially composite. Furthermore, one has freedom to decouple any number of composites. In general, however, non-perturbative dynamics affects RG flow and modifies the effective number of chiral generations in the IR. We will refer to these phenomena as *generation flow*.

It is then natural to ask whether generation flow can occur in scenarios where the number of generations is predicted from other data. This is particularly relevant for string model building (cf. e.g. [61] for a review), where one obtains the SM generations from string compactifications. We will argue that generation flow indeed occurs in some globally consistent string models. In these constructions, the true number of generations in the IR description can differ from the tree-level value that one obtains at the compactification scale. Hence, a search for 3-generation models in string theory has to go beyond the tree-level analysis.

The organization is as follows. In Section 3.2, we will review the RT mechanism of gapped chiral fermions. In Section 3.3, we construct models exhibiting generation flow towards a 3-generation theory with (a GUT completion of) the SM gauge group in the IR. Our first example is a $4 \rightsquigarrow 3$ model based on the RT mechanism where all the IR degrees of freedom are elementary. We then construct a generalization of the $4 \rightsquigarrow 3$ model where some of the third generation fields are composite. We point out that our construction is analogous to the NS mechanism [90, 114]. This motivates us to build a $2 \rightsquigarrow 3$ model with an upward generation flow. Furthermore, we discuss the stability of the chirally symmetric vacua in s-confining models under the deformations which induce generation flow. While such deformations may generally destabilize the vacua by non-perturbative dynamics (see [112] for a more detailed discussion), we argue that the chirally symmetric vacua survive in our models. In Section 3.4, we collect evidence for the existence of string models exhibiting generation flow by presenting

explicit examples.

3.2 s-confinement and Gapped Chiral Fermions

We begin by briefly reviewing dynamics of supersymmetric gapped fermion models introduced in [107]. In the following we will take the approach of [112] to building models of chiral gapped fermions. This approach starts with SUSY QCD models that exhibit confinement without chiral symmetry breaking on smooth moduli space [108].* For our purposes it is convenient to restrict attention to s-confinement in $\mathrm{SU}(2)_s$ SUSY QCD with six chiral doublet superfields and thus SU(6) chiral global symmetry. We review the dynamics of this model in the subsection 3.2.1. In the subsection 3.2.2, we discuss the deformation of the SUSY QCD required to arrive at mass gap models of [107].

3.2.1 s-confining $\mathrm{SU}(2)_s$ model

The model outlined above possesses $\mathrm{SU}(6)\times\mathrm{SU}(2)_s$ symmetry, where SU(6) is a chiral global symmetry while $\mathrm{SU}(2)_s$ is a strongly interacting s-confining gauge group. For future convenience we will assign quark superfields to $(\overline{\mathbf{6}},\mathbf{2})$ representation of the symmetry group. The theory possesses a set of classical D-flat directions which can be parameterized either in terms of squark VEVs or in terms of gauge invariant mesons which are classically defined as $M_{ij}\sim Q_iQ_j/\Lambda$, where we suppressed contraction of $\mathrm{SU}(2)_s$-color indices and the dynamical scale of the quantum theory Λ is introduced on dimensional grounds. The mesons M transform in the conjugate antisymmetric representation of the global SU(6) symmetry $\overline{\mathbf{15}}$. However, since quark VEVs satisfy a set of algebraic identities, not all meson VEVs are

*This dynamics is usually referred to as s-confinement. See [33] for a complete classification of such theories.

independent. These classical constraints imply a set of relations between the mesons,

$$\varepsilon^{i_1 \ldots i_6} M_{i_3 i_4} M_{i_5 i_6} = 0 \,. \tag{3.1}$$

One may implement these constraints in the composite description of the theory by postulating a dynamical superpotential

$$\mathscr{W}_s = \varepsilon^{i_1 \ldots i_6} M_{i_1 i_2} M_{i_3 i_4} M_{i_5 i_6} \equiv \mathrm{Pf}(M) \,. \tag{3.2}$$

The moduli space parameterized by mesons M together with the superpotential (3.2) coincides with the classical moduli space of the theory parameterized by quark VEVs satisfying D-flatness conditions. It was shown in [108] that the classical moduli space of vacua remains unmodified quantum mechanically and the IR physics is described in terms of weakly interacting mesons with the superpotential (3.2). While the chiral global symmetry of this model is broken at a generic point on the moduli space, the chiral symmetry remains unbroken at the origin where the theory exhibits confinement without chiral symmetry breaking. This is precisely the vacuum we are interested in.

3.2.2 Mass Gap Model

For phenomenological purposes we are interested in gauging SU(6) global symmetry of the s-confining model discussed in the previous subsection (more precisely we are interested in gauging a subgroup of SU(6), such as a GUT SU(5) or the SM group $\mathrm{SU}(3) \times \mathrm{SU}(2) \times \mathrm{U}(1)$). To this end, one must introduce a set of spectator fields charged under SU(6) but not $\mathrm{SU}(2)_s$ (so that the s-confining dynamics remains unaffected) to ensure a cancellation of the cubic SU(6) anomaly. This can be achieved, for example, by introducing spectators that transform in representations of SU(6) conjugate to those of elementary fields, i.e. by adding two spectators with quantum numbers given by $(\mathbf{6}, \mathbf{1})$. Alternatively, one can introduce

a single spectator S in an SU(6) representation conjugate to the one of the mesons, i.e. transforming as $(\mathbf{15}, \mathbf{1})$. In the former case, the theory remains chiral both in the UV and IR. This is because $\mathrm{SU}(2)_s$ is not yet confined in the UV and the matter fields transform in chiral representations of the full $\mathrm{SU}(6) \times \mathrm{SU}(2)_s$ symmetry, while the representations of IR degrees of freedom are chiral under SU(6). However, in the latter case, the chiral properties of the model change as the theory flows from the UV to the IR. While the UV theory is clearly chiral, the IR degrees of freedom, the mesons M and spectators S, transform in conjugate representations and thus form a single vector-like representation. By choosing to cancel anomalies with the spectator S in the antisymmetric representation, we will be able to construct a model that flows from a gapless, chiral phase in the UV to a gapped phase in the IR.

Since the matter content in the IR is non-chiral, a mass term, SM, is allowed in the IR superpotential. In terms of the UV degrees of freedom, this mass term corresponds to a marginal operator, SQ^2. Thus, we deform the s-confining model by a tree-level superpotential

$$\mathscr{W} = ySQ^2 = c\Lambda SM\,, \tag{3.3}$$

where the numerical coefficient c represents both an arbitrary Yukawa coupling y of the UV theory and the fact that the mass scale generated by confinement is not directly calculable.

At this point one might be tempted to conclude that a mass gap develops in the chirally symmetric vacuum at the origin, while the rest of the moduli space is lifted by the equations of motion for S and M. However, while ultimately correct, this conclusion is somewhat premature. Indeed, while lifting $\mathrm{SU}(2)_s$ D-flat directions, the deformation (3.3) introduces new classical flat directions, those parameterized by $\mathrm{SU}(2)_s$ singlets S. Since any VEVs for S would break the chiral symmetry, it is important to verify that the non-perturbative dynamical superpotential (3.2) does not destabilize these directions. A careful analysis [112]

of the full superpotential in (3.2) and (3.3) demonstrates that $\mathrm{SU}(2)_s$ dynamics generates an effective superpotential for gauge singlets S stabilizing them at the origin.[†] While referring the reader to [112] for the full analysis, we present a simple argument here. Consider the theory at large S where all quark superfields become heavy. In this region of the moduli space the low-energy physics is described in terms of a pure SYM $\mathrm{SU}(2)_s$ theory with dynamical scale given by $\Lambda_L^6 = \mathrm{Pf}(S)\,\Lambda^3$. The dynamics of the low-energy SYM in turn generates a gaugino condensate implying the existence of an effective superpotential

$$\mathscr{W}_{\rm dyn} = \Lambda_L^3 = \left(\Lambda^3\ \mathrm{Pf}(S)\right)^{1/2}. \tag{3.4}$$

It is easy to see that this superpotential stabilizes S near the origin.

The main lesson we learn from this example is a possibility that the RG flow may change the chiral properties of the theory and, in particular, may change the number of chiral generations. Here we define a chiral generation as a field transforming in an antisymmetric representation of the chiral symmetry accompanied by an appropriate number of fields in an antifundamental representation as required by anomaly cancellation conditions. Then the net number of generations is given by a difference between number of fields in an antisymmetric representation and in a conjugate antisymmetric representation, $\nu = n_{\square} - n_{\bar{\square}}$. For example, in our example with SU(6) chiral symmetry the number of generations is given by $n_{\mathbf{15}} - n_{\overline{\mathbf{15}}}$. This definition is chosen such that it can be used throughout this study, and coincides with what one calls a generation in SU(5) GUTs. From the SU(6) perspective, our UV model is a one-generation model containing an antisymmetric, $\mathbf{15}$, and two antifundamental, $\overline{\mathbf{6}}$, of SU(6). On the other hand, the IR theory has no massless chiral superfields even while the chiral symmetry remains unbroken.

While the construction of [107] decreases the number of chiral generations in the IR, we will

[†]We stress that this conclusion is model dependent, and there exist models where the $S = 0$ vacuum at the origin is destabilized, resulting in chiral symmetry breaking.

show in the following section that non-perturbative dynamics may also lead to an increase in the number of chiral generations. As we will see, the existence of generation flow offers immense opportunities for model building both in field theory (Section 3.3) and string theory (Section 3.4).

3.3 Generation Flows in GUTs

The supersymmetric gapped fermion model reviewed in the previous section is based on an $\mathrm{SU}(2)_s$ s-confining theory with SU(6) global symmetry. Generalizations to s-confining $\mathrm{SP}(2N)$ with $\mathrm{SU}(2N+4)$ global symmetry are straightforward [107].[‡] However, for phenomenological purposes one is interested in similar models with SU(5) or $\mathrm{SU}(3)\times\mathrm{SU}(2)\times\mathrm{U}(1)$ global symmetry which can then be identified with the GUT or the SM gauge group. As shown in [107], this can be easily achieved simply by considering the model of Section 3.2.2 and identifying GUT or SM gauge group with an appropriate subgroup of SU(6).

For example, to construct a one-generation $\mathrm{SU}(5)\times\mathrm{SU}(2)_s$ theory which behaves as a pure SYM SU(5) in the IR, one decomposes elementary fields of the model under SU(5) as follows

$$S:(\mathbf{15},\mathbf{1})\to T:(\mathbf{10},\mathbf{1})\oplus F:(\mathbf{5},\mathbf{1})\,,\quad Q:(\overline{\mathbf{6}},\mathbf{2})\to \overline{F}':(\overline{\mathbf{5}},\mathbf{2})\oplus\phi:(\mathbf{1},\mathbf{2})\,. \tag{3.5}$$

The tree-level superpotential (3.3) and dynamical superpotential (3.2) can be easily written in the SU(5) language. One can verify that the UV description corresponds to a one-generation model complemented by a single vector-like flavor in a fundamental representation. As we learned in Section 3.2, the s-confining dynamics leads to a unique ground state with an unbroken chiral symmetry and no light matter fields.

[‡]See also discussion in [112].

We are now ready to generalize the mass gap construction of RT [107] to obtain models where the number of chiral generations is changed through renormalization group flow but remains nonzero both in the UV and the IR. As we will see shortly, the RG flow may lead both to an increase and a decrease in the effective number of chiral generations. The latter can be achieved in two ways. In the first approach, as in the model of Section 3.2, some of the chiral elementary fields acquire masses by partnering with the chiral composites generated by confining dynamics. As a result, all the massless degrees of freedom in the IR are elementary fields of the theory. Just like in the model of Section 3.2, the chirally symmetric vacuum is a unique ground state of this theory. The second approach is reminiscent of the construction first introduced in [90, 114]. In this approach, some of the massless fields in the IR are composites even as other composites may become massive. Generically, models in this class retain the quantum moduli space and only one vacuum on this moduli space is chirally symmetric. Since IR degrees of freedom, including the massless composites, are to be identified with the SM multiplets, the motion along this moduli space is equivalent to motion along D-flat directions of a GUT or the SM. Note that the mechanism utilized in the second approach may also lead to an increase in the effective number of generations.

3.3.1 $4 \rightsquigarrow 3$ Generation Flow

We can now detail our general observations by building an explicit model of downward generation flow. Let us start with a more straightforward example, where the number of chiral generations decreases in the IR while all the composites are heavy. In particular, we construct a $4 \rightsquigarrow 3$ model, i.e. a model containing 4 generations in the UV and 3 generations in the IR. The matter fields of the model and their quantum numbers are presented in Table 3.1a. Note that this matter content comprises the fields appearing in (3.5) complemented by three chiral flavors of SU(5) i.e. three copies of $T \oplus \overline{F}$. Thus, this is a four-generation model. It is easy to see that $\mathrm{SU}(2)_s$ dynamics is not affected by the introduction of additional chiral

#	irrep	label
4	$(\mathbf{10},\mathbf{1})$	T
2	$(\overline{\mathbf{5}},\mathbf{1})$	$\overline{F}$
1	$(\overline{\mathbf{5}},\mathbf{2})$	$\overline{F}'$
1	$(\mathbf{1},\mathbf{2})$	ϕ
1	$(\mathbf{5},\mathbf{1})$	F
1	$(\overline{\mathbf{5}},\mathbf{1})$	$\overline{F}$

(a) Unconfined spectrum.

#	irrep	label
4	$(\mathbf{10},\mathbf{1})$	T
4	$(\overline{\mathbf{5}},\mathbf{1})$	$\overline{F},\overline{\mathcal{F}}$
1	$(\overline{\mathbf{10}},\mathbf{1})$	$\overline{\mathcal{T}}$
1	$(\mathbf{5},\mathbf{1})$	F

(b) Confined spectrum.

Table 3.1: Summary of the SU(5) $\times$ SU(2)$_s$ quantum numbers of the chiral superfield content of the 4$\rightsquigarrow$3 model. The vector-like pair at the bottom of Table 3.1a can be decoupled, resulting in a separate 4$\rightsquigarrow$3 model.

multiplets as long as one linear combination of the T_i's has the Yukawa coupling with $\overline{F}'$ and ϕ that is implied by the superpotential (3.3). Indeed, at low energies SU(2)$_s$ charged fields confine into $\overline{\mathcal{T}} \sim \overline{F}'\overline{F}'/\Lambda$ and $\overline{\mathcal{F}} \sim \overline{F}'\phi/\Lambda$. The transformation properties of the IR degrees of freedom are given in Table 3.1b. Finally, in the IR the superpotential (3.3) behaves like a mass term pairing composites $\overline{\mathcal{F}}$ and $\overline{\mathcal{T}}$ with F and one copy of T, respectively. Repeating the analysis of Section 3.2.2 one concludes that the classical flat directions parameterized by F and T are stabilized non-perturbatively.

Let us consider a generalization by noting that the symmetries of the model allow a mass term for the vector-like pair $F \oplus \overline{F}$. With this mass term, the full UV superpotential becomes

$$\mathscr{W} = y_1 T\overline{F}'\overline{F}' + y_2 F\overline{F}'\phi + mF\overline{F}\,. \tag{3.6}$$

Note that the additional mass term and $y_1 \neq y_2$ explicitly break the SU(6) symmetry. Neither F nor $\overline{F}$ are charged under SU(2)$_s$, thus the confined spectrum of the model (Table 3.1b) does not change. In the IR, the superpotential becomes

$$\mathscr{W} = \overline{\mathcal{T}}\,\overline{\mathcal{T}}\,\overline{\mathcal{F}} + c_1\Lambda T\overline{\mathcal{T}} + c_2\Lambda F\overline{\mathcal{F}} + mF\overline{F}\,, \tag{3.7}$$

where the first term is the s-confining superpotential Equation (3.2). A simple analysis shows that in the presence of the mass term the model possesses a quantum moduli space satisfying the condition

$$c_2\Lambda\overline{\mathcal{F}} + m\overline{F} = 0\,. \tag{3.8}$$

While at a generic point on the moduli space the chiral SU(5) symmetry is broken, the s-confining vacuum where one generation acquires a mass survives at $\overline{\mathcal{F}} = \overline{F} = 0$. This leaves three light generations, two made up entirely of elementary fields and another where the $\overline{\mathbf{5}}$ is made up of a linear combination of $\overline{\mathcal{F}}$ and $\overline{F}$. This lays out two interesting limits. In the limit $m \to 0$, the light generations are entirely composed of elementary fields, $\overline{\mathcal{F}} = 0$, and the chirally symmetric vacuum is stabilized as in Section 3.2.2. We refer to this as the RT limit because all composite fields decouple. In the limit $m \to \infty$, one of the three light generations has a composite $\overline{\mathbf{5}}$. We refer to this limit as the NS limit due to the appearance of light composite fields. At finite mass, there is a flat direction which can be parameterized by $\overline{\mathcal{F}}$. For the purposes of phenomenology, $\overline{\mathcal{F}}$ would play the role of a SM multiplet; motion along the moduli space of this model corresponds to motion along D-flat directions of a GUT (or the SM).

3.3.2 $2\rightsquigarrow 3$ Generation Flow

The NS limit of the model discussed above resulted in a theory with a composite $\overline{\mathbf{5}}$ while the number of $\mathbf{10}$'s (i.e. number of generations) was smaller in the IR. On the other hand, original models of [90, 114] had a composite $\mathbf{10}$ in the IR thus increasing the number of generations. That construction can be interpreted as an upward generation flow. Let us discuss a variation of that model where the starting point of RG flow contains two chiral generations while the end point in the IR has three chiral generations, i.e. a $2\rightsquigarrow 3$ model.

#	irrep	label
2	$(\mathbf{10},\mathbf{1})$	T
4	$(\overline{\mathbf{5}},\mathbf{1})$	$\overline{F}$
1	$(\mathbf{5},\mathbf{2})$	F'
1	$(\mathbf{1},\mathbf{2})$	ϕ

(a) Unconfined spectrum.

#	irrep	label
3	$(\mathbf{10},\mathbf{1})$	$T,\mathcal{T}$
3	$(\overline{\mathbf{5}},\mathbf{1})$	$\overline{F}$
1	$(\overline{\mathbf{5}},\mathbf{1})$	$\overline{F}$
1	$(\mathbf{5},\mathbf{1})$	$\mathcal{F}$

(b) Confined spectrum.

Table 3.2: Summary of the $\mathrm{SU}(5)\times\mathrm{SU}(2)_s$ quantum numbers of the chiral superfield content of the $2\rightsquigarrow 3$ model.

Once again we consider a model with the symmetry group $\mathrm{SU}(5)\times\mathrm{SU}(2)_s$, whose matter content and charges are given in Table 3.2a. The tree-level superpotential in terms of the UV degrees of freedom is

$$\mathscr{W} = y\overline{F}F'\phi\,. \tag{3.9}$$

When the non-perturbative dynamics is included, the IR superpotential becomes

$$\mathscr{W} = \mathcal{T}\mathcal{T}\mathcal{F} + c\Lambda\overline{F}\mathcal{F}\,, \tag{3.10}$$

where $\mathcal{T}\sim F'F'/\Lambda$ and $\mathcal{F}\sim F'\phi/\Lambda$.

It is convenient to analyze the behavior of this superpotential by going along a flat direction parameterized by $\overline{F}$. Without loss of generality we can assume that the VEV of $\overline{F}$ lives in a single component, say $\overline{F}_5$. At large VEV, the global symmetry is broken from SU(5) to SU(4), and one pair of doublets, the one corresponding to the $\mathcal{F}_5$ meson, becomes heavy and can be integrated out. Along this flat direction the superpotential becomes

$$\mathscr{W} = \mathcal{F}_5(\mathrm{Pf}'\,\mathcal{T} + \overline{F}_5)\,, \tag{3.11}$$

where prime on the Pfaffian indicates that it is taken only over the light mesons comprising a **6**-plet of the remaining SU(4) symmetry. Note that at this stage $\mathcal{F}_5$ is not a dynamical

field since it is a meson made out of heavy doublets. At the same time, the $\overline{F}_5$ VEV remains arbitrary albeit related to the $\mathcal{T}$ VEVs by the $\mathcal{F}_5$ equation of motion,

$$\mathrm{Pf}'\,\mathcal{T} + \overline{F}_5 = 0\,. \tag{3.12}$$

Upon a careful inspection of (3.11) and (3.12), one notices that they correspond to the superpotential and one of the equations of motion of a four-doublet theory with a deformed moduli space, a dynamical scale $\Lambda_L^6 = \overline{F}_5\Lambda^5$, and the meson $\mathcal{F}_5$ playing a role of Lagrange multiplier. We see that for each nonvanishing value of $\overline{F}_5$ the effective theory possesses a quantum deformed moduli space, i.e. it exhibits confinement with chiral symmetry breaking. Furthermore, the scale of chiral symmetry breaking is parameterized by $\overline{F}_5$. While the effective description in terms of four-doublet theory is only valid at large $\overline{F}_5$, the solution of the $\mathcal{F}_5$ equation of motion is valid everywhere on the quantum moduli space up to a SU(5) symmetry transformation. In particular, the chirally symmetric vacuum $\mathrm{Pf}'\,\mathcal{T} = \overline{F}_5 = 0$ belongs to the quantum moduli space.

Note that the models introduced in this section differ in their quantum moduli spaces and their low-energy spectra. In the RT limit of the $4\rightsquigarrow 3$ model, there is a unique, s-confining vacuum. All composite degrees of freedom become massive via the RT mechanism, and there are three light generations made out of the elementary fields. In the $2\rightsquigarrow 3$ model and the NS limit of the $4\rightsquigarrow 3$ model, there remains a quantum moduli space of vacua parameterized by the VEV of $\overline{\mathcal{F}}$ (or equivalently $\overline{F}$), respectively, which includes the chirally symmetric vacuum. In the $2\rightsquigarrow 3$ model, one of the three light generations contains a composite $\mathbf{10}$, while at finite mass, the $4\rightsquigarrow 3$ model has a $\overline{\mathbf{5}}$ which is partially composite and partially elementary.

In the following sections, we will show how these models can arise naturally in string model building, providing examples of phenomenologically viable string models which would have previously been ruled out by the tree-level analysis of the models.

3.4 Generation Flow in String Models

Given the possibility of generation flow discussed in Sections 3.2 and 3.3, we will now turn our attention to string model building. Why can generation flow be relevant for string models? In string phenomenology, one tries to connect string theory to the real world (cf. e.g. [61]). In practice, this often amounts to searching for a string compactification which reproduces the SM in its low-energy limit. When constructing a string model, one chooses a framework, such as one of the perturbative string theories, and compactifies it down to four dimensions. The step of compactification consists of making an assumption on the geometry of compact dimensions (in principle one also must show that the emerging setup is stable, i.e. string moduli describing the size and shape of compact space are stabilized). However, attempts to build realistic models often fail already at an earlier stage because the zero-modes do not comprise the SM matter. This could mean that one has chiral exotics, or just not the right number of generations. It is the latter possibility where generation flow, as discussed in Section 3.3, can be important.[§] In practice, when determining the number of generations, one looks at the tree-level predictions. However, as discussed in Sections 3.2 and 3.3, the number of generations obtained this way may differ from the true number of chiral generations in the low-energy effective theory.[¶] It is therefore interesting to study the question to which extent models of the type discussed earlier can be obtained from string theory.

It is not our purpose to construct a fully realistic model exhibiting generation flow. Rather, we will collect evidence for the existence of such models. To keep our discussion simple, and in order to relate our findings to Section 3.3, we will look for SU(5) models rather than

[§]It is conceivable that more generally chiral exotics can be removed along the lines of Section 3.2 (cf. [39] for an example). It will be interesting to work out the detailed conditions for this to happen.

[¶]It is known that chirality-changing phase transitions can occur in string compactifications [6, 47, 66]. In this work we focus on generation flow that can be understood in terms of field-theoretic supersymmetric gauge dynamics with an s-confining $\mathrm{SU}(2)_s$ as in Sections 3.2 and 3.3. It will be interesting to see whether there is a deeper relation between these phenomena.

models with SM gauge group. However, we expect that the results carry over to models with the SM gauge group after compactification.

3.4.1 Model Scans

In what follows, we focus on orbifold compactifications of the $(E_8 \times E_8')$ heterotic string [44,45], which can be efficiently constructed with the `orbifolder` [94]. We will collect evidence for the existence of globally consistent string compactifications that have either two or four generations of SM matter at tree level, but in fact have three generations in their low-energy effective description. That is, we will present evidence for the existence of stringy versions of the $4 \rightsquigarrow 3$ and $2 \rightsquigarrow 3$ models discussed in Section 3.3.

The `orbifolder` allows us to compute a 4D model from certain input data, which comprises the geometry of the orbifold and the so-called gauge embedding. The latter essentially describes how the geometric operations of the 6D space-like compact dimensions act on the $E_8 \times E_8'$ lattice. This determines not only what the residual gauge symmetry of the model is but also the spectrum. In more detail, the `orbifolder` provides us with the continuous and discrete gauge symmetries after compactification as well as the chiral spectrum of the model.

By using the `orbifolder`, we obtained a large sample of supersymmetric heterotic orbifold models with the following properties:

- orbifold geometry $\mathbb{Z}_2 \times \mathbb{Z}_4$ (1,1) (see [52] for the notation, and [87] for details of the geometry);
- 4D gauge group $\mathcal{G}_{4D} \supset SU(5) \times SU(2)_s$ (where we labeled the second factor "s" to indicate that this SU(2) plays the same role as in our earlier discussion in Sections 3.2 and 3.3);

- the SU(5) and $SU(2)_s$ gauge groups emerge each from a different E_8 factor of the original heterotic string;
- a net number of n SU(5) GUT generations, with no representation $(\mathbf{10}, \mathbf{2})$ *l*east one representation $(\overline{\mathbf{5}}, \mathbf{2})$ or $(\mathbf{5}, \mathbf{2})$;
- at least one "flavon" field transforming as $(\mathbf{1}, \mathbf{2})$; other fields of this type could in principle be decoupled from low energies;
- a (large) number of $SU(5) \times SU(2)_s$ singlets;
- additional non-Abelian gauge factors under which the SU(5) charged fields are singlets; and
- additional U(1) factors which can be broken along D-flat directions without breaking $SU(5) \times SU(2)_s$.

Our scan yielded several models in which s-confinement can change the number of chiral representations.

3.4.2 Models

Rather than providing the reader with an extensive survey, we focus on two sample models defined in the Appendix. In more detail, we discuss

- a 4$\rightsquigarrow$3 model (cf. Table 3.3a) in which the 4^{th} chiral generation acquires a mass and decouples through, and
- a 2$\rightsquigarrow$3 model (cf. Table 3.3b) in which the 3^{rd} chiral generation emerges from states that are vector-like under SU(5) through a variant of the RT effect, in which a chiral $\mathbf{10} \oplus \overline{\mathbf{5}}$ arises as a composite of $(\mathbf{5}, \mathbf{2}) \oplus (\mathbf{1}, \mathbf{2}) \oplus 2(\overline{\mathbf{5}}, \mathbf{1})$

4⇝3 model		
#	irrep	label
4	$(\mathbf{10},\mathbf{1})$	T
4	$(\overline{\mathbf{5}},\mathbf{1})$	F
7	$(\overline{\mathbf{5}},\mathbf{1})$	F
9	$(\mathbf{5},\mathbf{1})$	$\overline{F}$
1	$(\overline{\mathbf{5}},\mathbf{2})$	$\overline{F}'$
170	$(\mathbf{1},\mathbf{1})$	N
27	$(\mathbf{1},\mathbf{2})$	ϕ

(a) The first block contains four chiral generations of SU(5) matter.

2⇝3 model		
#	irrep	label
2	$(\mathbf{10},\mathbf{1})$	T
2	$(\overline{\mathbf{5}},\mathbf{1})$	F
10	$(\overline{\mathbf{5}},\mathbf{1})$	F
8	$(\mathbf{5},\mathbf{1})$	$\overline{F}$
1	$(\mathbf{5},\mathbf{2})$	F'
240	$(\mathbf{1},\mathbf{1})$	N
41	$(\mathbf{1},\mathbf{2})$	ϕ

(b) The first block represents two chiral families of an SU(5) GUT.

Table 3.3: Summary of the $\mathrm{SU}(5) \times \mathrm{SU}(2)_s$ quantum numbers of the (left-chiral) massless matter spectra of heterotic orbifold models with (a) 4⇝3 and (b) 2⇝3 SU(5) generation flow. These models have (a) four and (b) two chiral generations at tree level, respectively, but three chiral generations in the low-energy effective description due to $\mathrm{SU}(2)_s$ strong dynamics. The second (third) block of each table consists of states that are vector-like (invariant) under SU(5).

Both models have the virtue that the SU(5) and $\mathrm{SU}(2)_s$ factors come from different E_8's. Consequently, $\mathrm{SU}(2)_s$ can naturally be more strongly coupled than SU(5) (cf. e.g. [60]).

A Stringy 4⇝3 Model

The model defined by the parameters provided in Equation (A.1.1) results in the 4D gauge group $\mathcal{G}_{\mathrm{4D}} = \mathrm{SU}(5) \times \mathrm{SU}(2)_s \times [\mathrm{SU}(2)^5 \times \mathrm{U}(1)^6]$. The gauge factors in the brackets can be broken along D-flat directions. Since the Lagrange density is invariant under complexified gauge transformation, we can infer that nontrivial solutions to the F-term equations preserve supersymmetry [19, 85]. We are then left with $\mathcal{G}_{\mathrm{unbroken}} = \mathrm{SU}(5) \times \mathrm{SU}(2)_s$.

Before discussing the 4⇝3 properties of this model, let us comment on the possibility to break $\mathrm{SU}(2)_s$ along D-flat directions. In this case, we will obtain a vacuum with 4 generations of an SU(5) GUT, i.e. 4 copies of $\mathbf{10} \oplus \overline{\mathbf{5}}$ while the other states are now vector-like and pick up masses proportional to the VEVs of the SU(5) singlets that got switched on. According to the usual string phenomenology practices, we would thus label this model an unrealistic

4-generation model, not worth being considered further.

On the other hand, if we leave $\mathrm{SU}(2)_s$ unbroken, in a generic vacuum we obtain in an intermediate step a model with 4 copies of $(\mathbf{10},\mathbf{1})$, 2 copies of $\left(\overline{\mathbf{5}},\mathbf{1}\right)$, a $\left(\overline{\mathbf{5}},\mathbf{2}\right)$ and a $(\mathbf{1},\mathbf{2})$. Since string selection rules do not forbid the corresponding couplings, the other states of Table 3.3a acquire masses proportional to the VEVs of the $\mathrm{SU}(5)\times\mathrm{SU}(2)_s$ singlets. Conceivably, there also exist special string vacua that can allow for an extra massless vector-like pair $(\mathbf{5},\mathbf{1})\oplus(\overline{\mathbf{5}},\mathbf{1})$. This brings us to either of the 4$\rightsquigarrow$3 models discussed in Section 3.3, and summarized in Table 3.1a. As we have seen there, due to the $\mathrm{SU}(2)_s$ strong dynamics, $\left(\overline{\mathbf{5}},\mathbf{2}\right)$ and $(\mathbf{1},\mathbf{2})$ condense together to build a $\overline{\mathbf{5}}$ and condensates of $\left(\overline{\mathbf{5}},\mathbf{2}\right)$ yield an SU(5) antigeneration $\overline{\mathbf{10}}$. Since there are no string selection rules prohibiting the couplings, we thus expect this antigeneration to pair up with a linear combination of the 4 generations, and we are left with a 3-generation model at low energies.

An important condition for the strong $\mathrm{SU}(2)_s$ dynamics to play out as described is that $\mathrm{SU}(2)_s$ is much more strongly coupled than SU(5). Since these two gauge factors originate from different E_8's, it is plausible that this happens [46, 60, 113]. However, a detailed computation of the string thresholds is beyond the scope of this study.

A Stringy 2$\rightsquigarrow$3 Model

The model defined by the parameters provided in Equation (A.1.2) results in the 4D gauge group $\mathcal{G}_{4\mathrm{D}} = \mathrm{SU}(5)\times\mathrm{SU}(2)_s\times[\mathrm{SU}(2)^2\times\mathrm{U}(1)^9]$. As in the previous model, the gauge factors in parentheses can be spontaneously broken along D-flat directions while preserving supersymmetry. The corresponding massless spectrum after compactification is summarized in Table 3.3b, where we only display the quantum numbers with respect to $\mathrm{SU}(5)\times\mathrm{SU}(2)_s$. After switching on the VEVs of $\mathrm{SU}(5)\times\mathrm{SU}(2)_s$ singlets, we are left with 2 copies of $(\mathbf{10},\mathbf{1})$, 4 copies of $(\overline{\mathbf{5}},\mathbf{1})$, and 1 instance of $(\mathbf{5},\mathbf{2})$ and $(\mathbf{1},\mathbf{2})$, reproducing the spectrum of the 2$\rightsquigarrow$3

model presented in Table 3.2a.

If we also break $\mathrm{SU}(2)_s$ along D-flat directions, we obtain a vacuum with an SU(5) GUT symmetry and two generations of $\mathbf{10} \oplus \overline{\mathbf{5}}$. In the traditional approach, we would thus label the model as an unrealistic 2-generation model that is to be discarded.

However, this conclusion changes if we look at vacua where $\mathrm{SU}(2)_s$ confines. In this case, according to our discussion of the $2 \rightsquigarrow 3$ model in Section 3.3, we can obtain a third generation from $\mathrm{SU}(2)_s$ strong dynamics. In particular, the $(\mathbf{5}, \mathbf{2})$ builds a condensate that behaves as the $\mathbf{10}$-plet of a third generation of an SU(5) GUT. This means that this model admits 3-generation vacua and cannot be ruled out immediately.

Chapter 4

Metaplectic Flavor Symmetries from Magnetized Tori

(This section is heavily based on the publication with Yahya Almumin, Mu-Chun Chen, Michael Ratz, Saúl Ramos–Sánchez and Víctor Knapp-Pérez) [5]

4.1 Modular Flavor Symmetries

As discussed in section 1.2 of the introduction, we know that the SM of particle physics is an effective theory. This means that it has many parameters that have to be adjusted by hand to fit data. The bulk of these parameters resides in the flavor sector, i.e. concerns the fermion masses, mixing angles and $\mathcal{CP}$ phases. Any UV completion of the SM will have to explain these parameters. Turning this around, one may hope to get more insights on the UV completion by constructing a working theory of flavor. In chapters 2 and 3, we have observed that the number of generations is not an invariant notion across RG flows, and non-perturbative dynamics plays a significant role, particularly in the search for string models. When it comes to building string models, obtaining the correct number of chiral

fermions and generations is a challenging task. In this chapter, we explore a framework where modular symmetries present in the extra two dimensions of a torus not only result in chiral fermions, but also allow the magnetic flux on the torus to act as a parameter for determining the number of generations.

Modular symmetries have been at the forefront of string-inspired model building. Recently, a new approach to address the flavor problem has been put forward [49]: Yukawa couplings could be modular forms. There are two main ways in which this proposal has been utilized:

1. *symmetry based (SB)*, i.e. impose the modular flavor symmetry to construct the Lagrange density [8, 31, 35, 40–43, 76, 77, 79, 82, 84, 95, 99, 101, 123], and

2. *torus based (TB)*, in which one derives the symmetries from an underlying torus or related setup [13–15, 58, 68, 70–74, 78, 92, 98].

Both strategies have strong points and challenges. In the SB approach, very good fits to data have been achieved. However, this is, in part, possible because one can postulate the symmetry and other data like modular weights and representations at will. Apart from the arbitrariness of the flavor group and modular weights, the kinetic terms of the fields are not very constrained by the modular transformations [27]. The TB approach is much more restrictive, in particular when embedded into string theory [13–15, 92]. However, while these models have great promise and certainly fix the above–mentioned problems of arbitrariness, it is probably fair to say that they do not yet provide us with unequivocal predictions on flavor parameters that can be tested in the foreseeable future.

The purpose of this chapter is to explore the details of the relation between these approaches. More specifically, we derive metaplectic symmetries from magnetized tori. Earlier works on this subject include [68, 70–74, 78, 98]. To accomplish this, we work out closed–form expressions for the Yukawa couplings that are valid for arbitrary flux parameters, and thus

generalize the results of the pioneering work by Cremades, Ibáñez and Marchesano [30]. We also present consistent modular transformation laws for both even and odd numbers of generations. Models derived from magnetized tori also allow us to understand to which extent supersymmetry is crucial for modular flavor symmetries, which we will argue to be less important than usually assumed. Additional motivation for looking at magnetized tori, with and without supersymmetry, comes from the fact that even without supersymmetry interacting scalar masses seem to be protected from quantum corrections [20, 21, 53, 56].

4.1.1 Zero Modes on Tori with Magnetic Flux

Let us consider a gauge theory with two extra dimensions. Two of the extra dimensions are compactified on a 2–torus $\mathbb{T}^2$, which is endowed with a magnetic flux. Using the index theorem, we can show that the flux will give rise to chiral zero–modes.

The main goal of this section is to review some of the properties of the zero–modes. The wave functions of the zero modes of the Dirac operator on tori with magnetic flux have been worked out in [30]. They are given by

$$\psi^{j,M}(z,\tau,\zeta) = \mathcal{N}\, \mathrm{e}^{\pi\, \mathrm{i}\, M\, (z+\zeta)\, \frac{\mathrm{Im}(z+\zeta)}{\mathrm{Im}\,\tau}}\, \vartheta\begin{bmatrix} \frac{j}{M} \\ 0 \end{bmatrix}\big(M\,(z+\zeta), M\,\tau\big)\ . \tag{4.1.1}$$

Here, $M \in \mathbb{N}$ indicates the units of flux, $0 \leq j \leq M-1$ is an integer, z the coordinate in the extra dimensions, ζ a so–called Wilson line parameter, and τ the torus parameter or half-period ratio. The wave functions from equation (4.1.1) correspond to left–handed particles in 4D whereas there are no right–handed particles for positive M. On the other hand, for negative values of the integer M there are no solutions for left–handed particles, but there are $|M|$ right–handed particles described by $\psi^{j,M}(\bar{z},\bar{\tau},\bar{\zeta})$, with $0 \leq j \leq |M|-1$. Furthermore, notice that despite what the notation may suggest, the $\psi^{j,M}$ are neither holomorphic functions of z, nor of τ. ϑ denotes the so–called Jacobi ϑ–function, cf. appendix B.1. The

normalization is given by

$$\mathcal{N} = \left(\frac{2M\ \mathrm{Im}\,\tau}{\mathcal{A}^2}\right)^{1/4} , \tag{4.1.2}$$

where $\mathcal{A} = (2\pi R)^2 \mathrm{Im}\tau$ is the area of the torus (cf. appendix B.2). We find it instructive to derive the quantization condition on M. Let us follow the discussion by [30]. Consider a U(1) gauge group in the torus with a magnetic flux given by the gauge potential

$$A(z+\zeta) = \frac{B}{2\,\mathrm{Im}\,\tau}\,\mathrm{Im}\big((\bar{z}+\bar{\zeta})\mathrm{d}z\big) \ . \tag{4.1.3}$$

Then, if the wave function $\psi^{j,M}(z,\tau,\zeta)$ has charge q under this U(1), its transformation under torus translations are

$$\psi^{j,M}(z+1,\tau,\zeta) = \exp\left(\frac{\mathrm{i}\,qB}{2\,\mathrm{Im}\,\tau}\,\mathrm{Im}(z+\zeta)\right)\psi^{j,M}(z,\tau,\zeta) \ , \tag{4.1.4a}$$

$$\psi^{j,M}(z+\tau,\tau,\zeta) = \exp\left(\frac{\mathrm{i}\,qB}{2\,\mathrm{Im}\,\tau}\,\mathrm{Im}(z+\zeta)\bar{\tau}\right)\psi^{j,M}(z,\tau,\zeta) \ . \tag{4.1.4b}$$

In order to have consistency through a contractible loop in the torus, we must get the same wave function shifting $z \to z+\tau+1$ as in the case where we shift by $z \to z+1+\tau$. Then,

$$\begin{aligned}
\psi^{j,M}(z+\tau+1,\tau,\zeta) &= \exp\left(\frac{\mathrm{i}\,qB}{2\,\mathrm{Im}\,\tau}\,\mathrm{Im}\big((z+\zeta+1)\bar{\tau}\big)\right)\psi^{j,M}(z+1,\tau,\zeta) \\
&= \exp\left(\frac{\mathrm{i}\,qB}{2\,\mathrm{Im}\,\tau}\,\mathrm{Im}\big((z+\zeta+1)\bar{\tau}\big)\right)\exp\left(\frac{\mathrm{i}\,qB}{2\,\mathrm{Im}\,\tau}\,\mathrm{Im}(z+\zeta)\right)\psi^{j,M}(z,\tau,\zeta) \\
&= \exp\left(\mathrm{i}\,\frac{qB\,\mathrm{Im}\,\bar{\tau}}{2\,\mathrm{Im}\,\tau}\right)\exp\left(\frac{\mathrm{i}\,qB}{2\,\mathrm{Im}\,\tau}\,\mathrm{Im}\big(\bar{\tau}(z+\zeta)\big)\right) \\
&\qquad\qquad \times \exp\left(\frac{\mathrm{i}\,qB}{2\,\mathrm{Im}\,\tau}\,\mathrm{Im}(z+\zeta)\right)\psi^{j,M}(z,\tau,\zeta) \ ,
\end{aligned} \tag{4.1.5}$$

where we used first equation (4.1.4b) and then equation (4.1.4a). On the other hand,

$$\begin{aligned}\psi^{j,M}(z+\tau+1,\tau,\zeta) &= \exp\left(\frac{\mathrm{i}\,qB\,\mathrm{Im}(z+\zeta+\tau)}{2\,\mathrm{Im}\,\tau}\right)\psi^{j,M}(z+\tau,\tau,\zeta)\\ &= \exp\left(\mathrm{i}\frac{qB\,\mathrm{Im}(z+\zeta+\tau)}{2\,\mathrm{Im}\,\tau}\right)\exp\left(\frac{\mathrm{i}\,qB}{2\,\mathrm{Im}\,\tau}\,\mathrm{Im}\,\bar{\tau}(z+\zeta)\right)\psi^{j,M}(z,\tau,\zeta)\\ &= \exp\left(\mathrm{i}\frac{qB\,\mathrm{Im}\,\tau}{2\,\mathrm{Im}\,\tau}\right)\exp\left(\frac{\mathrm{i}\,qB}{2\,\mathrm{Im}\,\tau}\,\mathrm{Im}(\bar{\tau}(z+\zeta))\right)\exp\left(\frac{\mathrm{i}\,qB}{2\,\mathrm{Im}\,\tau}\,\mathrm{Im}(z+\zeta)\right)\psi^{j,M}(z,\tau,\zeta)\ ,\end{aligned} \tag{4.1.6}$$

where we used first equation (4.1.4a) and then equation (4.1.4b). Imposing that equation (4.1.5) and equation (4.1.6) yield the same wave function leads to the flux quantization condition

$$qB = 2\pi M\ , \tag{4.1.7}$$

with M an arbitrary integer. Therefore, in what follows, we will not consider q and B individually, but only the integer M instead. Then, we have

$$\psi^{j,M}(z+1,\tau,\zeta) = \exp\left(\frac{\mathrm{i}\,\pi M}{\mathrm{Im}\,\tau}\,\mathrm{Im}(z+\zeta)\right)\psi^{j,M}(z,\tau,\zeta)\ , \tag{4.1.8a}$$

$$\psi^{j,M}(z+\tau,\tau,\zeta) = \exp\left(\frac{\mathrm{i}\,\pi M}{\mathrm{Im}\,\tau}\,\mathrm{Im}(z+\zeta)\bar{\tau}\right)\psi^{j,M}(z,\tau,\zeta)\ . \tag{4.1.8b}$$

4.1.2 Yukawa Couplings

4.1.3 Couplings from Overlap Integrals

One of the main rationales of working out the wave functions in section 4.1.1 is that the overlaps of wave functions yield the (Yukawa) couplings of the model. Let us consider a $4+2$ dimensional theory which is compactified on a torus $\mathbb{T}^2$. There is a gauge group breaking

$\mathrm{U}(N) \to \mathrm{U}(N_a) \times \mathrm{U}(N_b) \times \mathrm{U}(N_c)$ with $N = N_a + N_b + N_c$ due to the introduction of a magnetic flux in the compact dimensions given by

$$F_{z\bar{z}} = \frac{\pi \mathrm{i}}{\mathrm{Im}\tau} \begin{pmatrix} \frac{m_a}{N_a} \mathbb{1}_{N_a \times N_a} & 0 & 0 \\ 0 & \frac{m_b}{N_b} \mathbb{1}_{N_b \times N_b} & 0 \\ 0 & 0 & \frac{m_c}{N_c} \mathbb{1}_{N_c \times N_c} \end{pmatrix} , \tag{4.1.9}$$

where we will assume that $s_\alpha = \frac{m_\alpha}{N_\alpha}$ is an integer for $\alpha \in \{a, b, c\}$. Then, in [30, equation (5.7)] one finds that Yukawa couplings of the 4D effective theory are given by

$$Y_{ijk}(\widetilde{\zeta}, \tau) = g\, \sigma_{abc} \int_{\mathbb{T}^2} \mathrm{d}^2 z\, \psi^{i,\mathcal{I}_{ab}}(z, \tau, \zeta_{ab})\, \psi^{j,\mathcal{I}_{ca}}(z, \tau, \zeta_{ca}) \left(\psi^{k,\mathcal{I}_{cb}}(z, \tau, \zeta_{cb})\right)^* . \tag{4.1.10}$$

Here, $\psi^{i,\mathcal{I}_{ab}}(z, \tau, \zeta_{ab})$ are the wave functions of equation (4.1.1) that represent chiral fermions bifundamentals transforming as $(\boldsymbol{N}_a, \overline{\boldsymbol{N}}_b)$ under $\mathrm{U}(N_a) \times \mathrm{U}(N_b)$, and similarly for $\psi^{j,\mathcal{I}_{ca}}$ and $\psi^{k,\mathcal{I}_{cb}}$. The multiplicities of $\mathcal{I}_{\alpha\beta}$ of these bifundamentals are given by

$$\mathcal{I}_{\alpha\beta} = s_\alpha - s_\beta \ , \tag{4.1.11}$$

which implies that

$$\mathcal{I}_{ab} + \mathcal{I}_{bc} + \mathcal{I}_{ca} = 0 \ . \tag{4.1.12}$$

Furthermore, g is the $(4+2)$–dimensional gauge coupling, and $\sigma_{abc} = \mathrm{sign}(\mathcal{I}_{ab}\mathcal{I}_{bc}\mathcal{I}_{ca})$ [30] is a sign which is equal to -1 throughout our discussion. The $\zeta_{\alpha\beta}$ are given by

$$\zeta_{\alpha\beta} = \frac{s_\alpha \zeta_\alpha - s_\beta \zeta_\beta}{s_\alpha - s_\beta} \tag{4.1.13}$$

for $\alpha, \beta \in \{a, b, c\}$. Finally, ζ_α are the Abelian Wilson lines associated to the group $\mathrm{U}(N_\alpha)$ for $\alpha \in \{a, b, c\}$. ζ_{cb} and ζ_{ca} are defined similarly. As one can see from equation (4.1.1),

the ζ_α represent translation of the torus origin. However, as shown in [30] if all three wave functions are shifted by the same Wilson line, then the values of the Yukawa couplings are unaffected.

4.1.4 Yukawa Couplings for Generic Flux Parameters

Let us now discuss how one can reduce the overlap integrals (4.1.10) to a linear combination of ϑ–functions. We follow the strategy of [30], but generalize the result to the cases $\mathcal{I}_{ab} > 1$ and/or $\gcd(\mathcal{I}_{ab}, \mathcal{I}_{ca}, \mathcal{I}_{bc}) > 1$, with $\mathcal{I}_{ab}, \mathcal{I}_{ca} > 0$ and $\mathcal{I}_{bc} < 0$. Note that the analogous discussion applies to the case in which $\mathcal{I}_{ab}$ and $\mathcal{I}_{ca}$ are negative [30, cf. the discussion around equation (5.6)].

In order to find closed–form expressions for the Yukawa couplings, one uses two important facts [30]:

1. products of ϑ–functions can be expanded in terms of ϑ–functions, see [30, equation (5.8)], and that
2. the ϑ–functions fulfill certain orthogonality and completeness relations.

These facts allow one to find analytic expressions for the Yukawa couplings (4.1.10) that do no longer involve integrals [30]. In more detail, starting from (4.1.10), one obtains (cf. [30, equation (5.15)])

$$Y_{ijk}(\widetilde{\zeta},\tau) = \mathcal{N}_{abc}\, \mathrm{e}^{\frac{H(\widetilde{\zeta},\tau)}{2}} \sum_{m\in\mathbb{Z}_{\mathcal{I}_{bc}}} \delta_{k,i+j+\mathcal{I}_{ab}\,m}\, \vartheta \begin{bmatrix} \frac{\mathcal{I}_{ca}i-\mathcal{I}_{ab}j+\mathcal{I}_{ab}\mathcal{I}_{ca}m}{-\mathcal{I}_{ab}\mathcal{I}_{bc}\mathcal{I}_{ca}} \\ 0 \end{bmatrix} \left(\widetilde{\zeta}, \tau\, |\mathcal{I}_{ab}\mathcal{I}_{bc}\mathcal{I}_{ca}|\right) , \tag{4.1.14}$$

where

$$\mathcal{N}_{abc} = g\,\sigma_{abc}\left(\frac{2\,\mathrm{Im}\,\tau}{\mathcal{A}^2}\right)^{1/4}\left|\frac{\mathcal{I}_{ab}\mathcal{I}_{ca}}{\mathcal{I}_{bc}}\right|^{1/4} \tag{4.1.15}$$

is a normalization constant and the Wilson line dependence is encoded in the quantities

$$\widetilde{\zeta} := -\mathcal{I}_{ab}\,\mathcal{I}_{ca}\,(\zeta_{ca}-\zeta_{ab}) = d^{\alpha\beta\gamma}\,s_\alpha\,\zeta_\alpha\,\mathcal{I}_{\beta\gamma} \tag{4.1.16}$$

and

$$\begin{aligned}\frac{H(\widetilde{\zeta},\tau)}{2} &:= \frac{\pi\mathrm{i}}{\mathrm{Im}\,\tau}(\mathcal{I}_{ab}\,\zeta_{ab}\;\mathrm{Im}\,\zeta_{ab}+\mathcal{I}_{bc}\,\zeta_{bc}\;\mathrm{Im}\,\zeta_{bc}+\mathcal{I}_{ca}\,\zeta_{ca}\;\mathrm{Im}\,\zeta_{ca})\\ &= \frac{\pi\mathrm{i}}{\mathrm{Im}\,\tau}|\mathcal{I}_{ab}\,\mathcal{I}_{bc}\,\mathcal{I}_{ab}|^{-1}\frac{\widetilde{\zeta}\;\mathrm{Im}\,\widetilde{\zeta}}{\mathrm{Im}\,\tau}\ .\end{aligned} \tag{4.1.17}$$

with

$$d^{\alpha\beta\gamma} = \begin{cases} 1\ , & \text{if } \{\alpha,\beta,\gamma\} \text{ is an even permutation of } \{1,2,3\}\ ,\\ 0\ , & \text{otherwise}\ , \end{cases} \tag{4.1.18}$$

where we have used [30, equation (5.28)]. Cremades et al. obtain then [30, equation (5.15)]

$$Y_{ijk}(\widetilde{\zeta},\tau) = \mathcal{N}_{abc}\mathrm{e}^{\frac{H(\widetilde{\zeta},\tau)}{2}}\,\vartheta\begin{bmatrix}-\left(\frac{j}{\mathcal{I}_{ca}}+\frac{k}{\mathcal{I}_{bc}}\right)/\mathcal{I}_{ab}\\ 0\end{bmatrix}\left(\widetilde{\zeta},\tau\,|\mathcal{I}_{ab}\mathcal{I}_{bc}\mathcal{I}_{ca}|\right) \text{ for } i=k-j \mod \mathcal{I}_{ab}\ . \tag{4.1.19}$$

This expression yields the correct couplings only if $\mathcal{I}_{ab}=1$, which implies that $d=1$, where

$$d := \gcd\big(|\mathcal{I}_{ab}|,|\mathcal{I}_{ca}|,|\mathcal{I}_{bc}|\big)\ . \tag{4.1.20}$$

To see that we need to demand that $d = 1$ for (4.1.19) to hold, notice that in (4.1.14) the integers i, j and k are only defined modulo $\mathcal{I}_{ab}$, $\mathcal{I}_{bc}$ and $\mathcal{I}_{ca}$, respectively. This is evident from the overlap integral (4.1.10), where e.g. $\psi^{i,\mathcal{I}_{ab}}(z,\tau,\zeta_{ab}) = \psi^{i+\mathcal{I}_{ab},\mathcal{I}_{ab}}(z,\tau,\zeta_{ab})$. However, if $\gcd(|\mathcal{I}_{ab}|,|\mathcal{I}_{ca}|) > 1$ or $|\mathcal{I}_{ab}| > 1$, shifting i (or j) by $|\mathcal{I}_{ab}|$ (or $(|\mathcal{I}_{ca}|)$, which leaves the wave functions invariant and hence has to produce the same overlap integral, leads to different results for the Yukawa couplings when using (4.1.19).

To obtain the general expression, let us look at [89, Proposition II.6.4. on p. 221]

$$\begin{aligned}\vartheta\begin{bmatrix}\frac{j}{\mathcal{I}_{ab}}\\0\end{bmatrix}(z_1,\mathcal{I}_{ab}\tau)\cdot\vartheta\begin{bmatrix}\frac{j}{\mathcal{I}_{ca}}\\0\end{bmatrix}(z_2,\mathcal{I}_{ca}\tau) = \sum_{m\in\mathbb{Z}_{\mathcal{I}_{ab}+\mathcal{I}_{ca}}}\vartheta\begin{bmatrix}\frac{i+j+\mathcal{I}_{ab}m}{\mathcal{I}_{ab}+\mathcal{I}_{ca}}\\0\end{bmatrix}\big(z_1+z_2,(\mathcal{I}_{ab}+\mathcal{I}_{ca})\tau\big)\\ \vartheta\begin{bmatrix}\frac{\mathcal{I}_{ca}i-\mathcal{I}_{ab}j+\mathcal{I}_{ab}\mathcal{I}_{ca}\,m}{\mathcal{I}_{ab}\mathcal{I}_{ca}(\mathcal{I}_{ab}+\mathcal{I}_{ca})}\\0\end{bmatrix}(\mathcal{I}_{ca}\,z_1-\mathcal{I}_{ab}\,z_2,\mathcal{I}_{ab}\mathcal{I}_{ca}(\mathcal{I}_{ab}+\mathcal{I}_{ca})\tau)\ ,\end{aligned}\tag{4.1.21}$$

which was used in [30]. In our wave functions, $z_1 = \mathcal{I}_{ab}\,(z+\zeta_{ab})$ and $z_2 = \mathcal{I}_{ca}\,(z+\zeta_{ca})$, so that in the overlap integral $z_1+z_2 = \mathcal{I}_{cb}\,(z+\zeta_{cb})$ and $\mathcal{I}_{ca}\,z_1-\mathcal{I}_{ab}\,z_2 = \widetilde{\zeta}$. One thus obtains (cf. [30, equation (5.12)])

$$\begin{aligned}\psi^{i,\mathcal{I}_{ab}}(z,\tau,\zeta_{ab})\cdot\psi^{j,\mathcal{I}_{ca}}(z,\tau,\zeta_{ca}) = \mathcal{A}^{-1/2}\,(2\,\mathrm{Im}\,\tau)^{1/4}\left|\frac{\mathcal{I}_{ab}\,\mathcal{I}_{ca}}{\mathcal{I}_{bc}}\right|^{1/4}\mathrm{e}^{\frac{H(\widetilde{\zeta},\tau)}{2}}\\ \sum_{m\in\mathbb{Z}_{|\mathcal{I}_{bc}|}}\psi^{i+j+\mathcal{I}_{ab}\,m,\mathcal{I}_{cb}}(z,\tau,\mathcal{I}_{cb})\,\vartheta\begin{bmatrix}\frac{\mathcal{I}_{ca}i-\mathcal{I}_{ab}j+\mathcal{I}_{ab}\mathcal{I}_{ca}\,m}{\mathcal{I}_{ab}\mathcal{I}_{ca}(\mathcal{I}_{ab}+\mathcal{I}_{ca})}\\0\end{bmatrix}\Big(\widetilde{\zeta},\mathcal{I}_{ab}\mathcal{I}_{ca}(\mathcal{I}_{ab}+\mathcal{I}_{ca})\tau\Big)\ .\end{aligned}\tag{4.1.22}$$

The product (4.1.22) gets projected on a third wave function $\psi^{k,\mathcal{I}_{ab}+\mathcal{I}_{ca}}$ via the overlap integral (4.1.10). This means that k has to "match", i.e. m has to be a solution of the congruence equation

$$\mathcal{I}_{ab}\,m+i+j = k \mod \mathcal{I}_{bc}\ .\tag{4.1.23}$$

Now observe that, since $\mathcal{I}_{ab}+\mathcal{I}_{bc}+\mathcal{I}_{ca}=0$, $\gcd\big(|\mathcal{I}_{ab}|,|\mathcal{I}_{cb}|\big)=d$ with d from equation (4.1.20). Equation (4.1.23) is a linear congruence equation for the variable m. It is known that (cf. e.g. [48, Lemma 3 on p. 37]) if

$$k-i-j=0 \mod d\,, \tag{4.1.24}$$

the linear congruence of equation (4.1.23) has d solutions. Otherwise there is no solution. Note that the condition (4.1.24) provides us with a selection rule for the Yukawa couplings, which can be interpreted as a $\mathbb{Z}_d$ flavor symmetry (cf. [1]). We thus know that the Yukawa couplings will be proportional to

$$\Delta^{(d)}_{i+j,k} := \begin{cases} 1\ , & \text{if } i+j=k \mod d\ , \\ 0\ , & \text{otherwise}\ . \end{cases} \tag{4.1.25}$$

Consider now combinations of i, j and k satisfying the selection rule (4.1.24). This means that

$$k-i-j=m'\,d \tag{4.1.26}$$

with some integer $m'=(k-i-j)/d$. Define now $\mathcal{I}'_{ab}=\mathcal{I}_{ab}/d$, $\mathcal{I}'_{ca}=\mathcal{I}_{ca}/d$ and $\mathcal{I}'_{bc}=\mathcal{I}_{bc}/d$, which are integers because of equation (4.1.20). We can thus divide equation (4.1.23) by d to get

$$|\mathcal{I}'_{ab}|\,m=m' \mod |\mathcal{I}'_{bc}|\ , \tag{4.1.27}$$

where $\gcd\big(|\mathcal{I}'_{ab}|,|\mathcal{I}'_{bc}|\big)=1$. Equation (4.1.27) can be solved with e.g. the `Mathematica` command `FindInstance`. However, as we shall discuss now, one can find a closed–form expression for the solution. The linear congruence (4.1.27) has one (inequivalent) solution $m=m_0$, which is given by $\big[|\mathcal{I}'_{ab}|\big]_{(|\mathcal{I}'_{bc}|)}m'$ where $\big[|\mathcal{I}'_{ab}|\big]_{(|\mathcal{I}'_{bc}|)}$ is the multiplicative inverse

of $|\mathcal{I}'_{ab}|$ modulo $|\mathcal{I}'_{bc}|$. According to Euler's theorem (cf. e.g. [48, Theorem 1 on p. 64]), the multiplicative inverse can be expressed via the Euler ϕ–function, $\big[|\mathcal{I}'_{ab}|\big]_{(|\mathcal{I}'_{bc}|)} = (\mathcal{I}'_{ab})^{\phi\left(|\mathcal{I}'_{bc}|\right)-1}$. This means that

$$m_0 = (\mathcal{I}'_{ab})^{\phi\left(|\mathcal{I}'_{bc}|\right)-1}\,\frac{k-i-j}{d} \mod |\mathcal{I}'_{bc}| \ . \tag{4.1.28}$$

Note that the Euler ϕ–function is implemented in `Mathematica` as `EulerPhi`. Relation (4.1.28) implies that one particular solution m_0 of equation (4.1.23) satisfies

$$\mathcal{I}_{ab}\, m_0 = (\mathcal{I}'_{ab})^{\phi\left(|\mathcal{I}'_{bc}|\right)}\,(k-i-j) \mod |\mathcal{I}_{bc}| \ . \tag{4.1.29}$$

Given the solution m_0 in equation (4.1.28), the d solutions of equation (4.1.23) are given by

$$m = m_0 - |\mathcal{I}'_{bc}|\, t \quad \text{for } t = 0, \ldots, (d-1) \ . \tag{4.1.30}$$

Thus, using equation (4.1.30) in (4.1.14), we see that the Yukawa couplings are given by

$$Y_{ijk}(\widetilde{\zeta},\tau) = \mathcal{N}_{abc}\mathrm{e}^{\frac{H(\widetilde{\zeta},\tau)}{2}}\,\Delta^{(d)}_{i+j,k}\sum_{t=0}^{d-1}\vartheta\begin{bmatrix}\frac{\mathcal{I}_{ca}i-\mathcal{I}_{ab}j+\mathcal{I}_{ab}\mathcal{I}_{ca}m_0}{|\mathcal{I}_{ab}\mathcal{I}_{bc}\mathcal{I}_{ca}|}+\frac{t}{d}\\ 0\end{bmatrix}\Big(\widetilde{\zeta},|\mathcal{I}_{ab}\mathcal{I}_{ca}\mathcal{I}_{bc}|\tau\Big) \ , \tag{4.1.31}$$

Equation (4.1.31) can be simplified further. Let us define

$$P := |\mathcal{I}_{ab}\mathcal{I}_{ca}\mathcal{I}_{bc}| \ , \tag{4.1.32a}$$

$$\lambda := \mathrm{lcm}\big(|\mathcal{I}_{ab}|,|\mathcal{I}_{ca}|,|\mathcal{I}_{bc}|\big) \ . \tag{4.1.32b}$$

Next we note that*

$$P = \lambda\, d^2 \ . \tag{4.1.33}$$

Then equation (4.1.31) can be recast as

$$Y_{ijk}(\widetilde{\zeta},\tau) = \mathcal{N}_{abc}\mathrm{e}^{\frac{H(\widetilde{\zeta},\tau)}{2}} \sum_{t=0}^{d-1} \vartheta\begin{bmatrix} \frac{1}{d}\left(\frac{\widehat{\alpha}_{ijk}}{\lambda}+t\right) \\ 0 \end{bmatrix}\Big(\widetilde{\zeta}, P\tau\Big) \ , \tag{4.1.34}$$

where

$$\widehat{\alpha}_{ijk} = \mathcal{I}'_{ca}\, i - \mathcal{I}'_{ab}\, j + \mathcal{I}'_{ca}\, \mathcal{I}_{ab}\, m_0 \tag{4.1.35}$$

is an integer. Using equation (4.1.28), $\widehat{\alpha}_{ijk}$ becomes

$$\widehat{\alpha}_{ijk} = \mathcal{I}'_{ca}\, i - \mathcal{I}'_{ab}\, j + \mathcal{I}'_{ca}\, (\mathcal{I}'_{ab})^{\phi\left(|\mathcal{I}'_{bc}|\right)}\, (k-i-j) \mod \lambda\, d \ . \tag{4.1.36}$$

Now we can use equation (B.1.4) to express the sum (4.1.34) as

$$\begin{aligned} Y_{ijk}(\widetilde{\zeta},\tau) &= \mathcal{N}_{abc}\mathrm{e}^{\frac{H(\widetilde{\zeta},\tau)}{2}} \sum_{t=0}^{d-1}\sum_{\ell=-\infty}^{\infty} \exp\left[\mathrm{i}\pi\left(\frac{1}{d}\frac{\widehat{\alpha}_{ijk}}{\lambda}+\frac{1}{d}t+\ell\right)^2 P\,\tau\right] \exp\left[2\pi\mathrm{i}\left(\frac{\widehat{\alpha}_{ijk}}{\lambda\, d}+\frac{t}{d}+\ell\right)\widetilde{\zeta}\right] \\ &= \mathcal{N}_{abc}\mathrm{e}^{\frac{H(\widetilde{\zeta},\tau)}{2}}\, \vartheta\begin{bmatrix} \frac{\widehat{\alpha}_{ijk}}{\lambda} \\ 0 \end{bmatrix}\left(\frac{\widetilde{\zeta}}{d}, \lambda\,\tau\right) \ . \end{aligned} \tag{4.1.37}$$

*To see this, consider two positive integers a and b, and define $c = \gcd(a,b) = \gcd\big(a,b,(a+b)\big)$ such that $a = a'\,c$ and $b = b'\,c$ with integers a' and b'. Then $\mathrm{lcm}\big(a,b,(a+b)\big) = c\ \mathrm{lcm}\big(a',b',(a'+b')\big)$. Since a', b' and $(a'+b')$ do not have a nontrivial common divisor,

$$\mathrm{lcm}\big(a,b,(a+b)\big) = c\,a'\,b'\,(a'+b') \ ,$$

so that

$$a\,b\,(a+b) = [\gcd\big(a,b,(a+b)\big)]^2\ \mathrm{lcm}\big(a,b,(a+b)\big) \ .$$

Here, $\ell' = d\,\ell + t$. When ℓ runs over all integers, and t runs from 0 to $d-1$, ℓ' runs over all integers. The $\widehat{\alpha}_{ijk}$ are integers. Therefore, the physical Yukawa couplings are given by

$$Y_{ijk}(\widetilde{\zeta},\tau) = \mathcal{N}_{abc}\,\mathrm{e}^{\frac{H(\widetilde{\zeta},\tau)}{2}}\,\Delta^{(d)}_{i+j,k}\,\vartheta\begin{bmatrix}\frac{\mathcal{I}'_{ca}\,i-\mathcal{I}'_{ab}\,j+\mathcal{I}'_{ca}\left(\mathcal{I}'_{ab}\right)^{\phi(|\mathcal{I}'_{bc}|)}\,(k-i-j)}{\lambda}\\ 0\end{bmatrix}\left(\frac{\widetilde{\zeta}}{d},\lambda\,\tau\right) \tag{4.1.38}$$

with d from equation (4.1.20), $\Delta^{(d)}_{i+j,k}$ from equation (4.1.25), λ from equation (4.1.32b) and assuming $\mathcal{I}_{ab}$, $\mathcal{I}_{ca} > 0$ and $\mathcal{I}_{bc} < 0$. Note that if $d = 1$ and $\mathcal{I}_{ab} = 1$, this formula reproduces equation (4.1.19). Further, *a priori* this expression does not rely on supersymmetry, it is simply derived from the overlap of wave functions. However, one may expect the scalar wave function to be subject to substantial corrections in non–supersymmetric theories. In section 4.1.10 we will argue that magnetized tori may not comply with these expectations, and that this formula may even be a good leading–order result in a non–supersymmetric theory. The normalization factors in equation (4.1.38) are

$$\mathcal{N}_{abc} = g\,\sigma_{abc}\left(\frac{2\,\mathrm{Im}\,\tau}{\mathcal{A}^2}\right)^{1/4}\lambda^{1/4}\left|\frac{1}{\mathcal{I}'_{bc}}\right|^{1/2} \tag{4.1.39}$$

with g being the gauge coupling. In equation (4.1.64) we will express the normalization in terms of Kähler potential terms. Notice that if there are nontrivial relative Wilson lines, the normalization of the fields changes compared to the case without Wilson lines [30, equation (7.37)]. This has to be taken into account when computing physical Yukawa couplings. In what follows, we will set the Wilson lines to zero, leaving the detailed study of their impact on the modular flavor symmetries for future work. As mentioned above, the selection rule (4.1.24) entails a $\mathbb{Z}_d$ symmetry. As we discuss in more detail in appendix B.4, out of *a priori* $P = \lambda\,d^2$ entries, at most $\lambda/2 + 1$ are distinct.

Modular Groups and Modular Forms of Matter Fields

We have reviewed most of the mathematical prerequisites of modular forms and modular symmetries in section 1.2.1. In this short subsection, we note the modular transformation properties of the matter fields. As already noted, [49] proposes that Yukawa couplings in quantum field theories can be modular forms, whereas, despite not being modular forms, "matter" superfields ϕ^i transform under a general modular transformation $\gamma \in \Gamma$ as

$$\phi^i \xmapsto{\gamma} (c\,\tau + d)^{k_\phi}\, \rho_{\boldsymbol{s}}(\gamma)_{ij}\, \phi^j \ . \tag{4.1.40}$$

Here $\rho_{\boldsymbol{s}}(\gamma)$ is the s-dimensional (reducible or irreducible) Γ'_N representation matrix. As for modular forms, the powers k_ϕ are also known as modular weights and are identical for the fields in the transformation. Thus, matter fields build a representation of the finite modular group Γ'_N, which can be adopted as a symmetry of the underlying (quantum) field theory. In this scenario, Γ'_N can be considered a "modular flavor symmetry".

In string–derived models, it is known that matter fields are subject to modular transformations similar to equation (4.1.40). Moreover, Yukawa couplings also transform as in equation (1.24). However, as we shall see in this section, the modular weights can be fractional and, hence, the emerging modular flavor symmetry is not necessarily one of the Γ'_N. Yet, to obtain fractional modular weights it is not necessary to go all the way to strings, they already emerge from simpler settings such as magnetized tori (see e.g. [68, 70–74, 78, 98]). As we discuss in detail in detail in section 4.1.5, this follows already from the τ–dependence of the normalization of the wave functions [30].

Finally, in field theories endowed with $\widetilde{\Gamma}_{4N}$ symmetries, the modular transformations of matter fields are given by

$$\phi^i \xmapsto{\widetilde{\gamma}} \varphi(\gamma,\tau)^{k_\phi}\, \rho_{\boldsymbol{s}}(\widetilde{\gamma})_{ij}\, \phi^j \ , \tag{4.1.41}$$

object	$\psi^{j,M}$	$\phi^{j,M}$	$\Omega^{j,M}$	Y_{ijk}	$\mathscr{W}$
modular weight k	$1/2$	$-1/2$	0	$1/2$	-1

Table 4.1.1: Modular weights of the $\mathbb{T}^2$ wave functions $\psi^{j,M}$, 4D fields $\phi^{j,M}$, 6D fields $\Omega^{j,M}$, Yukawa couplings Y_{ijk}, and superpotential $\mathscr{W}$.

where $\rho_{\boldsymbol{s}}(\widetilde{\gamma})$ is now a (reducible or irreducible) $\widetilde{\Gamma}_{4N}$ representation. As we shall see, this behavior is natural in toroidal compactifications with magnetic fluxes.

4.1.5 Normalization of the Wave Functions and Modular Weights

The wave functions in equation (4.1.1) satisfy

$$\int_{\mathbb{T}^2} \mathrm{d}^2 z \, |\psi^{j,M}(z,\tau,\zeta)|^2 = \mathcal{A} \int_0^1 \mathrm{d}x \int_0^1 \mathrm{d}y \, |\psi^{j,M}(x+\tau\, y,\tau,\zeta)|^2 \stackrel{!}{=} 1 \ , \tag{4.1.42}$$

where $\mathbb{T}^2$ denotes the fundamental domain of the torus, cf. appendix B.2. The normalization constant $\mathcal{N} \propto (\mathrm{Im}\,\tau)^{-1/4}$ in equation (4.1.2) is chosen in such a way that the normalization condition (4.1.42) holds. This implies, in particular, that the Kähler metric is proportional to $(\mathrm{Im}\,\tau)^{-1/2}$, i.e.

$$K_{i\bar{\imath}} \propto \frac{1}{(\mathrm{Im}\,\tau)^{1/2}} \ , \tag{4.1.43}$$

i.e. the modular weight of the 4D fields $\phi^{j,M}$ describing the zero modes is $k_\phi = -1/2$. We survey the modular weights of the fields, coupling and superpotential in table 4.1.1. The modular weights k_ψ of the wave functions can be inferred from their normalization factor $\mathcal{N}$ in equation (4.1.2) to be $k_\psi = +1/2$, as we shall also confirm through their explicit modular transformations, equation (4.1.62). Therefore, the 6D fields,

$$\Omega^{j,M} = \phi^{j,M}(x^\mu) \otimes \psi^{j,M}(z,\tau) \ , \tag{4.1.44}$$

have trivial modular weights, as they should. The modular weights of the Yukawa couplings, $k_Y = 1/2$, can be explicitly determined from their modular transformations, equations (B.5.8) and (B.5.10). Since the superpotential terms describing the Yukawa couplings involve three 4D fields and one coupling "constant", the superpotential $\mathscr{W}$ has modular weight $k_{\mathscr{W}} = 3k_\phi + k_Y = -1$. This means that under a modular transformation the superpotential picks up an automorphy factor

$$\mathscr{W} \overset{\gamma}{\longmapsto} (c\,\tau + d)^{-1}\mathscr{W} \ . \tag{4.1.45}$$

The automorphy factor $(c\,\tau + d)^{-1}$ can in general be "undone" by so–called Kähler transformations [121], under which

$$\mathscr{W} \mapsto \mathrm{e}^{-\mathscr{F}(\Phi)}\,\mathscr{W}(\Phi) \ , \tag{4.1.46a}$$

$$K(\Phi,\overline{\Phi}) \mapsto K(\Phi,\overline{\Phi}) + \mathscr{F}(\Phi) + \overline{\mathscr{F}(\Phi)} \ , \tag{4.1.46b}$$

where Φ denotes the collection of 4D superfields, and $\mathscr{F}$ a holomorphic function. In our case, the Kähler potential is, after setting the "matter" fields to zero and at the classical level, given by (cf. e.g. [30, equation (5.50)])

$$\widehat{K} = -\ln(\mathcal{S}+\overline{\mathcal{S}}) - \ln(\mathcal{T}+\overline{\mathcal{T}}) - \ln(\mathcal{U}+\overline{\mathcal{U}}) \subset K \ , \tag{4.1.47}$$

in terms of the axio–dilaton $\mathcal{S}$, the Kähler modulus $\mathcal{T}$ and the complex structure modulus $\mathcal{U}$. These chiral fields are related to the gauge coupling g, the torus volume $\mathcal{A}$ and τ according to $\mathrm{Re}\,\mathcal{S} \propto 1/g^2$, $\mathrm{Re}\,\mathcal{T} \propto \mathcal{A}$ and $\mathrm{Re}\,\mathcal{U} = \mathrm{Im}\,\tau$. Consequently, τ appears in the Kähler potential as

$$-\ln(\mathcal{U}+\overline{\mathcal{U}}) = -\ln(-\mathrm{i}\,\tau + \mathrm{i}\,\bar{\tau}) \ . \tag{4.1.48}$$

Given that

$$\tau - \bar{\tau} \overset{\gamma}{\longmapsto} |c\,\tau + d|^{-2}\,(\tau - \bar{\tau})\ , \tag{4.1.49}$$

it is easy to see that K under a modular transformation of τ becomes

$$K \overset{\gamma}{\longmapsto} K + \ln(c\,\tau + d) + \ln(c\,\bar{\tau} + d)\ . \tag{4.1.50}$$

A Kähler transformation (4.1.46) with $\mathscr{F} = -\ln(c\,\tau + d)$ then absorbs simultaneously the modular transformation of K and $\mathscr{W}$, see equation (4.1.45), yielding a modular invariant supersymmetric theory. That is, the supergravity Kähler function

$$G(\Phi, \overline{\Phi}) = K(\Phi, \overline{\Phi}) + \ln|\mathscr{W}(\Phi)|^2 \tag{4.1.51}$$

is automatically invariant under the simultaneous transformation (4.1.45) and (4.1.50). In other words, we cannot dial the modular weight of the superpotential at will, it is already determined by the (classical) Kähler potential of the torus (4.1.47). In particular, setting the modular weight of the superpotential to zero is not an option in this approach, we derive modular flavor symmetries from an explicit torus.

4.1.6 Boundary Conditions for the Transformed Wave Functions

It has been stated in the literature [71, 98] that the wave functions given by equation (4.1.1) do not satisfy the boundary conditions given by the lattice periodicity when transformed under equation (1.21) for odd units of flux, M. If true, this would mean that a physical wave function gets mapped to an unphysical one just by looking at an equivalent torus, which would indicate that either the expressions for the wave functions were incorrect, or there is something fundamentally wrong with odd M. In this case, simple explanations of three

generations would be at stake.

However, as we shall see, the transformed wave functions do obey the correct boundary conditions, both for even and odd M. The important point is that, if our original wave function $\psi^{j,M}(z,\tau,0)$ satisfied conditions for τ, after a modular transformation $\tau \mapsto \tau'$ the transformed wave function $\psi^{j,M}(z,\tau',0)$ needs to fulfill the conditions for τ', and not for τ.

For the modular S transformations, the boundary conditions, given by equations (4.1.8a) and (4.1.8b), are now

$$\begin{aligned}
\psi^{j,M}\left(-\frac{z}{\tau}+1,-\frac{1}{\tau},0\right) &= \exp\left(\mathrm{i}\pi M\frac{\mathrm{Im}(-z/\tau)}{\mathrm{Im}(-1/\tau)}\right)\psi^{j,M}\left(-\frac{z}{\tau},-\frac{1}{\tau},0\right) \\
&= \exp\left(-\mathrm{i}\pi M\frac{\mathrm{Im}\, z\bar{\tau}}{\mathrm{Im}\,\tau}\right)\psi^{j,M}\left(-\frac{z}{\tau},-\frac{1}{\tau},0\right)\,, \qquad (4.1.52a)\\
\psi^{j,M}\left(-\frac{z}{\tau}-\frac{1}{\tau},-\frac{1}{\tau},0\right) &= \exp\left(\mathrm{i}\pi M\frac{\mathrm{Im}(-z/\tau)(-1/\bar{\tau})}{\mathrm{Im}(-1/\tau)}\right)\psi^{j,M}\left(-\frac{z}{\tau},-\frac{1}{\tau},0\right) \\
&= \exp\left(\frac{\mathrm{i}\pi M\,\mathrm{Im}\, z}{\mathrm{Im}\,\tau}\right)\psi^{j,M}\left(-\frac{z}{\tau},-\frac{1}{\tau},0\right)\,. \qquad (4.1.52b)
\end{aligned}$$

The fact that the transformed wave functions follow the boundary condition is a consequence of the wave functions being functions of z and τ, which we can just replace by their image under S. Nonetheless we verify this explicitly in appendix B.3.1.

Next, under the modular T transformation given by equation (1.21) the transformed boundary conditions, equations (4.1.8a) and (4.1.8b), are

$$\begin{aligned}
\psi^{j,M}(z+1,\tau+1,0) &= \exp\left(\mathrm{i}\,\frac{\pi M}{\mathrm{Im}\,\tau}\mathrm{Im}\, z\right)\psi^{j,M}(z,\tau+1,0)\,, \qquad (4.1.53a)\\
\psi^{j,M}(z+\tau+1,\tau+1,0) &= \exp\left(\mathrm{i}\,\frac{\pi M}{\mathrm{Im}\,\tau}\,\mathrm{Im}\big((\bar{\tau}+1)z\big)\right)\psi^{j,M}(z,\tau+1,0)\,. \qquad (4.1.53b)
\end{aligned}$$

We can make the same argument as above but also verify the statement explicitly in appendix B.3.2.

However, the transformed wave function equation (B.3.6), i.e. the wave functions "living" on a torus with torus parameter $\tau' = \tau + 1$ do not follow the original boundary conditions of equations (4.1.8a) and (4.1.8b) with τ. Indeed, from equation (B.3.6) we get

$$\begin{aligned}
\psi^{j,M}(z+\tau,\tau+1,0) &= \widetilde{\mathcal{N}} \mathrm{e}^{\frac{\mathrm{i}\,\pi M}{\mathrm{Im}\,\tau}[z\,\mathrm{Im}\,z + z\,\mathrm{Im}\,\tau + \tau\,\mathrm{Im}\,z + \tau\,\mathrm{Im}\,\tau]} \vartheta \begin{bmatrix} \frac{j}{M} \\ \frac{M}{2} \end{bmatrix} (Mz + M\tau, M\tau) \\
&= \widetilde{\mathcal{N}} \mathrm{e}^{\frac{\mathrm{i}\,\pi M}{\mathrm{Im}\,\tau}[z\,\mathrm{Im}\,z + z\,\mathrm{Im}\,\tau + \tau\,\mathrm{Im}\,z + \tau\,\mathrm{Im}\,\tau]} \mathrm{e}^{-\mathrm{i}\,\pi M\tau - 2\pi\mathrm{i}\,(Mz + \frac{M}{2})} \vartheta \begin{bmatrix} \frac{j}{M} \\ \frac{M}{2} \end{bmatrix} (Mz, M\tau) \\
&= \mathrm{e}^{-\pi\mathrm{i}\,M} \mathrm{e}^{\frac{\mathrm{i}\,\pi M}{\mathrm{Im}\,\tau}(z\,\mathrm{Im}\,\tau + \tau\,\mathrm{Im}\,z + \tau\,\mathrm{Im}\,\tau - \tau\,\mathrm{Im}\,\tau - 2z\,\mathrm{Im}\,\tau)} \widetilde{\mathcal{N}} \mathrm{e}^{i\pi M z \frac{\mathrm{Im}\,z}{\mathrm{Im}\,\tau}} \vartheta \begin{bmatrix} \frac{j}{M} \\ \frac{M}{2} \end{bmatrix} (Mz, M\tau) \\
&= \mathrm{e}^{-\pi\mathrm{i}\,M} \, \exp\left(\mathrm{i}\,\frac{M\pi}{\mathrm{Im}\,\tau}\,\mathrm{Im}\,\bar{\tau} z \right) \psi^{j,M}(z,\tau+1,0) \ , \qquad (4.1.54)
\end{aligned}$$

where $\widetilde{\mathcal{N}} := \mathrm{e}^{-\mathrm{i}\pi\, j\left(1-\frac{j}{M}\right)} \mathcal{N}$ and we have used equation (B.1.5b) in the second line. Thus, we find that

$$\psi^{j,M}(z+\tau,\tau+1,0) = \mathrm{e}^{-\pi\mathrm{i}\,M} \exp\left(\mathrm{i}\,\frac{M\pi}{\mathrm{Im}\,\tau}\,\mathrm{Im}\,\bar{\tau} z \right) \psi^{j,M}(z,\tau+1,0) \ . \qquad (4.1.55)$$

Therefore, for odd M equation (4.1.55) differs from equation (4.1.8b) by a phase. However, there is also no reason why the transformed wave functions should obey boundary conditions for τ instead of $\tau' = \tau + 1$. Nevertheless, this fact will have important implications for the explicit form of the T–transformation, as we shall see in section 4.1.7.

4.1.7 Modular Flavor Symmetries

Modular Transformations of the Wave Functions $\psi^{j,M}$

Crucially, physics should not depend on how we choose to parametrize the underlying torus. That is, if we subject the half–period ratio τ of the torus to a modular transformation, the physical predictions of the theory have to stay the same. This means that there should be

a dictionary between theories with seemingly different but equivalent values of τ, which are related by modular transformations.

Let us now study the action of T, under which $z \mapsto z$ and $\tau \mapsto \tau + 1$. We wish to establish a dictionary between the wave functions on a torus with parameter τ and an equivalent torus with parameter $\tau + 1$. Let us now consider [71, equation (37)],

$$\psi^{j,M}(z,\tau,0) \xmapsto{T} \psi^{j,M}(z,\tau+1,0) = \mathrm{e}^{\mathrm{i}\pi\frac{j^2}{|M|}}\, \psi^{j,M}(z,\tau,0)\ . \tag{4.1.56}$$

As shown in [71], this relation holds for even units of magnetic flux M. However, for odd M a relation of the form

$$\psi^{j,M}(z,\tau+1,0) = \sum_{j'=0}^{M-1} [\rho(T)]_{jj'}\, \psi^{j'}(z,\tau,0) \tag{4.1.57}$$

cannot be true because according to equation (4.1.55) both sides have different periodicities. That is, on the left–hand side of the equality (4.1.56) we see a function that is supposed to be "periodic" under $z \mapsto z + \tau'$ whereas on the right–hand side the function is supposed to be "periodic" under $z \mapsto z + \tau$. According to equation (4.1.55), for odd M only one of these "periodicities" can hold.

At first sight, this statement may appear odd. One might think that the zero modes $\psi^{j,M}$ form a basis of eigenmodes of the Dirac operator with eigenvalue 0. So one may expect that the transformed wave functions can be expanded in terms of the original ones as in equation (4.1.57). However, this argument is incorrect. When we write down our wave functions we make a choice for the origin of the torus. *A priori* there are arbitrarily many choices possible, which may be parametrized by Δz in $\psi^{j,M}(z + \Delta z, \tau, 0)$. So, on general

grounds we only know that

$$\psi^{j,M}(z,\tau+1,0) = \sum_{j'=0}^{M-1} [\rho(T)]_{jj'}\, \psi^{j'}(z+\Delta z,\tau,0) \tag{4.1.58}$$

for some appropriate real constant Δz. As we shall see, an appropriate choice of Δz will allow us to express the transformed wave functions in terms of the original one also for odd M. More concretely, we will impose that $z \mapsto z+\Delta z$, with some real constant Δz that we are going to find. Inserting this ansatz leads to (cf. equation (B.3.9))

$$\psi^{j,M}(z+\Delta z,\tau+1,0) = \widetilde{\mathcal{N}} \mathrm{e}^{\mathrm{i}\,\pi M \Delta z \frac{\mathrm{Im}\, z}{\mathrm{Im}\,\tau}} \mathrm{e}^{\mathrm{i}\,\pi M z \frac{\mathrm{Im}\, z}{\mathrm{Im}\,\tau}} \vartheta\begin{bmatrix} \frac{j}{M} \\ 0 \end{bmatrix}(M(z+\Delta z+1/2), M\tau) \tag{4.1.59}$$

Thus, if $N := M(\Delta z + 1/2)$ is an integer, we might use equation (B.1.5a), which we recast here in a slightly different form

$$\vartheta\begin{bmatrix} \frac{j}{M} \\ 0 \end{bmatrix}(Mz+N,\tau) = \mathrm{e}^{2\pi \mathrm{i}\, N \alpha}\, \vartheta\begin{bmatrix} \frac{j}{M} \\ 0 \end{bmatrix}(Mz, M\tau)\ , \tag{4.1.60}$$

to get rid of the extra factor in the z coordinate of the ϑ function. Finally, after the redefinition $z \mapsto z-\Delta z$, we obtain

$$\psi^{j,M}(z,\tau,0) \overset{T}{\longmapsto} \mathrm{e}^{\mathrm{i}\pi M \Delta z \frac{\mathrm{Im}(z)}{\mathrm{Im}\,\tau}}\, \mathrm{e}^{\mathrm{i}\pi \frac{j^2}{|M|} + 2\mathrm{i}\pi j \Delta z}\, \psi^{j,M}(z-\Delta z,\tau,0)\ . \tag{4.1.61}$$

Note that in order to get an integer N, it is sufficient to demand an integer or half–integer Δz for even M. For $\Delta z = 0$ equation (4.1.61) reproduces equation (4.1.56). However, for odd M we need a half–integer Δz. Specifically, for $\Delta z = 1/2$ we find that (see appendix B.3

for details)

$$\psi^{j,M}(z,\tau,0) \overset{S}{\longmapsto} \frac{\mathrm{e}^{\mathrm{i}\frac{\pi}{4}}}{\sqrt{M}}\bigg(-\frac{\tau}{|\tau|}\bigg)^{1/2}\sum_{k=0}^{M-1}\mathrm{e}^{2\pi\mathrm{i}jk/M}\,\psi^{k,M}(z,\tau,0)$$
$$= -\bigg(-\frac{\tau}{|\tau|}\bigg)^{1/2}\Big[\rho(S)^{\psi}_{M}\Big]_{jk}\psi^{k,M}(z,\tau,0)\ , \tag{4.1.62a}$$
$$\psi^{j,M}(z,\tau,0) \overset{T}{\longmapsto} \mathrm{e}^{\mathrm{i}\pi M\frac{\mathrm{Im}\,z}{2\,\mathrm{Im}\,\tau}}\,\mathrm{e}^{\mathrm{i}\pi j(j/M+1)}\,\psi^{j,M}(z-1/2,\tau,0)$$
$$= \mathrm{e}^{\mathrm{i}\pi M\frac{\mathrm{Im}\,z}{2\,\mathrm{Im}\,\tau}}\Big[\rho(T)^{\psi}_{M}\Big]_{jk}\psi^{k,M}(z-1/2,\tau,0)\ , \tag{4.1.62b}$$

where

$$\Big[\rho(S)^{\psi}_{M}\Big]_{jk} := -\frac{\mathrm{e}^{\mathrm{i}\pi/4}}{\sqrt{M}}\exp\bigg(\frac{2\pi\mathrm{i}\,j\,k}{M}\bigg)\ , \tag{4.1.63a}$$
$$\Big[\rho(T)^{\psi}_{M}\Big]_{jk} := \exp\bigg[\mathrm{i}\pi\,j\bigg(\frac{j}{M}+1\bigg)\bigg]\delta_{jk}\ . \tag{4.1.63b}$$

As we shall confirm shortly in equation (4.1.73), the matrices (4.1.63) equal, up to a phase in equation (4.1.63a), representation matrices of the generators of finite metaplectic modular groups. They are compatible with [58, 70–72], but (4.1.63a) differs from [98] by the $\mathrm{e}^{\mathrm{i}\pi/4}$ phase. For even M, the T transformation can rather be represented as in equations (4.1.62) and (4.1.63) or equation (4.1.56) due to the freedom of choosing half–integer or integer Δz. However, since the Yukawa integral involves wave functions with both odd and even fluxes M, we need to be consistent in our choice of Δz to cancel the z–dependent phase appearing in equation (4.1.62b) (cf. equation (B.5.3)). Specifically, we need $\Delta z = 1/2$ for the T transformation also for even M, in which case our results differ from [58, 70, 71, 98] by phase factors which are absent in equation (4.1.56). Nevertheless, the modular T transformation of the 2D compact wave functions for odd M was excluded in [58, 70, 71, 98]. In [72] they were introduced through the so–called Scherk–Schwarz phases. In particular, our equations (4.1.62) and (4.1.63) are consistent with their discussion in [72, equation (126)]. However, as discussed in section 4.1.6, we disagree with the statement made in [58, 70–72,

98] that the modular transformed wave functions do not follow the appropriate boundary conditions. As we have shown, the T transformation can generally *not* be represented by a matrix multiplication of the set of wave functions, but necessarily goes beyond this. However, as we discuss in appendix B.5, the extra exponential factors in equation (4.1.62b) get canceled in the overlap integral (4.1.10), thus allowing us to define a matrix representation for the transformation of the 4D fields, which derive from equation (4.1.63).

Modular Flavor Symmetries in the Effective 4D Theory

Let us now define proper "modular flavor transformation" for the 4D fields. The first thing to notice is that these transformations *cannot be unique*, at least not in models of this type.[†] The reason is that there are additional symmetries at play, such as the remnant gauge factors, and we can always add an extra transformation to our transformation law. That is to say that the details of the representation matrices of a modular flavor symmetries acting on the fields are somewhat ambiguous. Let us start with something unambiguous: the transformation of the Yukawa couplings. As we have seen in equation (4.1.38), there are *a priori* λ Yukawa couplings, out of which at most $\lambda/2+1$ are independent, as shown in appendix B.4.

Let us make an important distinction between "physical Yukawa coupling" Y_{ijk} and "holomorphic Yukawa couplings" $\mathcal{Y}_{ijk}$ [67], which are related by (cf. [30, equation (5.41)])

$$Y_{ijk}(\tau) = \mathrm{e}^{\widehat{K}/2}\,\frac{\mathcal{Y}_{ijk}(\tau)}{(K_{i\bar{i}}\,K_{j\bar{j}}\,K_{k\bar{k}})^{1/2}}\ . \tag{4.1.64}$$

Here, $\widehat{K}$ stands for the Kähler potential of the moduli, which is, in our truncated setup, at tree level given by equation (4.1.47). The formula for the Yukawa couplings (4.1.38), which we obtained from the overlap integral (4.1.10), contains the normalization factor (4.1.39),

[†]It has been suggested that the modular flavor symmetries can be defined by the requirement that the 6D fields remain invariant [98]. However, apart from the fact that this prescription fails for odd M since the 2D coordinates gets shifted (cf. equation (4.1.62b)), it is not clear to us why one should impose this very requirement.

which is not holomorphic. In our case, the matter field Kähler metric is proportional to $(\mathrm{Im}\,\tau)^{-1/2}$ (cf. equation (4.1.43)), so (cf. [30, section 5.3])

$$\frac{\mathrm{e}^{\widehat{K}/2}}{(K_{i\bar{i}}\,K_{j\bar{j}}\,K_{k\bar{k}})^{1/2}} = \mathcal{N}_{abc} \propto g\left(\frac{\mathrm{Im}\,\tau}{\mathcal{A}^2}\right)^{1/4} . \tag{4.1.65}$$

While $Y_{ijk}(\tau)$ is normalized and thus "physical", it is not holomorphic. On the other hand, the superpotential coupling

$$\mathcal{Y}_{ijk}(\tau) = \vartheta\begin{bmatrix}\widehat{\alpha}_{ijk}/\lambda\\ 0\end{bmatrix}(0,\lambda\,\tau) \tag{4.1.66}$$

is a proper modular form. Here, we have made use of the fact that the upper characteristic is of the form $\widehat{\alpha}_{ijk}/\lambda$ with some integer $\widehat{\alpha}_{ijk}$, cf. the discussion below equation (4.1.38), and we set, as done throughout this section, the Wilson lines to zero. Further, all additional non–zero factors appearing in equation (4.1.38) must be included in the Kähler potential, so that they are canceled in the holomorphic couplings through the redefinition (4.1.64). The holomorphic coupling $\mathcal{Y}_{ijk}(\tau)$ differs from the physical coupling between canonically normalized fields by a non–holomorphic factor. The modular transformations are seemingly non–unitary because of the automorphy factor has generally not modulus 1. However, the automorphy factors get canceled, cf. our discussion below equation (4.1.71).

As shown in appendix B.5, the λ–plet of Yukawa couplings transforms with the simple transformation law

$$\mathcal{Y}_{\widehat{\alpha}}(\tau) \overset{\widetilde{\gamma}}{\longmapsto} \mathcal{Y}_{\widehat{\alpha}}(\widetilde{\gamma}\,\tau) = \pm(c\,\tau+d)^{1/2}\,\rho_{\boldsymbol{\lambda}}(\widetilde{\gamma})_{\widehat{\alpha}\widehat{\beta}}\,\mathcal{Y}_{\widehat{\beta}}(\tau)\ , \tag{4.1.67}$$

where $\widehat{\alpha}$ and $\widehat{\beta}$ are integers that label the distinct Yukawa couplings, and we use the metaplectic element $\widetilde{\gamma} \in \widetilde{\Gamma}$ instead of $\gamma \in \Gamma$ because the Yukawa couplings have weight $k_Y = 1/2$.

The transformation matrices of the modular generators are given by

$$\rho_{\boldsymbol{\lambda}}(\widetilde{S})_{\widehat{\alpha}\widehat{\beta}} = -\frac{\mathrm{e}^{\mathrm{i}\pi/4}}{\sqrt{\lambda}}\,\exp\!\left(\frac{2\pi\mathrm{i}\,\widehat{\alpha}\,\widehat{\beta}}{\lambda}\right)\,, \tag{4.1.68a}$$

$$\rho_{\boldsymbol{\lambda}}(\widetilde{T})_{\widehat{\alpha}\widehat{\beta}} = \exp\!\left(\frac{\mathrm{i}\pi\,\widehat{\alpha}^2}{\lambda}\right)\delta_{\widehat{\alpha}\widehat{\beta}}\,. \tag{4.1.68b}$$

These matrices are symmetric and unitary, so that

$$[\rho_{\boldsymbol{\lambda}}(\widetilde{S})_{\widehat{\alpha}\widehat{\beta}}]^{-1} = [\rho_{\boldsymbol{\lambda}}(\widetilde{S})_{\widehat{\alpha}\widehat{\beta}}]^{*} \quad \text{and} \quad [\rho_{\boldsymbol{\lambda}}(\widetilde{T})_{\widehat{\alpha}\widehat{\beta}}]^{-1} = [\rho_{\boldsymbol{\lambda}}(\widetilde{T})_{\widehat{\alpha}\widehat{\beta}}]^{*}\,. \tag{4.1.69}$$

Since there can be relations between the Yukawa couplings, this may not be an irreducible representation. The relations between the Yukawa couplings depend on the choice of fluxes. We will specify the irreducible representations of the Yukawa couplings in our survey of models in section 4.1.8. The modular transformations of the Yukawa couplings given by equation (4.1.10) were also studied in [98]. Although an explicit general formula for any combination of $\mathcal{I}_{\alpha\beta}$ was not given in their work, our results from equation (4.1.68) match their result up to the phase $\mathrm{e}^{\mathrm{i}\frac{\pi}{4}}$ in the model described in section 4.1.8. This phase is crucial to have the transformation matrices (4.1.68) satisfy the presentation (1.31) and, thus, give rise to representations of a finite metaplectic modular group, as was noted in [58]. Note also that there is an extra minus in our equation (4.1.68) compared to [98, equations (64) and (108)] and [58]. However, this sign comes only from our convention that the automorphy factor is $\varphi(S,\tau) = -\sqrt{-\tau}$ in equation (1.30).

Next, we discuss modular flavor symmetries. They are, by definition, symmetry transformations of the 4D Lagrange density. In our present discussion, we are thus seeking transformations of the 4D fields, $\phi^{j,M}$, which are such that superpotential couplings

$$\mathscr{W} \supset \mathcal{Y}_{ijk}(\tau)\,\phi^{i,\mathcal{I}_{ab}}\,\phi^{j,\mathcal{I}_{ca}}\,\phi^{k,\mathcal{I}_{cb}} \tag{4.1.70}$$

are invariant up to Kähler transformations, cf. the discussion around (4.1.45). Here, $\mathcal{I}_{cb} = -\mathcal{I}_{bc} = \mathcal{I}_{ab} + \mathcal{I}_{ca} > 0$. That is, our modular flavor transformations are given by

$$\phi^{j,M} \xmapsto{\widetilde{\gamma}} \pm(c\,\tau + d)^{-1/2} \left[\rho^{\phi}_{M}(\widetilde{\gamma})\right]^{-1}_{jk} \phi^{k,M} \ . \tag{4.1.71}$$

Notice that, due to equations (4.1.67) and (4.1.71), the superpotential acquires modular weight $k_{\mathscr{W}} = -1$, see equation (4.1.45). The corresponding automorphy factor gets canceled by the transformation of τ in the Kähler potential followed by a Kähler transformation, see our discussion around equation (4.1.49). Therefore, the requirement that the modular transformations be a symmetry amounts to demanding that

$$\begin{aligned}\mathcal{Y}_{ijk}(\widetilde{\gamma}\,\tau) \left[\rho^{\phi}_{\boldsymbol{\mathcal{I}_{ab}}}(\widetilde{\gamma})\right]^{-1}_{ii'} \phi^{i',\mathcal{I}_{ab}} \left[\rho^{\phi}_{\boldsymbol{\mathcal{I}_{ca}}}(\widetilde{\gamma})\right]^{-1}_{jj'} \phi^{j',\mathcal{I}_{ca}} \left[\rho^{\phi}_{\overline{\boldsymbol{\mathcal{I}_{cb}}}}(\widetilde{\gamma})\right]^{-1}_{kk'} \phi^{k',\mathcal{I}_{cb}} \\ \overset{!}{=} \mathcal{Y}_{ijk}(\tau)\, \phi^{i,\mathcal{I}_{ab}}\, \phi^{j,\mathcal{I}_{ca}}\, \phi^{k,\mathcal{I}_{cb}} \ .\end{aligned} \tag{4.1.72}$$

As already mentioned, this condition does not fix the transformation laws of the 4D fields uniquely. However, we can use the transformation properties of the $\mathbb{T}^2$ wave functions, (cf. equations (B.5.3) and (B.5.4)), to infer the matrix structure of the transformations. One way in which we may infer the transformations of the 4D fields is by using the *quasi–*inverse transformations of the compact wave functions, that is, the inverse transformations of equation (4.1.63). However, a more convenient choice is

$$\rho^{\phi}_{\boldsymbol{M}}(\widetilde{S})_{jk} = -\frac{\mathrm{e}^{\mathrm{i}\pi(3M+1)/4}}{\sqrt{M}} \exp\left(\frac{2\pi\mathrm{i}\, j\, k}{M}\right) \ , \tag{4.1.73a}$$

$$\rho^{\phi}_{\boldsymbol{M}}(\widetilde{T})_{jk} = \exp\left[\mathrm{i}\pi\, j\left(\frac{j}{M} + 1\right)\right] \delta_{jk} \ , \tag{4.1.73b}$$

where we have chosen the transformation (4.1.63a) multiplied by a phase $\mathrm{e}^{3\mathrm{i}\pi\frac{M}{4}}$ in the S matrix representation. These matrices fulfill equation (4.1.69), too. This choice has the virtue that $\rho_{\overline{\boldsymbol{M}}}(\widetilde{\gamma}) = [\rho_{\boldsymbol{M}}(\widetilde{\gamma})]^*$ and that, as we will demonstrate in section 4.1.8, it yields the

correct representation matrices for the group $\widetilde{\Gamma}_{2\lambda}$.

We also note that, as far as the Yukawa couplings are concerned, there is a U(1) symmetry due to the condition of equation (4.1.12), which acts as

$$\phi^{j,\mathcal{I}_{\alpha\beta}} \xmapsto{\mathrm{U}(1)} \mathrm{e}^{\mathrm{i}q\alpha\mathcal{I}_{\alpha\beta}}\phi^{j,\mathcal{I}_{\alpha\beta}} \ , \tag{4.1.74}$$

where $\alpha, \beta \in \{a, b, c\}$ as in equation (4.1.11). Here, $\phi^{\mathcal{I}_{ab}}, \phi^{\mathcal{I}_{ca}}$ have a charge $+1$ and $\phi^{\mathcal{I}_{cb}}$ a charge -1. This U(1) factor allows one to install "extra" phases of the above type. Note that while the T–transformed wave functions, for odd M, cannot be expanded in terms of untransformed wave functions, the additional factor in our dictionary (4.1.62b) cancels in the overlap integrals (4.1.10) so that there is a meaningful, well–defined modular flavor transformation of the 4D fields also for odd M. Our proposal in equation (4.1.73) for the transformations of 4D fields $\phi^{j,M}$ for even values of M differs from the results in [98]. While [98] assumes that the modular transformations of the 4D fields coincide with those of the 2D wave functions, we assume the 4D fields transform quasi–inversely to the 2D wave functions. Furthermore, we have an extra phase $\mathrm{e}^{3\mathrm{i}\pi\frac{M}{4}}$, which is useful to achieve metaplectic group representations. Note that we specify the T transformation, rather than just the T^2 representation as in [98].

4.1.8 An Example Model

In this subsection, we note an important toy model. While far from realistic, this highlights how modular flavor symmetries derive from some simple magnetized tori with even and odd numbers of repetitions of matter fields. For the example model will use the representation matrices stated in equation (4.1.73) for the $\mathcal{I}_{cb}$–plet of ϕ^k 4D fields, while the $\mathcal{I}_{ab}$–plet of ϕ^i and $\mathcal{I}_{ca}$–plet of ϕ^j 4D fields will transform in the conjugate representation. On the other hand, the λ–plet of Yukawa couplings will follow the representation matrices found in equa-

tion (4.1.68). We will show that the modular flavor symmetries in such models are given by $\widetilde{\Gamma}_{2\lambda}$ with λ being the least common multiple of matter repetition numbers (4.1.32b). Furthermore, using equation (4.1.33) one can see that for a fixed total number of Yukawa couplings P, the largest number of independent Yukawa couplings, that is the largest λ, is obtained by having the least possible d. Although we have proposed the representation matrices for the 4D fields in equation (4.1.73), the ones for the Yukawa couplings equation (4.1.68) are unambiguous. For the model we discuss here, we will find that the representations $\rho_{\boldsymbol{\lambda}}$ satisfy equation (1.31) together with the finiteness conditions (1.32)–(1.33) for $N = 2, 3$, with $\lambda = 2N$. Thus, the modular transformations of the Yukawa couplings build representations of the finite metaplectic group $\widetilde{\Gamma}_{2\lambda}$. In [58] it was also noted that, for even numbers of flavors, the Yukawa couplings transform as a λ–plet under the metaplectic group. However, in [58] it does not get mentioned that for $\lambda > 2$ this representation is reducible, which is rather easy to see from our general compact expression (4.1.38), but less obvious when one represents the Yukawa coupling as the sum (4.1.22). Moreover, we will demonstrate that the transformations of the 4D fields encoded in $\rho^{\phi}_{\boldsymbol{\mathcal{I}_{\alpha\beta}}}$ build representations of the same group, so that $\widetilde{\Gamma}_{2\lambda}$ can be regarded as the modular flavor symmetry of the models. We are hence led to conjecture that, with λ from equation (4.1.32b),

magnetized tori with $\lambda = \mathrm{lcm}(\#\text{ of flavors})$ exhibit a $\widetilde{\Gamma}_{2\lambda}$ modular flavor symmetry . (4.1.75)

Model with $\boldsymbol{\mathcal{I}_{ab} = \mathcal{I}_{ca} = 3}$ and $\boldsymbol{\mathcal{I}_{bc} = -6}$

Let us consider a three generation toy model, based on a super–Yang–Mills theory in six dimensions with gauge group U(4) [98]. The two extra dimensions are compactified on $\mathbb{T}^2$,

field	$\mathrm{SU}(2) \times \mathrm{U}(1)_a \times \mathrm{U}(1)_b \times \mathrm{U}(1)_c$ quantum numbers	# of copies
L	$\mathbf{2}_{(1,-1,0)}$	$\mathcal{I}_{ab} = 2 - (-1) = 3$
R	$\mathbf{1}_{(0,+1,-1)}$	$\mathcal{I}_{bc} = -1 - (5) = -6$
H	$\mathbf{2}_{(-1,0,1)}$	$\mathcal{I}_{ca} = 5 - (2) = 3$

Table 4.1.2: Matter content of the 336 model.

and the U(4) gauge symmetry gets broken to $\mathrm{SU}(2) \times \mathrm{U}(1)_a \times \mathrm{U}(1)_b \times \mathrm{U}(1)_c$ by the fluxes

$$F = \frac{\pi \mathrm{i}}{\mathrm{Im}\,\tau} \begin{pmatrix} \mathbb{1}_{2\times 2} & 0 & 0 \\ 0 & -3 & 0 \\ 0 & 0 & 3 \end{pmatrix} , \tag{4.1.76}$$

where we used equation (4.1.9). The chiral matter content of the supersymmetric model is given in table 4.1.2. They decompose into three generations of L particles, six generations of R particles and three generations of H particles. The superpotential of this model is given by

$$\mathscr{W} \supset \mathcal{Y}_{ijk} L^i H^j R^k , \tag{4.1.77}$$

where the (holomorphic) Yukawa couplings are given by equation (4.1.38),

$$\mathcal{Y}_{ijk}(\tau) = \vartheta \begin{bmatrix} \frac{k-2j}{6} \\ 0 \end{bmatrix} (0, 6\tau) . \tag{4.1.78}$$

Here we used the values from table 4.1.2 and assumed zero Wilson lines. The explicit transformation matrices for the L^i and H^j are given by (4.1.73) for $M = 3$, and are the

conjugates of

$$\rho^{\phi}_{\mathbf{3}}(\widetilde{S}) = -\frac{1}{\sqrt{3}}\begin{pmatrix} \mathrm{i} & \mathrm{i} & \mathrm{i} \\ \mathrm{i} & \mathrm{e}^{-\frac{5\mathrm{i}\pi}{6}} & \mathrm{e}^{-\frac{\mathrm{i}\pi}{6}} \\ \mathrm{i} & \mathrm{e}^{-\frac{\mathrm{i}\pi}{6}} & \mathrm{e}^{-\frac{5\mathrm{i}\pi}{6}} \end{pmatrix} \quad \text{and} \quad \rho^{\phi}_{\mathbf{3}}(\widetilde{T}) = \begin{pmatrix} 1 & 0 & 0 \\ 0 & \mathrm{e}^{-\frac{2\mathrm{i}\pi}{3}} & 0 \\ 0 & 0 & \mathrm{e}^{-\frac{2\mathrm{i}\pi}{3}} \end{pmatrix} . \tag{4.1.79}$$

The explicit transformation matrices for the R^k fields are given by equation (4.1.73) for $M = 6$

$$\rho^{\phi}_{\mathbf{6}}(\widetilde{S}) = -\mathrm{i}\,\frac{\mathrm{e}^{\mathrm{i}\frac{\pi}{4}}}{\sqrt{6}}\begin{pmatrix} 1 & 1 & 1 & 1 & 1 & 1 \\ 1 & \mathrm{e}^{\frac{\pi\mathrm{i}}{3}} & \mathrm{e}^{\frac{2\pi\mathrm{i}}{3}} & -1 & \mathrm{e}^{-\frac{2\pi\mathrm{i}}{3}} & \mathrm{e}^{-\frac{\pi\mathrm{i}}{3}} \\ 1 & \mathrm{e}^{\frac{2\pi\mathrm{i}}{3}} & \mathrm{e}^{-\frac{2\pi\mathrm{i}}{3}} & 1 & \mathrm{e}^{\frac{2\pi\mathrm{i}}{3}} & \mathrm{e}^{-\frac{2\pi\mathrm{i}}{3}} \\ 1 & -1 & 1 & -1 & 1 & -1 \\ 1 & \mathrm{e}^{-\frac{2\pi\mathrm{i}}{3}} & \mathrm{e}^{\frac{2\pi\mathrm{i}}{3}} & 1 & \mathrm{e}^{-\frac{2\pi\mathrm{i}}{3}} & \mathrm{e}^{\frac{2\pi\mathrm{i}}{3}} \\ 1 & \mathrm{e}^{-\frac{\pi\mathrm{i}}{3}} & \mathrm{e}^{-\frac{2\pi\mathrm{i}}{3}} & -1 & \mathrm{e}^{\frac{2\pi\mathrm{i}}{3}} & \mathrm{e}^{\frac{\pi\mathrm{i}}{3}} \end{pmatrix} , \tag{4.1.80a}$$

$$\rho^{\phi}_{\mathbf{6}}(\widetilde{T}) = \mathrm{diag}\big(1, \mathrm{e}^{-\frac{5\pi\mathrm{i}}{6}}, \mathrm{e}^{\frac{2\pi\mathrm{i}}{3}}, \mathrm{i}, \mathrm{e}^{\frac{2\pi\mathrm{i}}{3}}, \mathrm{e}^{-\frac{5\pi\mathrm{i}}{6}}\big) . \tag{4.1.80b}$$

As discussed at the end of section 4.1.2, there are only $\lambda/2 + 1 = 4$ independent Yukawa couplings,[‡]

$$Y_0 := Y_{i=j,j,k=2j} , \qquad Y_1 := Y_{i=j+1,j,k=2j+1} = Y_5 := Y_{i=j+2,j,k=2j+5} , \tag{4.1.81a}$$

$$Y_3 := Y_{i=j,j,k=2j+3} , \qquad Y_2 := Y_{i=j+2,j,k=2j+2} = Y_4 := Y_{i=j+1,j,k=2j+4} , \tag{4.1.81b}$$

where i and j are understood to be modulo 3, and k modulo 6. The six–plet of holomorphic Yukawa coupling coefficients $\mathcal{Y}_{\mathbf{6}} = (\mathcal{Y}_0, \mathcal{Y}_1, \mathcal{Y}_2, \mathcal{Y}_3, \mathcal{Y}_4, \mathcal{Y}_5)^T$ obeys the transformation law

[‡]The relations given in equation (4.1.81) are valid for both holomorphic and non–holomorphic Yukawa couplings.

equation (4.1.67) under modular transformations, with the matrix representations

$$\rho_{\mathbf{6}}(\widetilde{S}) = -\mathrm{i}\,\rho^{\phi}_{\mathbf{6}}(\widetilde{S}) \quad \text{and} \quad \rho_{\mathbf{6}}(\widetilde{T}) = \mathrm{diag}\big(1, \mathrm{e}^{\frac{\pi\mathrm{i}}{6}}, \mathrm{e}^{\frac{2\pi\mathrm{i}}{3}}, -\mathrm{i}, \mathrm{e}^{\frac{2\pi\mathrm{i}}{3}}, \mathrm{e}^{\frac{\pi\mathrm{i}}{6}}\big)\ . \tag{4.1.82}$$

However, the 6×6 matrices can be reduced to a 4–dimensional representation due to the relation between the Yukawa couplings in equation (4.1.81). Using the projection matrix

$$P_{6\to4} = \begin{pmatrix} 1 & 0 & 0 & 0 \\ 0 & \frac{1}{\sqrt{2}} & 0 & 0 \\ 0 & 0 & \frac{1}{\sqrt{2}} & 0 \\ 0 & 0 & 0 & 1 \\ 0 & 0 & \frac{1}{\sqrt{2}} & 0 \\ 0 & \frac{1}{\sqrt{2}} & 0 & 0 \end{pmatrix}\ , \tag{4.1.83}$$

we can define the **4**–plet of independent Yukawa couplings through $\mathcal{Y}_{\mathbf{4}} = P^{T}_{6\to4}\mathcal{Y}_{\mathbf{6}}$, which transform as modular forms with the representation matrices given by

$$\rho_{\mathbf{4}}(\widetilde{S}) = P^{T}_{6\to4}\rho_{\mathbf{6}}(\widetilde{S})P_{6\to4} = -\frac{\mathrm{e}^{\mathrm{i}\frac{\pi}{4}}}{\sqrt{6}}\begin{pmatrix} 1 & \sqrt{2} & \sqrt{2} & 1 \\ \sqrt{2} & 1 & -1 & -\sqrt{2} \\ \sqrt{2} & -1 & -1 & \sqrt{2} \\ 1 & -\sqrt{2} & \sqrt{2} & -1 \end{pmatrix}\ , \quad \text{and} \tag{4.1.84a}$$

$$\rho_{\mathbf{4}}(\widetilde{T}) = P^{T}_{6\to4}\,\rho_{\mathbf{6}}(\widetilde{T})\,P_{6\to4} = \begin{pmatrix} 1 & 0 & 0 & 0 \\ 0 & \mathrm{e}^{\frac{\pi\mathrm{i}}{6}} & 0 & 0 \\ 0 & 0 & \mathrm{e}^{\frac{2\pi\mathrm{i}}{3}} & 0 \\ 0 & 0 & 0 & -\mathrm{i} \end{pmatrix}\ . \tag{4.1.84b}$$

The representation matrices in equations (4.1.79), (4.1.80), (4.1.82) and (4.1.84) fulfill the conditions (1.31) for $N = 3$ and (1.33), which implies that this model exhibits a $\widetilde{\Gamma}_{2\lambda=12}$ finite modular symmetry of order 2304. The fact that there are only four distinct Yukawa entries implies that the 6–dimensional representation of the Yukawa couplings decomposes into $\widetilde{\Gamma}_{12}$ irreducible representations according to $\mathbf{6} = \mathbf{4} \oplus \mathbf{2}$, as we have confirmed, where the doublet vanishes. As we shall discuss below, this can be also attributed to the existence of an outer automorphism. Using the character tables (cf. [103, section 3.4]), we find that the matter triplets and six–plets are reducible as well, $\mathbf{3} = \mathbf{2''} \oplus \mathbf{1'}$ and $\mathbf{6'} = \mathbf{4'} \oplus \mathbf{2'}$, where we added primes to indicate that these are different representation matrices, and that the singlet is nontrivial. We have verified that the reducible representation $\mathbf{6'}$ provides us with a faithful representation content of $\widetilde{\Gamma}_{12}$ and its tensor products yield all other representations of the group. The six $\mathcal{Y}_{\widehat{\alpha}}$ have been identified in [98], where they have been represented as sums of three different ϑ–functions each, and the relations $Y_1 = Y_5$ and $Y_2 = Y_4$ have been missed. The latter relations are actually quite interesting as they can be thought of as $i \leftrightarrow j$ exchange symmetries,

$$Y_{ijk}(\tau) = Y_{jik}(\tau) \ . \tag{4.1.85}$$

However, the wave functions labeled i and j, i.e. the L^i and H^j, have *different* quantum numbers in 4D (and in the upstairs theory). This means that this symmetry is not an "ordinary" flavor symmetry but an outer automorphism of the low-energy gauge symmetry. Note that the existence of this very outer automorphism depends on the specifics of the model. Examples for such outer automorphisms include the so–called left–right parity [88]. It is known that such symmetries can originate as discrete remnants of gauge symmetries either by dialing appropriate VEVs [23, 69] or by orbifolding [16]. As the exchange of the U(1) factors is part of the original U(4) gauge symmetry of the model, we have identified yet another way in which these outer automorphism can emerge from an explicit gauge

symmetry.

A geometric interpretation of Yukawa couplings. It is instructive to discuss the geometrical interpretation of these results. We have derived the couplings by computing the overlaps of wave functions, see (4.1.10). The result is that, up to a normalization factor, the Yukawa couplings are given by

$$Y_{\widehat{\alpha}} \propto (\operatorname{Im}\tau)^{-1/4}\,\vartheta\begin{bmatrix}\widehat{\alpha}/\lambda\\ 0\end{bmatrix}(0,\lambda\,\tau) = (\operatorname{Im}\tau)^{-1/4}\sum_{\ell=-\infty}^{\infty}\mathrm{e}^{-\pi\,\lambda(\operatorname{Im}\tau-\mathrm{i}\,\operatorname{Re}\tau)(\widehat{\alpha}/\lambda+\ell)^2}\ , \tag{4.1.86}$$

where we have used equation (B.1.4). Here we choose to highlight the fact that the terms are exponentially suppressed by $\mathrm{e}^{-\pi\,\lambda\,\operatorname{Im}\tau\,\xi}$ with some $\xi > 0$ in order to compare our result for the Yukawa couplings with a simple overlap of Gaussians. For simplicity, we just consider two Gaussians, and consider

$$y(a,b_1,b_2) = \int_{-\infty}^{\infty}\mathrm{d}x\,\mathcal{N}_{b_1}\,\mathrm{e}^{-x^2/b_1}\,\mathcal{N}_{b_2}\,\mathrm{e}^{-(x-a)^2/b_2} = \frac{\mathrm{e}^{-a^2/(b_1+b_2)}}{\sqrt{\pi}\sqrt{b_1+b_2}} \tag{4.1.87}$$

with Gaussian normalization factors $\mathcal{N}_b = 1/\sqrt{b\pi}$. In order to compute the overlap on the torus, one does not only have to compute the overlap of a given Gaussian of width b_1, say, with one Gaussian of width b_2, but with all images of the second Gaussian under torus translations. This leads to an expression which is qualitatively similar to the sum on the right–hand side of equation (4.1.86).

Turning this around, the upper characteristics $\widehat{\alpha}$ in equations (4.1.38) and (4.1.86), or, more precisely, $\min\bigl(|\widehat{\alpha}/\lambda|, |1-\widehat{\alpha}/\lambda|\bigr)$ with $0 \leq |\widehat{\alpha}/\lambda| < 1$, has the interpretation of a "distance between the loci of the states", i.e. a in figure 4.1.1. We illustrate this by plotting some sample Yukawa couplings in figure 4.1.2. This geometric intuition may conceivably provide us with an understanding of the observed hierarchies of fermion masses. Apart from the

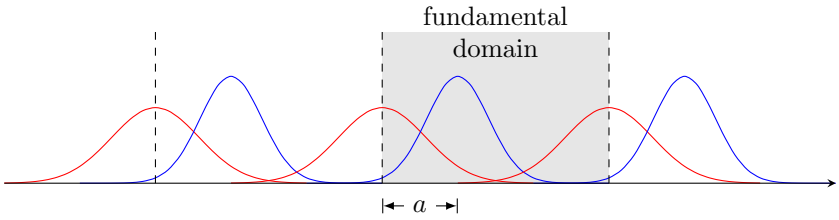

Figure 4.1.1: Overlap of two Gaussians on a torus. The overlap of a given, say red, curve is not just the overlap with one blue curve but with infinitely many of them, thus leading to an expression of the form (4.1.86).

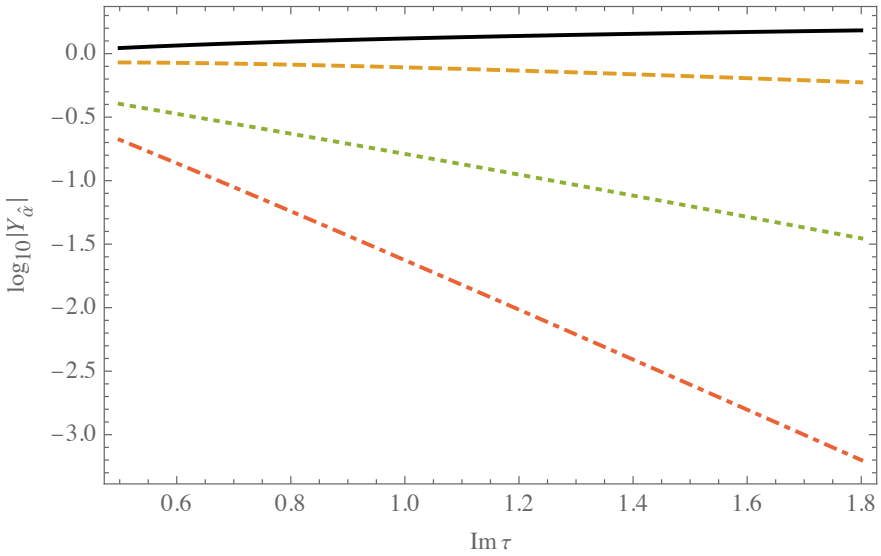

Figure 4.1.2: Dependence of the magnitude of the Yukawa couplings $Y_{\widehat{\alpha}}$ for $\mathrm{Re}\,\tau = 0.1$. The black solid, orange dashed, green dotted and red dash–dotted curves represent $\widehat{\alpha} = 0$, 1, 2 and 3, respectively. There is an exponential suppression with $\mathrm{Im}\,\tau$ that depends on the "distance" between the wave functions $\widehat{\alpha}$, i.e. the $\mathrm{Im}\,\tau$ dependence is more pronounced for larger $\widehat{\alpha}$.

fact that the kinetic terms are under control, the geometric interpretation may be one of the strongest motivations for deriving the modular flavor symmetries from explicit tori.

4.1.9 Comments on the Relation to Bottom–up Constructions

As we have seen, the models derived from explicit tori give rise to the finite metaplectic groups, which have been discussed e.g. in [84] in the context of bottom–up model building. The models presented here do not attempt to make an immediate connection to particle phenomenology. At first sight, it seems to be hard to derive the models of [84] from tori for

at least two reasons:

1. our fields all have modular weight $-1/2$ while in [84] they come with a variety of weights, and

2. we have additional symmetries like the outer automorphism symmetry (4.1.85) and residual gauge factors.

On the other hand, deriving the modular transformations from an explicit higher–dimensional model has the virtue that normalization of the fields is known at tree level, and that otherwise free parameters get fixed. Of course, the Kähler potential is not exact, apart from the usual 4D corrections there are additional terms contributing (cf. [36]), yet the point that there is a zeroth order classical form plus corrections, which are under control. On the other hand, in the SB approach every invariant Kähler potential is as good as others [27], and there are thus large uncertainties. An additional benefit of deriving the modular flavor symmetries from explicit tori is the geometrical intuition one can develop for the Yukawa couplings, cf. our discussion at the end of section 4.1.8.

One may now wonder if the price that one has to pay for all these benefits is the inability to construct semi–realistic models. In what follows, we will argue that this is not the case. First of all, the $\mathbb{T}^2$ model is just a building block of a more complete story. As explained in [30], these models are dual to some intersecting D–brane constructions. Moreover, the couplings of the latter are closely related to heterotic string compactifications [3], which provide us with a large number of potentially realistic models [61].[§] These more complete settings come with a variety of modular weights [59]. Second, even if one is not adding more dimensions to the construction, fields with higher modular weights can emerge as composites of fields with modular weight $-1/2$. That is, if "quarks" of a model with an $SU(N_c)$ have modular weights

[§]We adopt the convention to call models with realistic and unrealistic features "semi–realistic" while "potentially realistic" models are constructions that have no obviously unrealistic features, but have not yet been analyzed in enough detail to be called realistic.

$-1/2$, then the "baryons" will have weights $-N_c/2$.

4.1.10 Comments on the Role of Supersymmetry

Let us comment on the role SUSY plays in the discussion. While Cremades et al. work in a supersymmetric theory, they mention [30, see the beginning of section 5.3] that their derivation "in principle is valid for toroidal compactifications where supersymmetry might be broken explicitly". Of course, if one wants to claim that the couplings that one has computed are Yukawa couplings, one needs to make sure that one computes the overlap between two fermionic and one bosonic zero–modes. In supersymmetric models there is no problem because the superpartners are described by the same wave functions.

In a model without low–energy SUSY one may be worried that quantum corrections lead to uncontrollable corrections to the wave function of the scalar. This is generally a very valid concern, yet is as recently been observed that in the magnetized tori there is an interesting cancellation of corrections to the scalar mass [20, 21, 53, 56]. While this has not yet led to a complete solution of the hierarchy problem in the SM, it does suggest that in the context of the very models that we were led to consider for the sake of deriving modular flavor symmetries the situation is "better" than in other nonsupersymmetric completions of the SM with a high UV scale. In fact, similar cancellations have been reported in [38], where they were attributed to modular symmetries.

In a bit more detail, one could imagine a torus compactification in which the Yukawa couplings emerge as outlined in [30], namely as the overlap of three wave functions. These wave functions describe two fermions and one scalar, such as the SM Higgs. If the scalars remain light, they will still be approximate zero–modes, and thus the profile is approximately given by equation (4.1.1). So the Yukawa couplings will, to some good approximation, be the ones of equation (4.1.10). So supersymmetry is not instrumental for having models with modular

flavor symmetries.

4.2 Another Concluding Poem

This is another poem I wrote on the work in this chapter:

Take two dimensions you don't live in,
And put them on a torus.
Add to them the magnetic flux,
And the strings strum into a chorus!

The couplings are now modular forms,
Thus a single theta function,
They look like the wavefunctions did,
Without the GCD assumption!

And the boundary conditions are just fine,
The fluxes are chill being odd,
We get our three generations,
To this please just applaud!

Chapter 5

Quasi–Eclectic Modular Flavor Symmetries

(This section is heavily based on the publication with Mu-Chun Chen, Víctor Knapp-Pérez, Mario Ramos-Hamud, Saúl Ramos–Sánchez and Michael Ratz) [24]

5.1 Eclectic Symmetries

In this thesis, we have primarily concerned ourselves with the problem of the flavor sector: determining the number of generations, the neutrino masses, Yukawa couplings, etc. We have seen in chapter 4 that modular flavor symmetries [31,41,49,75,82,84,95,101] present an exciting new approach to the flavor problem. Very simple settings can, in principle, provide us with a surprisingly good fit to data while making a comparatively large number of nontrivial, testable predictions. For more details and models, Feruglio's paper [51] is a great reference. What is the new ingredient of Feruglio's models [49] which appears to make the traditional A_4 models [10, 86] even more compelling? The challenges in traditional models (see e.g. [65] for an extended list of examples and references) lie mainly in the flavon sector. More specifically,

one has to align the flavons at some appropriate values, see e.g. [57] for a discussion and further references. However, often flavons naturally settle at symmetry–enhanced points (see e.g. [80]), which are typically not entirely realistic. As a consequence, the traditional flavor models often require an extended flavon sector, which introduces a number of free parameters, thus limiting the number of nontrivial predictions. Models with modular flavor symmetries evade these arguments because the flavons get replaced by multiplets of modular forms. One then faces the lesser challenge to find, and eventually justify, appropriate values of the half–period ratio τ which the modular forms depend on. The resulting models are very elegant and describe data surprisingly well [51].

However, there is a price one has to pay. The modular flavor symmetries, which we will review in some more detail in Section 4.1.7, are nonlinearly realized. As a consequence, the Kähler potential is not under control [27], i.e. there is no preferred field basis. This introduces additional parameters, thus limiting the predictive power of the construction. On the other hand, in the framework of traditional flavor symmetries the Kähler potential is under control. It is still subject to possibly important corrections [25, 26], but one has at least a perturbative expansion in $\varepsilon = \langle\xi\rangle/\Lambda$, where $\langle\xi\rangle$ denotes the VEV of a so–called flavon and Λ is the cut–off scale.

In this chapter, we show that a hybrid scheme allows us to combine the advantages of both approaches while largely avoiding their limitations. The simplest models of this hybrid approach have a flavor symmetry of the form

$$G_{\text{flavor}} = G_{\text{traditional}} \times G_{\text{modular}} \ , \tag{5.1.1}$$

and a flavon χ, which is charged under both $G_{\text{traditional}}$ and G_{modular}. Once χ acquires a VEV, the flavor symmetry will be broken to its diagonal subgroup,

$$G_{\text{flavor}} = G_{\text{traditional}} \times G_{\text{modular}} \xrightarrow{\langle\chi\rangle} G_{\text{diagonal}} \ . \tag{5.1.2}$$

Matter fields are assumed to transform under $G_{\text{traditional}}$, which is why their Kähler potential is under control [25, 26, 93]. However, after the breaking (5.1.2), their couplings will be effectively given by modular forms.

Our setup is heavily inspired by the scheme of "eclectic flavor groups" [91], which arise naturally in string models [12, 92, 93] and magnetized toroidal compactifications [98]. Generally in top–down models (cf. e.g. [5, 73, 74, 78]) one can, at least in principle, compute the Kähler potential, but at this point it is probably also fair to say that this approach has not yet provided us with completely realistic predictive models. These groups are the result of combining nontrivially a traditional and a modular flavor group, such that G_{modular} is a subgroup of the outer automorphisms of $G_{\text{traditional}}$. Hence, eclectic groups represent a more complex hybrid scheme than Equation (5.1.1), sharing the feature of a controlled Kähler potential due to $G_{\text{traditional}}$. The purpose of the present work is to show how one can, in a bottom–up effective field theory (EFT) approach, combine modular flavor symmetries with perturbative control over the Kähler potential. We leave the question of an explicit stringy completion for future work.

5.1.1 Modular and Eclectic Flavor Symmetries

The half–period ratio or modulus τ of a torus does not uniquely characterize a given torus. Rather, different τ related by transformations in the so–called modular group $\mathrm{PSL}(2,\mathbb{Z})$ describe the same torus. Under an arbitrary element $\gamma \in \mathrm{PSL}(2,\mathbb{Z})$, the modulus and matter superfields Φ_j transform as

$$\tau \xmapsto{\gamma} \gamma\,\tau := \frac{a\,\tau + b}{c\,\tau + d}\ , \tag{5.1.3a}$$

$$\Phi_j \xmapsto{\gamma} (c\,\tau + d)^{k_j}\,\rho_{\boldsymbol{r}_j}(\gamma)\,\Phi_j\ , \quad \text{where } \gamma := \begin{pmatrix} a & b \\ c & d \end{pmatrix} \tag{5.1.3b}$$

with $\det\gamma = 1$ and $a, b, c, d \in \mathbb{Z}$. Further, k_j denotes the so–called modular weight of the matter superfield Φ_j, which can build an r_j–dimensional representation of some finite modular group* Γ_N, $N = 2, 3, \ldots$. $\rho_{\boldsymbol{r}_j}(\gamma)$ corresponds to the $r_j \times r_j$ matrix representation of γ in the finite modular group. This transformation of the matter fields indicates that Γ_N can be regarded as a modular flavor symmetry [31, 49], which is however nonlinearly realized, as is evident from Equation (5.1.3a). Finally, note that the action of the modular flavor symmetry is accompanied by $(c\tau + d)^{k_j}$, which is known as automorphy factor.

Note that, as a consequence of Equation (5.1.3a),

$$(-\mathrm{i}\tau + \mathrm{i}\bar{\tau})^k \overset{\gamma}{\longmapsto} \big((c\,\tau + d)(c\,\bar{\tau} + d)\big)^{-k}(-\mathrm{i}\tau + \mathrm{i}\bar{\tau})^k \ , \tag{5.1.4}$$

for an arbitrary k. This implies that an invariant under the finite modular group is given by

$$(-\mathrm{i}\tau + \mathrm{i}\bar{\tau})^{k_j}\big(\bar{\Phi}_j\Phi_j\big)_{\mathbf{1}} \ , \tag{5.1.5}$$

where the subindex $\mathbf{1}$ refers to the trivial Γ_N singlet(s) resulting from tensoring the superfield Φ_j with its conjugate.

To complete a supersymmetric model based on modular flavor symmetries, we must specify its superpotential and Kähler potential. In terms of the matter fields Φ_j, the superpotential can be expressed as a polynomial of the form

$$\mathscr{W}(\Phi) = \sum_{i,j,k} \hat{Y}_{\boldsymbol{s}}^{(k_Y)}(\tau)\,\Phi_i\Phi_j\Phi_k + \text{higher order terms} \ , \tag{5.1.6}$$

where $\hat{Y}_{\boldsymbol{s}}^{(k_Y)}(\tau)$ are modular forms of level N and modular weights k_Y transforming as an s–dimensional representation of Γ_N. In general, the superpotential is constrained to transform

*We restrict here to Γ_N finite modular groups, but our discussion can be readily extended to their double cover Γ'_N and metaplectic extensions (cf. [5, 82–84, 96, 120, 123]).

according to

$$\mathscr{W}(\Phi) \overset{\gamma}{\longmapsto} \mathscr{W}(\Phi') := (c\tau + d)^{k_{\mathscr{W}}} \mathscr{W}(\Phi)\,. \tag{5.1.7}$$

In our case, given our bottom-up approach, we choose the superpotential to be modular invariant, i.e., $k_{\mathscr{W}} = 0$. This amounts to demanding $\boldsymbol{s}\otimes\boldsymbol{r}_i\otimes\boldsymbol{r}_j\otimes\boldsymbol{r}_k \overset{!}{\supset} \mathbf{1}$ and $k_Y \overset{!}{=} -k_i - k_j - k_k$.

The Kähler potential of matter fields in models endowed with a modular flavor symmetry is typically assumed to take the canonical form

$$\mathscr{K}(\Phi, \bar{\Phi}) \supset \sum_j (-\mathrm{i}\tau + \mathrm{i}\bar{\tau})^{k_j} |\Phi^j|^2\,, \tag{5.1.8}$$

as in [49]. However, the nonlinear realization of this symmetry implies that there are additional terms with free coefficients, which are at the same footing as the canonical terms, thus limiting the predictive power of the model [27].

Eclectic Flavor Symmetries

The so–called eclectic flavor symmetries [91] arise naturally in string models [12, 92, 93] and magnetized toroidal compactifications [98]. They are given by group–theoretic unions of a traditional (flavor) symmetry, $G_{\text{traditional}}$, and a modular symmetry, G_{modular},

$$G_{\text{eclectic}} = G_{\text{traditional}} \cup G_{\text{modular}}\ , \tag{5.1.9}$$

such that the modular symmetry is built out of outer automorphisms of $G_{\text{traditional}}$, $G_{\text{modular}} \subset \text{Out}(G_{\text{traditional}})$. The union "$\cup$" in Equation (5.1.9) is to be understood as the multiplicative closure of the groups.

Crucially, G_{eclectic} has representations which transform nontrivially under both $G_{\text{traditional}}$ and

G_{modular}. This means that, by giving a VEV to a representation of that kind, we can break G_{eclectic} to a diagonal subgroup which inherits properties from $G_{\text{traditional}}$ as well as G_{modular}.

Even though eclectic groups can also be built from a bottom–up perspective [91], in this work we refrain from working out an explicit eclectic model. Rather, in what follows we will analyze the somewhat simpler situation in which the union "$\cup$" in Equation (5.1.9) gets replaced by a direct product, i.e. $G_{\text{quasi-eclectic}} = G_{\text{traditional}} \times G_{\text{modular}}$. As we shall see, the emerging scheme is still simple enough to be analyzed and at the same time illustrates how the desirable properties of $G_{\text{traditional}}$ and G_{modular} get inherited by the diagonal group.

5.2 A Simple Quasi–eclectic Example

5.2.1 Symmetries and Representations

To illustrate the main points of our quasi–eclectic scheme, let us consider a model by Feruglio [49], but with a slight twist. We will take the original flavor symmetry to be

$$G_{\text{flavor}} = A_4^{\text{traditional}} \times \Gamma_3 \ , \tag{5.2.1}$$

where Γ_3 can be thought of as a modular version of A_4. The quantum numbers of the states are listed in Table 5.2.1. We take the superpotential to have modular weight $k_{\mathscr{W}} = 0$.

5.2.2 Diagonal Breaking

Let us now *assume* that the flavon χ attains a "diagonal" VEV, i.e. in the real basis

$$\langle \chi_i^a \rangle = v_1 \, \mathbb{1}_3 \ . \tag{5.2.2}$$

	$(E_1^{\mathcal{C}}, E_2^{\mathcal{C}}, E_3^{\mathcal{C}})$	L	H_d	H_u	χ	φ	S_χ	S_φ	Y
$\mathrm{SU}(2)_\mathrm{L} \times \mathrm{U}(1)_Y$	$\mathbf{1}_1$	$\mathbf{2}_{-1/2}$	$\mathbf{2}_{-1/2}$	$\mathbf{2}_{1/2}$	$\mathbf{1}_0$	$\mathbf{1}_0$	$\mathbf{1}_0$	$\mathbf{1}_0$	$\mathbf{1}_0$
$A_4^{\text{traditional}}$	$(\mathbf{1_0}, \mathbf{1_2}, \mathbf{1_1})$	$\mathbf{3}$	$\mathbf{1}_0$	$\mathbf{1}_0$	$\mathbf{3}$	$\mathbf{3}$	$\mathbf{1}_0$	$\mathbf{1}_0$	$\mathbf{1}_0$
$\mathbb{Z}_3^\chi$	0	0	0	1	1	0	1	0	0
$\mathbb{Z}_3^\varphi$	1	0	1	0	0	1	0	1	0
Γ_3	$\mathbf{1}_0$	$\mathbf{1}_0$	$\mathbf{1}_0$	$\mathbf{1}_0$	$\mathbf{3}$	$\mathbf{1}_0$	$\mathbf{1}_0$	$\mathbf{1}_0$	$\mathbf{3}$
k	$(k_{E_1}, k_{E_2}, k_{E_3})$	k_L	k_{H_d}	k_{H_u}	k_χ	k_φ	k_S	k_S	k_Y
modular weights	$(1, 1, 1)$	-1	0	0	0	0	0	0	2

Table 5.2.1: Variation of model 1 of [49]. $E_i^{\mathcal{C}}$, L, H_u and H_d are the superfields of the charged leptons, left–handed doublets, up–type Higgs and down–type Higgs, respectively. S_χ and S_φ are part of the VEV alignment, see Appendix C.1. In our notation, $A_4 \cong \Gamma_3$ has the representations $\mathbf{3}, \mathbf{1}_0, \mathbf{1}_1$ and $\mathbf{1}_2$, whose tensor products are given e.g. in [49, Appendix C].

In the complex basis, this diagonal VEV has the shape[†]

$$\langle \chi_i^a \rangle = v_1 \begin{pmatrix} 1 & 0 & 0 \\ 0 & 0 & 1 \\ 0 & 1 & 0 \end{pmatrix} . \tag{5.2.3}$$

We discuss the alignment of the flavon in Appendix C.1. Similarly to Feruglio, we introduce a flavon φ (as in [49]). Here, a is a Γ_3 index and i an $A_4^{\text{traditional}}$ index. The VEV (5.2.3) breaks $A_4^{\text{traditional}} \times \Gamma_3$ to $\Gamma_3^{\text{diagonal}}$. Both Γ_3 and $\Gamma_3^{\text{diagonal}}$ are nonlinearly realized.

[†]The relation between these bases is explained in Appendix C.2.

5.2.3 Charged Lepton Yukawa Couplings

The charged fermion masses are obtained just like in [49]. Since we assigned them the $\mathbf{1}_0$, $\mathbf{1}_1$ and $\mathbf{1}_2$ under $A_4^{\text{traditional}}$, respectively, we can write down superpotential terms[‡]

$$\mathscr{W}_e = \frac{\widetilde{y}_e}{\Lambda} H_d (L\varphi E_1^{\mathcal{C}})_{\mathbf{1}_0} + \frac{\widetilde{y}_\tau}{\Lambda} H_d (L\varphi E_2^{\mathcal{C}})_{\mathbf{1}_0} + \frac{\widetilde{y}_\mu}{\Lambda} H_d (L\varphi E_3^{\mathcal{C}})_{\mathbf{1}_0} \,, \tag{5.2.4}$$

which involve the three free parameters $\widetilde{y}_e$, $\widetilde{y}_\mu$ and $\widetilde{y}_\tau$, and the cut–off scale Λ of the model. Here, a $\mathbf{1}_0$ subscript indicates a contraction to a G_{flavor} singlet. In order to get a diagonal charged lepton Yukawa coupling matrix, we will take the VEV of φ to be

$$\langle \varphi_i \rangle = v_2 \begin{pmatrix} 1 \\ 0 \\ 0 \end{pmatrix} \tag{5.2.5}$$

in the complex basis and

$$\langle \varphi_i \rangle = \frac{v_2}{\sqrt{3}} \begin{pmatrix} 1 \\ 1 \\ 1 \end{pmatrix} \tag{5.2.6}$$

in the real basis, similarly to Feruglio's model [49]. This choice will be justified in Appendix C.1. Equation (5.2.4) along with Equation (5.2.5) gives the charged lepton mass matrix

$$m_e = v_d \frac{v_2}{\Lambda} \operatorname{diag}(\widetilde{y}_e, \widetilde{y}_\tau, \widetilde{y}_\mu) \,, \tag{5.2.7}$$

[‡]Following Feruglio's model (cf. [49, discussion between Equations (39) and (40)]), we exchange here $\widetilde{y}_\mu$ and $\widetilde{y}_\tau$ to best fit data.

where v_d is the VEV of H_d, as usual. Like in [49], we introduced three parameters, $\widetilde{y}_e$, $\widetilde{y}_\mu$ and $\widetilde{y}_\tau$. These parameters can be used to reproduce the observed charged lepton masses. In order to reproduce the observed τ lepton mass, $\varepsilon_2 := v_2/\Lambda$ cannot become too small. This sector does not really contain any novel ingredients, nor does it by itself make nontrivial predictions. Some ideas to address the question of fermion mass hierarchies can be found in e.g. [50, 97, 100].

5.2.4 The Weinberg Operator

Like in Feruglio's model [49] the new ingredients are in the Weinberg operator, which emerges from the superpotential couplings

$$\mathscr{W}_\nu = \frac{1}{\Lambda^2}[(H_u \cdot L)\,\chi\,(H_u \cdot L)\,Y]_{\mathbf{1}_0}\ . \tag{5.2.8}$$

To construct the couplings at the component level, we first contract $Y\chi$ to Γ_3 singlets. Since χ consists of three Γ_3 **3**–plets, we obtain an $A_4^{\text{traditional}}$ triplet

$$[(Y\chi)_{(\mathbf{3},\mathbf{1}_0)}]_i = Y_1\chi_i^1 + Y_2\chi_i^3 + Y_3\chi_i^2\ , \tag{5.2.9}$$

where i is an $A_4^{\text{traditional}}$ index. Here, $(\boldsymbol{r}, \boldsymbol{r'})$ means that the contraction transforms as $(\boldsymbol{r}, \boldsymbol{r'})$ under $A_4^{\text{traditional}} \times \Gamma_3$. This $A_4^{\text{traditional}}$ triplet can be contracted with the unique $A_4^{\text{traditional}}$ triplet that emerges from combining the $A_4^{\text{traditional}}$ triplet L with itself,

$$(LL)_{(\mathbf{3},\mathbf{1}_0)} = \frac{2}{\sqrt{3}}\begin{pmatrix} L_1^2 - L_2L_3 \\ L_3^2 - L_1L_2 \\ L_2^2 - L_1L_3 \end{pmatrix}\ . \tag{5.2.10}$$

After inserting the "diagonal" VEV (5.2.3), the effective superpotential coincides, up to an irrelevant prefactor, with the one proposed in [49],

$$\mathscr{W}_\nu = \frac{v_1}{\Lambda^2}[(H_u \cdot L)\, Y\, (H_u \cdot L)]_{\mathbf{1}_0} \ . \tag{5.2.11}$$

In particular, the matrix structure of the Weinberg operator is identical to the one in [49]. That is, the neutrino mass matrix is given by

$$m_\nu = \frac{v_u^2 \varepsilon_1}{\sqrt{3}\Lambda} \begin{pmatrix} 2Y_1(\tau) & -Y_3(\tau) & -Y_2(\tau) \\ -Y_3(\tau) & 2Y_2(\tau) & -Y_1(\tau) \\ -Y_2(\tau) & -Y_1(\tau) & 2Y_3(\tau) \end{pmatrix} , \tag{5.2.12}$$

where $\varepsilon_1 = v_1/\Lambda$ and v_u is the VEV of H_u. Then this matrix has only three free real parameters: Λ, $\mathrm{Re}\,\tau$ and $\mathrm{Im}\,\tau$.

5.2.5 Kinetic Terms

Before χ and φ attain VEVs, the Kähler potential of the charged leptons is diagonal because of the presence of $A_4^{\text{traditional}}$. Therefore, the Kähler potential is under control. After the breaking to the diagonal flavor symmetry,

$$K_L \ = \ L^\dagger L + \mathcal{O}(\varepsilon_1^2) + \mathcal{O}(\varepsilon_2^2) \ . \tag{5.2.13}$$

This is because the corrections to the Kähler potential come from terms involving[§] χ and φ. A priori these terms are not known. In this work we ask how much we can limit the effects of these terms in a bottom–up approach.

[§]Terms including the fields L and the modular forms Y (see e.g. [27, Equation (12)]) are restricted by $A_4^{\text{traditional}}$ to be just the product of the $L^\dagger L$ and $Y^\dagger Y$ trivial singlets of $A_4^{\text{traditional}}$, and are hence diagonal too.

Let us first turn our attention to χ. χ enters the leptonic superpotential only through the Weinberg operator, yielding Equation (5.2.12). Therefore, we cannot place a stringent lower bound on the size of v_1.

On the other hand, the magnitude of the VEV of φ, v_2, is bounded from below by the requirement to reproduce a realistic τ Yukawa coupling, y_τ. The value y_τ depends on the Higgs VEV ratio $\tan\beta$, $y_\tau = \sqrt{1+\tan^2\beta}\, m_\tau / v_{\rm EW} \sim 10^{-2}\sqrt{1+\tan^2\beta}$ (at tree level), where $v_{\rm EW}$ denotes the electroweak VEV. In [31], the best fits to data are obtained for small $\tan\beta$, in which case y_τ is suppressed, and the lower bound on v_2 is less stringent.

At first glance, one may suspect to find linear contributions to the Kähler metric,

$$K \supset (\varphi L L^\dagger)_{\mathbf{1}_0} \quad \text{and/or} \quad \left(\varphi\, E_i^{\mathcal{C}} (E_i^{\mathcal{C}})^\dagger\right)_{\mathbf{1}_0} . \tag{5.2.14}$$

However, the terms (5.2.14) are forbidden due to the symmetry $\mathbb{Z}_3^\varphi$ (cf. Table 5.2.1). Thus, the first nontrivial flavon–dependent contributions to the Kähler metric are given by $(L\varphi)^\dagger(L\varphi)$ and $(\varphi\varphi^\dagger)(EE^\dagger)$, which we will call ΔK_L and ΔK_R, respectively. Let us first focus on the L contribution. Considering the discrete charges of L and φ, we identify seven $A_4^{\rm traditional}$ invariant terms from the product $(\mathbf{3}\otimes\mathbf{3}\otimes\mathbf{3}\otimes\mathbf{3})$. After inserting on the VEV of φ (5.2.5), these are reduced to only three nonvanishing invariant contributions to ΔK_L, which are associated with three independent coefficients C_i. The resulting contribution to the Kähler metric, in the complex basis, is

$$\Delta K_L \;=\; \frac{v_2^2}{3\Lambda^2}\begin{pmatrix} 3C_1+4C_2 & 0 & 0 \\ 0 & 3C_1-2C_2+2\sqrt{3}C_3 & 0 \\ 0 & 0 & 3C_1-2C_2-2\sqrt{3}C_3 \end{pmatrix}, \tag{5.2.15}$$

which can be decomposed as

$$\Delta K_L \;=\; \varepsilon_2^2\left(C_1\,\mathbb{1}_3 + \frac{2C_2}{3}\,\mathrm{diag}(2,-1,-1) + \frac{2C_3}{\sqrt{3}}\,\mathrm{diag}(0,1,-1)\right)\,. \tag{5.2.16}$$

In the case of the R contribution, after evaluating in Equation (5.2.5), we get nine invariant terms from which only three are nonvanishing. The resulting contribution, in both complex and real basis, is

$$\Delta K_R \;=\; \varepsilon_2^2\,\mathrm{diag}(D_1, D_2, D_3)\;, \tag{5.2.17}$$

where D_i is defined similarly as in Equation (5.2.15).

The impact of these corrections can be estimated using the discussion in [25,26]. We see that the corrections of the mixing angles come from ΔK_L only. Generically, the solar angle θ_{12} is the most sensitive angle in a scheme with inverted mass ordering, its correction gets enhanced by a factor $m_1^2/\Delta m^2_{\mathrm{sol}}$, which is about 34 in the Feruglio model. The corrections are also proportional to $\varepsilon_2^2 = v_2^2/\Lambda^2 \gtrsim y_\tau^2$. Furthermore since the unperturbed theory has diagonal kinetic terms, the coefficients of the Kähler corrections are also not arbitrarily large. For corrections associated with the coefficient C_i of the Kähler metric ΔK_L in Equation (5.2.16), we find

$$\Delta\theta_{12} \simeq C_i\left(\frac{\varepsilon_2}{0.03}\right)^2 \cdot \begin{cases} 0\;, & \text{if } i=1\;,\\ -0.05\;, & \text{if } i=2\;,\\ 0.01\;, & \text{if } i=3\;. \end{cases} \tag{5.2.18}$$

While an exact computation of the coefficient C_i would require a UV completion of the model (cf. e.g. [2, 7]), we make the EFT assumption that the coefficients are at most of the order unity. Equation (5.2.18) shows that, if the correction is proportional to the unit matrix,

θ_{12} does not change, as expected. For small $\tan\beta$, $\varepsilon_2 \sim 0.03$ is possible, and the Kähler corrections are comparable to the experimental uncertainties. However, for large $\tan\beta$, the model we discuss here requires additional ingredients to allow us to make precise predictions.

Altogether we see that the Kähler corrections are controlled by ε_2, which also governs the charged lepton Yukawa couplings. In this regard this bottom–up analysis is somewhat reminiscent of minimal flavor violation (MFV) [22, 28, 34]. We can hence conclude that the quasi–eclectic scheme presented here allows us to construct predictive bottom–up models with modular flavor symmetries.

Chapter 6

Conclusions and Final Words

We have illustrated various modern tools for understanding physics beyond the Standard Model. In particular, we focused on modular flavor symmetries and non-perturbative dynamics which induce chirality flows in supersymmetric gauge theories. We started by studying non-perturbative dynamics underlying chirality flows in strongly interacting SUSY gauge theories. In our analysis, we identified stability conditions for chirally symmetric vacua in various gauge groups and developed model-building tools to construct multiple models exhibiting chirality flows. We also showed how the straightforward approach that works in most gauge groups fails in the case of SO groups due to the absence of true s-confinement. In particular, 'the s-confining branch' is unstable, leading to a runaway potential even under small mass deformations of the theory.

Further, we explored the consequences of chirality-changing RG flows in the context of string theory. We noted that non-perturbative s-confining dynamics change the effective number of chiral generations in such stringy models. The non-perturbative dynamics may increase the number of generations by generating new chiral composites in IR or decrease the generations due to the appearance of a mass gap. Using the construction of explicit models from string

compactifications, we highlighted the importance of considering generation flow in the search for realistic string models by undergoing more thorough analyses.

In the second part, we studied modular flavor symmetries derived from tori with magnetic fluxes. Using simple mathematical tools, we derived closed-form expressions for Yukawa couplings for general flux parameters and showed that odd-generation models deriving from such setups are not inconsistent, contrary to previous papers. This played an important role in understanding the full symmetry group of the theory, for various models. One very interesting conclusion here is that, unlike bottom-up approaches, these Yukawa couplings suffer no ambiguities and are determined exactly in such setups!

Finally, building upon the achievements of Feruglio's models, we proposed a novel approach to fix the kinetic terms in bottom-up scenarios, by working in an eclectic scheme. We started with the product of a modular group and a traditional discrete flavor group and introduced flavon VEVs that break them into their diagonal subgroups. This helped us build on the predictive capacity of our framework while aligning vacuum expectation values, and controlling the Kähler terms. Due to this, we were able to achieve the desired symmetry-breaking patterns. This opens up new avenues for exploration of such hybrid schemes not only applied to neutrino models but also quark sectors.

In summary, we have used non-perturbative physics in supersymmetric theories to show how the chiral structure of theories can be altered by introducing mass gaps, and how this affects string model searches. Furthermore, we used modular symmetries in both top-down and bottom-up approaches to show how these can help build predictive models. As we continue to explore these in more detail, we might hope to understand new physics emerging from experiments, with valuable insights from such theoretical structures.

Finally speaking of the PhD journey itself: While there were both bad days and good days, the support I have received from my advisors, other faculty, my colleagues, and friends has

been invaluable. The vibrant atmosphere at this department has made UCI the best place I have ever worked in, and although the future awaits, the PhD life is something I will always, always miss. I want to finish the conclusions with this poem about my PhD journey:

The road felt infinite ahead of me,
And infinitely steep,
For I didn't know how long I'd work
And think how deep!

There were many easy days,
And difficult ones, some
Days filled with nervousness and anxiety,
And then the laughter ones would come.

So at the end of this long, great journey
I do feel a bit saddened,
But if something ending makes you sad,
It must've been incredible when it happened.

Bibliography

[1] H. Abe, K.-S. Choi, T. Kobayashi, and H. Ohki. Magnetic flux, Wilson line and orbifold. *Phys. Rev. D*, 80:126006, 2009.

[2] Y. Abe, T. Higaki, T. Kobayashi, S. Takada, and R. Takahashi. 4D effective action from the non-Abelian DBI action with a magnetic flux background. *Phys. Rev. D*, 104(12):126020, 2021.

[3] S. A. Abel and A. W. Owen. N-point amplitudes in intersecting brane models. *Nucl. Phys.*, B682:183–216, 2004.

[4] I. Affleck, M. Dine, and N. Seiberg. Dynamical Supersymmetry Breaking in Supersymmetric QCD. *Nucl. Phys.*, B241:493–534, 1984.

[5] Y. Almumin, M.-C. Chen, V. Knapp-Pérez, S. Ramos-Sánchez, M. Ratz, and S. Shukla. Metaplectic Flavor Symmetries from Magnetized Tori. *JHEP*, 05:078, 2021.

[6] L. B. Anderson, J. Gray, N. Raghuram, and W. Taylor. Matter in transition. *JHEP*, 04:080, 2016.

[7] I. Antoniadis, E. Gava, K. S. Narain, and T. R. Taylor. Superstring threshold corrections to Yukawa couplings. *Nucl. Phys. B*, 407:706–724, 1993.

[8] T. Asaka, Y. Heo, T. H. Tatsuishi, and T. Yoshida. Modular A_4 invariance and leptogenesis. *JHEP*, 01:144, 2020.

[9] J. J. Atick, L. J. Dixon, and A. Sen. String Calculation of Fayet-Iliopoulos D Terms in Arbitrary Supersymmetric Compactifications. *Nucl. Phys.*, B292:109–149, 1987.

[10] K. S. Babu, E. Ma, and J. W. F. Valle. Underlying A(4) symmetry for the neutrino mass matrix and the quark mixing matrix. *Phys. Lett.*, B552:207–213, 2003.

[11] D. Bailin and A. Love. Orbifold compactifications of string theory. *Phys. Rept.*, 315:285–408, 1999.

[12] A. Baur, M. Kade, H. P. Nilles, S. Ramos-Sanchez, and P. K. S. Vaudrevange. Completing the eclectic flavor scheme of the $\mathbb{Z}_2$ orbifold. *JHEP*, 06:110, 2021.

[13] A. Baur, M. Kade, H. P. Nilles, S. Ramos-Sanchez, and P. K. S. Vaudrevange. Siegel modular flavor group and CP from string theory. *Phys. Lett. B*, 816:136176, 2021.

[14] A. Baur, M. Kade, H. P. Nilles, S. Ramos-Sánchez, and P. K. S. Vaudrevange. The eclectic flavor symmetry of the $\mathbb{Z}_2$ orbifold. *JHEP*, 02:018, 2021.

[15] A. Baur, H. P. Nilles, A. Trautner, and P. K. Vaudrevange. Unification of Flavor, CP, and Modular Symmetries. *Phys. Lett. B*, 795:7–14, 2019.

[16] S. Biermann, A. Mütter, E. Parr, M. Ratz, and P. K. S. Vaudrevange. Discrete remnants of orbifolding. *Phys. Rev. D*, 100(6):066030, 2019.

[17] P. Binétruy, S. Lavignac, and P. Ramond. Yukawa textures with an anomalous horizontal abelian symmetry. *Nucl. Phys.*, B477:353–377, 1996.

[18] P. Binétruy and P. Ramond. Yukawa textures and anomalies. *Phys. Lett. B*, 350:49–57, 1995.

[19] F. Buccella, J. P. Derendinger, S. Ferrara, and C. A. Savoy. Patterns of Symmetry Breaking in Supersymmetric Gauge Theories. *Phys. Lett. B*, 115:375–379, 1982.

[20] W. Buchmüller, M. Dierigl, and E. Dudas. Flux compactifications and naturalness. *JHEP*, 08:151, 2018.

[21] W. Buchmüller, M. Dierigl, E. Dudas, and J. Schweizer. Effective field theory for magnetic compactifications. *JHEP*, 04:052, 2017.

[22] A. J. Buras, P. Gambino, M. Gorbahn, S. Jäger, and L. Silvestrini. Universal unitarity triangle and physics beyond the standard model. *Phys. Lett.*, B500:161–167, 2001.

[23] D. Chang, R. N. Mohapatra, and M. K. Parida. Decoupling Parity and SU(2)-R Breaking Scales: A New Approach to Left-Right Symmetric Models. *Phys. Rev. Lett.*, 52:1072, 1984.

[24] M. Chen, V. Knapp–Pérez, M. Ramos–Hamud, S. Ramos–Sánchez, M. Ratz, and S. Shukla. Quasi–eclectic modular flavor symmetries. *Physics letters. B*, 824:136843, 1 2022.

[25] M.-C. Chen, M. Fallbacher, M. Ratz, and C. Staudt. On predictions from spontaneously broken flavor symmetries. *Phys. Lett. B*, 718:516–521, 2012.

[26] M.-C. Chen, Y. Fallbacher, Maximilian and, M. Ratz, and C. Staudt. Predictivity of models with spontaneously broken non-Abelian discrete flavor symmetries. *Nucl. Phys. B*, 873:343–371, 2013.

[27] M.-C. Chen, S. Ramos-Sánchez, and M. Ratz. A note on the predictions of models with modular flavor symmetries. *Phys. Lett. B*, 801:135153, 2020.

[28] R. S. Chivukula and H. Georgi. Composite Technicolor Standard Model. *Phys. Lett.*, B188:99, 1987.

[29] H. Cohen and F. Strömberg. *Modular Forms: a classical approach*. American Mathematical Soc., 8 2017.

[30] D. Cremades, L. Ibáñez, and F. Marchesano. Computing Yukawa couplings from magnetized extra dimensions. *JHEP*, 05:079, 2004.

[31] J. C. Criado and F. Feruglio. Modular Invariance Faces Precision Neutrino Data. *SciPost Phys.*, 5(5):042, 2018.

[32] C. Csaki, M. Schmaltz, and W. Skiba. A Systematic approach to confinement in N=1 supersymmetric gauge theories. *Phys. Rev. Lett.*, 78:799–802, 1997.

[33] C. Csaki, M. Schmaltz, and W. Skiba. Confinement in N=1 SUSY gauge theories and model building tools. *Phys. Rev. D*, 55:7840–7858, 1997.

[34] G. D'Ambrosio, G. F. Giudice, G. Isidori, and A. Strumia. Minimal flavor violation: An Effective field theory approach. *Nucl. Phys. B*, 645:155–187, 2002.

[35] F. J. de Anda, S. F. King, and E. Perdomo. $SU(5)$ grand unified theory with A_4 modular symmetry. *Phys. Rev. D*, 101(1):015028, 2020.

[36] P. Di Vecchia, A. Liccardo, R. Marotta, and F. Pezzella. Kahler Metrics and Yukawa Couplings in Magnetized Brane Models. *JHEP*, 03:029, 2009.

[37] F. Diamond and J. Shurman. *A first course in modular forms*. Springer Science and Business Media, 3 2006.

[38] K. R. Dienes. Modular invariance, finiteness, and misaligned supersymmetry: New constraints on the numbers of physical string states. *Nucl. Phys. B*, 429:533–588, 1994.

[39] P. Dimopoulos, G. K. Leontaris, and N. D. Tracas. Supercompositeness inspired from superstrings. *Z. Phys. C*, 76:327–331, 1997.

[40] G.-J. Ding and F. Feruglio. Testing Moduli and Flavon Dynamics with Neutrino Oscillations. *JHEP*, 06:134, 2020.

[41] G.-J. Ding, F. Feruglio, and X.-G. Liu. Automorphic Forms and Fermion Masses. *JHEP*, 01:037, 2021.

[42] G.-J. Ding, S. F. King, and X.-G. Liu. Neutrino mass and mixing with A_5 modular symmetry. *Phys. Rev. D*, 100(11):115005, 2019.

[43] G.-J. Ding, S. F. King, X.-G. Liu, and J.-N. Lu. Modular S_4 and A_4 symmetries and their fixed points: new predictive examples of lepton mixing. *JHEP*, 12:030, 2019.

[44] L. J. Dixon, J. A. Harvey, C. Vafa, and E. Witten. Strings on Orbifolds. *Nucl. Phys. B*, 261:678–686, 1985.

[45] L. J. Dixon, J. A. Harvey, C. Vafa, and E. Witten. Strings on Orbifolds. 2. *Nucl. Phys. B*, 274:285–314, 1986.

[46] L. J. Dixon, V. Kaplunovsky, and J. Louis. Moduli dependence of string loop corrections to gauge coupling constants. *Nucl. Phys. B*, 355:649–688, 1991.

[47] M. R. Douglas and C.-g. Zhou. Chirality change in string theory. *JHEP*, 06:014, 2004.

[48] U. Dudley. *Elementary Number Theory: Second Edition*. Dover Books on Mathematics. Dover Publications, 2012.

[49] F. Feruglio. *Are neutrino masses modular forms?*, pages 227–266. nill, 2019.

[50] F. Feruglio, V. Gherardi, A. Romanino, and A. Titov. Modular invariant dynamics and fermion mass hierarchies around $\tau = i$. *JHEP*, 05:242, 2021.

[51] F. Feruglio and A. Romanino. Lepton flavor symmetries. *Rev. Mod. Phys.*, 93(1):015007, 2021.

[52] M. Fischer, M. Ratz, J. Torrado, and P. K. S. Vaudrevange. Classification of symmetric toroidal orbifolds. *JHEP*, 01:084, 2013.

[53] D. Ghilencea and H. M. Lee. Wilson lines and UV sensitivity in magnetic compactifications. *JHEP*, 06:039, 2017.

[54] M. B. Green, J. H. Schwarz, and E. Witten. *Superstring Theory: Volume 1, Introduction*. Cambridge University Press, 7 1988.

[55] M. B. Green, J. H. Schwarz, and E. Witten. *Superstring Theory: Volume 2, Loop Amplitudes, Anomalies and Phenomenology*. Cambridge University Press, 7 1988.

[56] T. Hirose and N. Maru. Cancellation of One-loop Corrections to Scalar Masses in Yang-Mills Theory with Flux Compactification. *JHEP*, 08:054, 2019.

[57] M. Holthausen and M. A. Schmidt. Natural Vacuum Alignment from Group Theory: The Minimal Case. *JHEP*, 01:126, 2012.

[58] K. Hoshiya, S. Kikuchi, T. Kobayashi, Y. Ogawa, and H. Uchida. Classification of three-generation models by orbifolding magnetized $T^2 \times T^2$. *PTEP*, 2021(3):033B05, 2021.

[59] L. E. Ibáñez and D. Lüst. Duality anomaly cancellation, minimal string unification and the effective low-energy Lagrangian of 4-D strings. *Nucl. Phys.*, B382:305–364, 1992.

[60] L. E. Ibáñez and H. P. Nilles. Low-Energy Remnants of Superstring Anomaly Cancellation Terms. *Phys. Lett. B*, 169:354–358, 1986.

[61] L. E. Ibáñez and A. M. Uranga. *String theory and particle physics: An introduction to string phenomenology*. Cambridge University Press, 2 2012.

[62] W. R. Inc. Mathematica, Version 14.0. Champaign, IL, 2024.

[63] K. A. Intriligator and P. Pouliot. Exact superpotentials, quantum vacua and duality in supersymmetric SP(N(c)) gauge theories. *Phys. Lett. B*, 353:471–476, 1995.

[64] K. A. Intriligator and N. Seiberg. Duality, monopoles, dyons, confinement and oblique confinement in supersymmetric SO(N(c)) gauge theories. *Nucl. Phys. B*, 444:125–160, 1995.

[65] H. Ishimori, T. Kobayashi, H. Ohki, Y. Shimizu, H. Okada, and M. Tanimoto. Non-Abelian Discrete Symmetries in Particle Physics. *Prog. Theor. Phys. Suppl.*, 183:1–163, 2010.

[66] S. Kachru and E. Silverstein. Chirality changing phase transitions in 4-D string vacua. *Nucl. Phys. B*, 504:272–284, 1997.

[67] V. S. Kaplunovsky and J. Louis. Model independent analysis of soft terms in effective supergravity and in string theory. *Phys. Lett. B*, 306:269–275, 1993.

[68] Y. Kariyazono, T. Kobayashi, S. Takada, S. Tamba, and H. Uchida. Modular symmetry anomaly in magnetic flux compactification. *Phys. Rev. D*, 100(4):045014, 2019.

[69] T. W. B. Kibble, G. Lazarides, and Q. Shafi. Walls Bounded by Strings. *Phys. Rev.*, D26:435, 1982.

[70] S. Kikuchi, T. Kobayashi, H. Otsuka, S. Takada, and H. Uchida. Modular symmetry by orbifolding magnetized $T^2 \times T^2$: realization of double cover of Γ_N. *JHEP*, 11:101, 2020.

[71] S. Kikuchi, T. Kobayashi, S. Takada, T. H. Tatsuishi, and H. Uchida. Revisiting modular symmetry in magnetized torus and orbifold compactifications. *Phys. Rev. D*, 102(10):105010, 2020.

[72] S. Kikuchi, T. Kobayashi, and H. Uchida. Modular flavor symmetries of three-generation modes on magnetized toroidal orbifolds. *Phys. Rev. D*, 104(6):065008, 2021.

[73] T. Kobayashi, S. Nagamoto, S. Takada, S. Tamba, and T. H. Tatsuishi. Modular symmetry and non-Abelian discrete flavor symmetries in string compactification. *Phys. Rev. D*, 97(11):116002, 2018.

[74] T. Kobayashi, S. Nagamoto, and S. Uemura. Modular symmetry in magnetized/intersecting D-brane models. *PTEP*, 2017(2):023B02, 2017.

[75] T. Kobayashi, N. Omoto, Y. Shimizu, K. Takagi, M. Tanimoto, and T. H. Tatsuishi. Modular A4 invariance and neutrino mixing. *The Journal of high energy physics/The journal of high energy physics*, 2018(11), 11 2018.

[76] T. Kobayashi, Y. Shimizu, K. Takagi, M. Tanimoto, and T. H. Tatsuishi. A_4 lepton flavor model and modulus stabilization from S_4 modular symmetry. *Phys. Rev. D*, 100(11):115045, 2019. [Erratum: Phys.Rev.D 101, 039904 (2020)].

[77] T. Kobayashi, Y. Shimizu, K. Takagi, M. Tanimoto, T. H. Tatsuishi, and H. Uchida. CP violation in modular invariant flavor models. *Phys. Rev. D*, 101(5):055046, 2020.

[78] T. Kobayashi and S. Tamba. Modular forms of finite modular subgroups from magnetized D-brane models. *Phys. Rev. D*, 99(4):046001, 2019.

[79] T. Kobayashi, K. Tanaka, and T. H. Tatsuishi. Neutrino mixing from finite modular groups. *Phys. Rev. D*, 98(1):016004, 2018.

[80] L. Kofman et al. Beauty is attractive: Moduli trapping at enhanced symmetry points. *JHEP*, 05:030, 2004.

[81] O. Lebedev, H. P. Nilles, S. Raby, S. Ramos-Sánchez, M. Ratz, P. K. S. Vaudrevange, and A. Wingerter. A mini-landscape of exact MSSM spectra in heterotic orbifolds. *Phys. Lett.*, B645:88, 2007.

[82] X.-G. Liu and G.-J. Ding. Neutrino Masses and Mixing from Double Covering of Finite Modular Groups. *JHEP*, 08:134, 2019.

[83] X.-G. Liu, C.-Y. Yao, and G.-J. Ding. Modular invariant quark and lepton models in double covering of S_4 modular group. *Phys. Rev. D*, 103(5):056013, 2021.

[84] X.-G. Liu, C.-Y. Yao, B.-Y. Qu, and G.-J. Ding. Half-integral weight modular forms and application to neutrino mass models. *Phys. Rev. D*, 102(11):115035, 2020.

[85] M. A. Luty and W. Taylor. Varieties of vacua in classical supersymmetric gauge theories. *Phys. Rev. D*, 53:3399–3405, 1996.

[86] E. Ma and G. Rajasekaran. Softly broken A(4) symmetry for nearly degenerate neutrino masses. *Phys. Rev.*, D64:113012, 2001.

[87] D. K. Mayorga Peña, H. P. Nilles, and P.-K. Oehlmann. A Zip-code for Quarks, Leptons and Higgs Bosons. *JHEP*, 12:024, 2012.

[88] R. N. Mohapatra and G. Senjanovic. Neutrino Mass and Spontaneous Parity Violation. *Phys. Rev. Lett.*, 44:912, 1980.

[89] D. Mumford. *Tata Lectures on Theta I.* Birkhäuser, 1. edition, 1983.

[90] A. E. Nelson and M. J. Strassler. A Realistic supersymmetric model with composite quarks. *Phys. Rev. D*, 56:4226–4237, 1997.

[91] H. P. Nilles, S. Ramos-Sánchez, and P. K. Vaudrevange. Eclectic Flavor Groups, 2020.

[92] H. P. Nilles, S. Ramos-Sánchez, and P. K. S. Vaudrevange. Eclectic flavor scheme from ten-dimensional string theory – I. Basic results. *Phys. Lett. B*, 808:135615, 2020.

[93] H. P. Nilles, S. Ramos-Sánchez, and P. K. S. Vaudrevange. Lessons from eclectic flavor symmetries. *Nucl. Phys. B*, 957:115098, 2020.

[94] H. P. Nilles, S. Ramos-Sánchez, P. K. S. Vaudrevange, and A. Wingerter. The Orbifolder: A Tool to study the Low Energy Effective Theory of Heterotic Orbifolds. *Comput. Phys. Commun.*, 183:1363–1380, 2012.

[95] P. Novichkov, J. Penedo, S. Petcov, and A. Titov. Generalised CP Symmetry in Modular-Invariant Models of Flavour. *JHEP*, 07:165, 2019.

[96] P. P. Novichkov, J. T. Penedo, and S. T. Petcov. Double cover of modular S_4 for flavour model building. *Nucl. Phys. B*, 963:115301, 2021.

[97] P. P. Novichkov, J. T. Penedo, and S. T. Petcov. Fermion mass hierarchies, large lepton mixing and residual modular symmetries. *JHEP*, 04:206, 2021.

[98] H. Ohki, S. Uemura, and R. Watanabe. Modular flavor symmetry on a magnetized torus. *Phys. Rev. D*, 102(8):085008, 2020.

[99] H. Okada and M. Tanimoto. CP violation of quarks in A_4 modular invariance. *Phys. Lett. B*, 791:54–61, 2019.

[100] H. Okada and M. Tanimoto. Modular invariant flavor model of A_4 and hierarchical structures at nearby fixed points. *Phys. Rev. D*, 103(1):015005, 2021.

[101] J. Penedo and S. Petcov. Lepton Masses and Mixing from Modular S_4 Symmetry. *Nucl. Phys. B*, 939:292–307, 2019.

[102] J. Polchinski. *String theory. Vol. 1: An introduction to the bosonic string.* Cambridge Monographs on Mathematical Physics. Cambridge University Press, 12 2007.

[103] P. Ramond. *Group theory: A physicist's survey.* nill, 2010.

[104] S. Ramos-Sánchez. Towards Low Energy Physics from the Heterotic String. *Fortsch. Phys.*, 10:907–1036, 2009.

[105] S. Ramos-Sanchez, M. Ratz, Y. Shirman, S. Shukla, and M. Waterbury. Generation flow in field theory and strings. *JHEP*, 10:144, 2021.

[106] S. Ramos–Sánchez, M. Ratz, Y. Shirman, S. Shukla, and M. Waterbury. Generation flow in field theory and strings. *The Journal of high energy physics/The journal of high energy physics*, 2021(10), 10 2021.

[107] S. S. Razamat and D. Tong. Gapped Chiral Fermions. *Phys. Rev. X*, 11(1):011063, 2021.

[108] N. Seiberg. Exact results on the space of vacua of four-dimensional SUSY gauge theories. *Phys. Rev. D*, 49:6857–6863, 1994.

[109] N. Seiberg. Electric — magnetic duality in supersymmetric non–Abelian gauge theories. *Nucl.Phys.*, B435:129–146, 1995.

[110] Y. Shirman. Dynamical supersymmetry breaking versus runaway behavior in supersymmetric gauge theories. *Phys. Lett. B*, 389:287–293, 1996.

[111] Y. Shirman, S. Shukla, and M. Waterbury. Chirality changing RG flows: dynamics and models. *The Journal of high energy physics/The journal of high energy physics*, 2023(6), 6 2023.

[112] Y. Shirman, S. Shukla, and M. Waterbury. Chirality changing RG flows: dynamics and models. *JHEP*, 06:168, 2023.

[113] S. Stieberger. (0,2) heterotic gauge couplings and their M theory origin. *Nucl. Phys. B*, 541:109–144, 1999.

[114] M. J. Strassler. Generating a fermion mass hierarchy in a composite supersymmetric standard model. *Phys. Lett. B*, 376:119–126, 1996.

[115] J. Terning. *Modern supersymmetry*. OUP Oxford, 1 2009.

[116] D. Tong. Line Operators in the Standard Model. *JHEP*, 07:104, 2017.

[117] D. Tong. Comments on symmetric mass generation in 2d and 4d. *JHEP*, 07:001, 2022.

[118] P. K. S. Vaudrevange. *Grand Unification in the Heterotic Brane World*. PhD thesis, Bonn U., 2008.

[119] M. Viazovska. The sphere packing problem in dimension 8. *Annals of mathematics*, 185(3), 5 2017.

[120] X. Wang, B. Yu, and S. Zhou. Double covering of the modular A_5 group and lepton flavor mixing in the minimal seesaw model. *Phys. Rev. D*, 103(7):076005, 2021.

[121] J. Wess and J. Bagger. *Supersymmetry and supergravity*. Princeton University Press, Princeton, NJ, USA, 1992.

[122] A. Wiles. Modular elliptic curves and Fermat's Last theorem. *Annals of mathematics*, 141(3):443, 5 1995.

[123] C.-Y. Yao, X.-G. Liu, and G.-J. Ding. Fermion masses and mixing from the double cover and metaplectic cover of the A_5 modular group. *Phys. Rev. D*, 103(9):095013, 2021.

Appendix A

(This appendix first appeared in the publication with Saul Ramos-Sanchez, Michael Ratz, Yuri Shirman and Michael Waterbury) [106]

A.1 Orbifold Model Definitions

In the bosonic formulation, a $\mathbb{Z}_2 \times \mathbb{Z}_4$ (1,1) heterotic orbifold compactification is defined by the shifts V_1 and V_2 of order 2 and 4, respectively, as well as six discrete Wilson lines W_a, $a = 1, \ldots, 6$ of order 2. These Wilson lines are restricted to satisfy $W_1 = W_2$ and $W_5 = W_6$ to be compatible with the $\mathbb{Z}_2 \times \mathbb{Z}_4$ point group of the compactification.* These parameters can be used as input in the `orbifolder` [94] to obtain the corresponding massless spectrum and compute the superpotential of the associated low-energy effective field theory.

A.1.1 Details of the 4⇝3 heterotic orbifold model

One heterotic orbifold model with geometry $\mathbb{Z}_2 \times \mathbb{Z}_4$ (1,1) which yields 4⇝3 generations via the RT scheme is defined by the following shifts and Wilson lines (with $W_4 = 0$):

$$V_1 = \left(-\tfrac{7}{4}, -\tfrac{1}{4}, -\tfrac{1}{4}, -\tfrac{1}{4}, -\tfrac{1}{4}, -\tfrac{1}{4}, \tfrac{1}{4}, \tfrac{7}{4}\right), (0,0,0,0,0,0,0,0)\,, \tag{A.1.1a}$$

*See e.g. [11, 104, 118] for reviews on orbifold compactifications, and [87, Section 4] for more details on this specific orbifold geometry.

$$V_2 = \left(\tfrac{3}{8}, \tfrac{1}{8}, \tfrac{1}{8}, \tfrac{1}{8}, \tfrac{3}{8}, \tfrac{9}{8}, -\tfrac{3}{8}, -\tfrac{3}{8}\right), \left(-1, 0, 0, 0, \tfrac{1}{4}, \tfrac{1}{4}, \tfrac{1}{4}, \tfrac{3}{4}\right), \tag{A.1.1b}$$

$$W_1 = W_2 = (0, 0, 0, 0, 0, 0, 0, 0), \left(-1, -1, \tfrac{1}{2}, \tfrac{3}{2}, -\tfrac{1}{2}, 0, \tfrac{1}{2}, 0\right), \tag{A.1.1c}$$

$$W_3 = (0, 0, 0, 0, 0, 0, 0, 0), \left(-\tfrac{5}{4}, -\tfrac{5}{4}, \tfrac{1}{4}, \tfrac{3}{4}, \tfrac{3}{4}, \tfrac{7}{4}, -\tfrac{3}{4}, \tfrac{7}{4}\right), \tag{A.1.1d}$$

$$W_5 = W_6 = \left(-1, -1, 0, 1, \tfrac{3}{2}, \tfrac{1}{2}, \tfrac{1}{2}, \tfrac{3}{2}\right), (0, 0, 0, 0, 0, 0, 0, 0). \tag{A.1.1e}$$

The effective massless matter spectrum before decoupling of vector-like representations and $\mathrm{SU}(2)_s$ confinement, obtained by the `orbifolder` is summarized in Table 3.3a.

A.1.2 Details of the 2↝3 heterotic orbifold model

The orbifold parameters that define the $\mathbb{Z}_2 \times \mathbb{Z}_4$ (1,1) heterotic orbifold model presented in section 3.4.2 are

$$V_1 = \left(-\tfrac{1}{4}, -\tfrac{1}{4}, \tfrac{1}{4}, \tfrac{1}{4}, \tfrac{1}{4}, \tfrac{1}{4}, \tfrac{1}{4}, \tfrac{9}{4}\right), (0, 0, 0, 0, 0, 0, 0, 2), \tag{A.1.2a}$$

$$V_2 = \left(\tfrac{1}{8}, \tfrac{9}{8}, -\tfrac{7}{8}, -\tfrac{1}{8}, -\tfrac{1}{8}, -\tfrac{1}{8}, \tfrac{9}{8}, \tfrac{7}{8}\right), \left(-\tfrac{1}{2}, 0, 0, 0, \tfrac{1}{4}, \tfrac{1}{4}, \tfrac{3}{4}, -\tfrac{3}{4}\right), \tag{A.1.2b}$$

$$W_1 = W_2 = (1, 0, -2, -1, 0, 1, -1, -2), \left(\tfrac{1}{4}, -\tfrac{3}{4}, -\tfrac{1}{4}, \tfrac{7}{4}, -\tfrac{3}{4}, \tfrac{3}{4}, -\tfrac{5}{4}, \tfrac{5}{4}\right), \tag{A.1.2c}$$

$$W_3 = \left(-\tfrac{5}{4}, \tfrac{5}{4}, \tfrac{5}{4}, -\tfrac{7}{4}, -\tfrac{5}{4}, -\tfrac{5}{4}, \tfrac{1}{4}, -\tfrac{5}{4}\right), \left(\tfrac{7}{4}, \tfrac{5}{4}, \tfrac{7}{4}, \tfrac{7}{4}, \tfrac{5}{4}, \tfrac{9}{4}, -\tfrac{1}{4}, \tfrac{9}{4}\right), \tag{A.1.2d}$$

$$W_5 = W_6 = \left(-2, -\tfrac{1}{2}, 0, 1, -\tfrac{1}{2}, 1, \tfrac{1}{2}, \tfrac{3}{2}\right), \left(-\tfrac{7}{4}, -\tfrac{1}{4}, -\tfrac{5}{4}, -\tfrac{5}{4}, \tfrac{7}{4}, \tfrac{1}{4}, -\tfrac{3}{4}, -\tfrac{7}{4}\right), \tag{A.1.2e}$$

and $W_4 = 0$. Using these parameters as input of the `orbifolder`, one finds the massless matter spectrum before decoupling of vector-like representations and $\mathrm{SU}(2)_s$ confinement shown in Table 3.3b.

Appendix B

(This appendix first appeared in the publication with Yahya Almumin, Mu-Chun Chen, Michael Ratz, Saul Ramos-Sanchez and Victor Knapp-Perez) [5]

B.1 ϑ–functions

In this appendix, we collect some relevant facts on the ϑ–functions. Our conventions are based on [89] and [102]. One defines

$$\vartheta\left[\begin{smallmatrix}\alpha\\ \beta\end{smallmatrix}\right](z,\tau) := S_\beta\, T_\alpha\, \vartheta(z,\tau) = \mathrm{e}^{2\pi \mathrm{i}\,\alpha\,\beta}\, T_\alpha\, S_\beta\, \vartheta(z,\tau)\ , \tag{B.1.1}$$

where [89, p. 4]

$$\vartheta(z,\tau) := \sum_{\ell\in\mathbb{Z}} \exp(\mathrm{i}\,\pi\,\ell^2\,\tau)\, \exp(2\pi\mathrm{i}\,\ell\,z) \tag{B.1.2}$$

with $\mathrm{Im}\,\tau > 0$, and [89, p. 6]

$$(S_\beta f)(z) \;:=\; f(z+\beta)\ , \tag{B.1.3a}$$

$$(T_\alpha f)(z) \;:=\; \mathrm{e}^{\mathrm{i}\,\pi\,\alpha^2\,\tau + 2\pi\mathrm{i}\,\alpha\,z}\, f(z+\alpha\,\tau)\ . \tag{B.1.3b}$$

This immediately gives us (cf. [102, p. 214 f.])

$$\vartheta\left[\begin{smallmatrix}\alpha\\ \beta\end{smallmatrix}\right](z,\tau) = \sum_{\ell=-\infty}^{\infty} \mathrm{e}^{\mathrm{i}\pi\,(\alpha+\ell)^2\,\tau}\,\mathrm{e}^{2\pi\mathrm{i}\,(\alpha+\ell)\,(z+\beta)}\ . \tag{B.1.4}$$

For an integer $n \in \mathbb{Z}$ one has torus periodicities

$$\vartheta\left[\begin{smallmatrix}\alpha\\ \beta\end{smallmatrix}\right](z+n,\tau) = \mathrm{e}^{2\pi\mathrm{i}\,n\,\alpha}\,\vartheta\left[\begin{smallmatrix}\alpha\\ \beta\end{smallmatrix}\right](z,\tau)\ , \tag{B.1.5a}$$

$$\vartheta\left[\begin{smallmatrix}\alpha\\ \beta\end{smallmatrix}\right](z+n\,\tau,\tau) = \mathrm{e}^{-\mathrm{i}\pi\,n^2\,\tau-2\pi\mathrm{i}\,n\,(z+\beta)}\,\vartheta\left[\begin{smallmatrix}\alpha\\ \beta\end{smallmatrix}\right](z,\tau)\ . \tag{B.1.5b}$$

Further, the ϑ–function have several periodicities in the characteristics α and β,

$$\vartheta\left[\begin{smallmatrix}\alpha+1\\ \beta\end{smallmatrix}\right](z,\tau) = \vartheta\left[\begin{smallmatrix}\alpha\\ \beta\end{smallmatrix}\right](z,\tau)\ , \tag{B.1.6a}$$

$$\vartheta\left[\begin{smallmatrix}\alpha\\ \beta+1\end{smallmatrix}\right](z,\tau) = \mathrm{e}^{2\pi\mathrm{i}\,\alpha}\,\vartheta\left[\begin{smallmatrix}\alpha\\ \beta\end{smallmatrix}\right](z,\tau)\ . \tag{B.1.6b}$$

The behavior under modular transformation is

$$\vartheta\left[\begin{smallmatrix}\alpha\\ \beta\end{smallmatrix}\right](z,\tau+1) = \mathrm{e}^{-\mathrm{i}\,\pi\,\alpha\,(\alpha+1)}\,\vartheta\left[\begin{smallmatrix}\alpha\\ \beta+\alpha+\frac{1}{2}\end{smallmatrix}\right](z,\tau)\ , \tag{B.1.7a}$$

$$\vartheta\left[\begin{smallmatrix}\alpha\\ \beta\end{smallmatrix}\right]\left(-\frac{z}{\tau},-\frac{1}{\tau}\right) = \sqrt{-\mathrm{i}\,\tau}\,\mathrm{e}^{2\pi\mathrm{i}\left(\frac{z^2}{2\tau}+\alpha\,\beta\right)}\,\vartheta\left[\begin{smallmatrix}-\beta\\ \alpha\end{smallmatrix}\right](z,\tau)\ . \tag{B.1.7b}$$

Another useful formula is

$$\vartheta\left[\begin{smallmatrix}0\\ j/M\end{smallmatrix}\right]\left(z,\frac{\tau}{M}\right) = \sum_{k=0}^{M-1} e^{2\pi\mathrm{i}jk/M}\vartheta\begin{bmatrix}\frac{k}{M}\\ 0\end{bmatrix}(Mz,M\tau)\ . \tag{B.1.8}$$

B.2 Torus Integration

The torus is defined by two lattice vectors, which can be chosen as $e_1 = 2\pi R$ and $e_2 = 2\pi R\,\tau$, where the real, dimensionful quantity R sets the length of one lattice vector, and τ with

$\mathrm{Im}\,\tau > 0$ is the half–period ratio. In this basis, the torus metric reads

$$G = (2\pi R)^2 \begin{pmatrix} 1 & \mathrm{Re}\,\tau \\ \mathrm{Re}\,\tau & |\tau|^2 \end{pmatrix} . \tag{B.2.1}$$

We can define the *fundamental domain* of the torus as

$$\mathbb{T}^2 = \{ z \in \mathbb{C} \; ; \quad z = x\, e_1 + y\, e_2 \;\; \text{with} \;\; 0 \leq x, y \leq 1 \} . \tag{B.2.2}$$

It is straightforward to verify that the Jacobian of the transformation $(\mathrm{Re}\, z, \mathrm{Im}\, z) \mapsto (x, y)$ is given by $(2\pi R)^2\, \mathrm{Im}\,\tau$. Therefore, the integrals of an arbitrary function $f(z)$ over the fundamental domain are given by

$$\int\limits_{\mathbb{T}^2} \mathrm{d}^2 z\, f(z) = (2\pi R)^2\, \mathrm{Im}\,\tau \int\limits_0^1 \mathrm{d}x \int\limits_0^1 \mathrm{d}y\, f(x e_1 + y e_2) . \tag{B.2.3}$$

Let us now look at constant modes on the torus, or, equivalently integrate over the torus $\mathbb{T}^2$ to determine its volume. We then have

$$\mathrm{vol(torus)} = \int\limits_{\mathbb{T}^2} \mathrm{d}^2 z\, 1 = (2\pi R)^2\, \mathrm{Im}\,\tau =: \mathcal{A} . \tag{B.2.4}$$

B.3 Explicit Verification of the Boundary Conditions for the Transformed Waveunctions

B.3.1 The *S* Transformation

We now compute the S transformation, $\tau \mapsto -1/\tau$ (cf. equation (1.21)), of equation (4.1.1). We have

$$\begin{aligned}
\psi^{j,M}\left(-\frac{z}{\tau},-\frac{1}{\tau},0\right) &= \left(\frac{2M\,\mathrm{Im}\,\frac{-1}{\tau}}{\mathcal{A}^2}\right)^{1/4}\exp\left(\mathrm{i}\pi M\frac{z}{\tau}\frac{\mathrm{Im}\,\frac{z}{\tau}}{\mathrm{Im}\,\frac{-1}{\tau}}\right)\vartheta\left[\begin{smallmatrix}\frac{j}{M}\\0\end{smallmatrix}\right]\left(-\frac{Mz}{\tau},-\frac{M}{\tau}\right)\\
&= \frac{\mathcal{N}}{\sqrt{|\tau|}}\exp\left(\mathrm{i}\pi M\frac{z}{\tau}\frac{\mathrm{Im}\,z\bar{\tau}}{\mathrm{Im}\,\tau}\right)\sqrt{-\mathrm{i}\frac{\tau}{M}}\mathrm{e}^{2\pi M\mathrm{i}\frac{z^2}{2\tau}}\,\vartheta\left[\begin{smallmatrix}0\\\frac{j}{M}\end{smallmatrix}\right]\left(z,\frac{\tau}{M}\right)\\
&= \frac{\mathcal{N}}{\sqrt{|\tau|}}\exp\left(\mathrm{i}\pi M\frac{z}{\tau}\frac{\mathrm{Im}\,z\bar{\tau}}{\mathrm{Im}\,\tau}\right)\sqrt{-\mathrm{i}\frac{\tau}{M}}\mathrm{e}^{\mathrm{i}\pi M\frac{z^2}{\tau}}\sum_{k=0}^{M-1}\mathrm{e}^{2\pi\mathrm{i}\,jk/M}\,\vartheta\left[\begin{smallmatrix}\frac{k}{M}\\0\end{smallmatrix}\right](Mz,M\tau)\\
&= \frac{\mathrm{e}^{\frac{\mathrm{i}\pi}{4}}}{\sqrt{M}}\left(-\frac{\tau}{|\tau|}\right)^{1/2}\sum_{k=0}^{M-1}\mathrm{e}^{\frac{2\pi\mathrm{i}jk}{M}}\left[\mathcal{N}\exp\left(\frac{\mathrm{i}\pi Mz}{\tau}\frac{\mathrm{Im}\,z\bar{\tau}}{\mathrm{Im}\,\tau}+\mathrm{i}M\pi\frac{z^2}{\tau}\right)\vartheta\left[\begin{smallmatrix}\frac{k}{M}\\0\end{smallmatrix}\right](Mz,M\tau)\right]\\
&= \frac{\mathrm{e}^{\mathrm{i}\frac{\pi}{4}}}{\sqrt{M}}\left(-\frac{\tau}{|\tau|}\right)^{1/2}\sum_{k=0}^{M-1}\mathrm{e}^{\frac{2\pi\mathrm{i}jk}{M}}\mathcal{N}\mathrm{e}^{i\pi Mz\frac{\mathrm{Im}\,z}{\mathrm{Im}\,\tau}}\,\vartheta\left[\begin{smallmatrix}\frac{j}{M}\\0\end{smallmatrix}\right](Mz,M\tau)\ , \qquad \text{(B.3.1)}
\end{aligned}$$

where we used (4.1.2), (B.1.7b) and (B.1.8) in the first, second and third lines respectively. We thus arrive at (B.3.2). Therefore, the S modular transformation of the zero modes is

$$\psi^{j,M}\left(-\frac{z}{\tau},-\frac{1}{\tau},0\right) = \frac{\mathrm{e}^{\mathrm{i}\frac{\pi}{4}}}{\sqrt{M}}\left(-\frac{\tau}{|\tau|}\right)^{1/2}\sum_{k=0}^{M-1}\mathrm{e}^{2\pi\mathrm{i}jk/M}\,\psi^{k,M}(z,\tau,0)\ . \qquad \text{(B.3.2)}$$

It is straightforward to see that the wave function of equation (B.3.2) satisfies the boundary conditions of equations (4.1.52a) and (4.1.52b). Note that

$$\psi^{j,M}\left(-\frac{z}{\tau}+1,-\frac{1}{\tau},0\right) = \psi^{j,M}\left(-\frac{(z-\tau)}{\tau},-\frac{1}{\tau},0\right)$$

$$= \frac{\mathrm{e}^{\mathrm{i}\frac{\pi}{4}}}{\sqrt{M}}\left(-\frac{\tau}{|\tau|}\right)^{1/2}\sum_{k=0}^{M-1}\mathrm{e}^{\frac{2\pi\mathrm{i}jk}{M}}\,\psi^{k,M}(z-\tau,\tau,0) = \exp\left(-\mathrm{i}\pi M\frac{\mathrm{Im}\,z\bar{\tau}}{\mathrm{Im}\,\tau}\right)\psi^{j,M}\left(-\frac{z}{\tau},-\frac{1}{\tau},0\right) \tag{B.3.3}$$

and

$$\begin{aligned}\psi^{j,M}\left(-\frac{z}{\tau}-\frac{1}{\tau},-\frac{1}{\tau},0\right) &= \psi^{j,M}\left(-\frac{(z+1)}{\tau},-\frac{1}{\tau},0\right)\\ = \frac{\mathrm{e}^{\mathrm{i}\frac{\pi}{4}}}{\sqrt{M}}\left(-\frac{\tau}{|\tau|}\right)^{1/2}\sum_{k=0}^{M-1}\mathrm{e}^{\frac{2\pi\mathrm{i}jk}{M}}\psi^{k,M}(z+1,\tau,0) &= \exp\left(\frac{\mathrm{i}\pi M\,\mathrm{Im}\,z}{\mathrm{Im}\,\tau}\right)\psi^{j,M}\left(-\frac{z}{\tau},-\frac{1}{\tau},0\right).\end{aligned} \tag{B.3.4}$$

Thus, from equations (B.3.3) and (B.3.4) we can see that the S transformed zero mode follows the boundary conditions of equations (4.1.52a) and (4.1.52b) for both odd and even M.

B.3.2 The T Transformation

Now, we compute the transformed wave function $\psi^{j,M}(z,\tau+1,0)$ and check that it satisfies both equation (4.1.53a) and equation (4.1.53b). Applying the T modular transformation in equation (4.1.1) gives

$$\begin{aligned}\psi^{j,M}(z,\tau+1,0) &= \mathcal{N}\mathrm{e}^{\mathrm{i}\pi\,Mz\frac{\mathrm{Im}\,z}{\mathrm{Im}\,\tau}}\vartheta\begin{bmatrix}\frac{j}{M}\\0\end{bmatrix}\big(Mz,M(\tau+1),0\big)\\ &= \mathrm{e}^{-\mathrm{i}\,\pi j\left(\frac{j}{M}+1\right)}\,\mathcal{N}\mathrm{e}^{\mathrm{i}\,\pi Mz\frac{\mathrm{Im}\,z}{\mathrm{Im}\,\tau}}\,\vartheta\begin{bmatrix}\frac{j}{M}\\j+\frac{M}{2}\end{bmatrix}(Mz,M\tau)\\ &= \mathrm{e}^{-\mathrm{i}\,\pi j\left(\frac{j}{M}+1\right)}\,\mathcal{N}\mathrm{e}^{\mathrm{i}\,\pi Mz\frac{\mathrm{Im}\,z}{\mathrm{Im}\,\tau}}\,\mathrm{e}^{2\pi\mathrm{i}\,\frac{j}{M}j}\vartheta\begin{bmatrix}\frac{j}{M}\\\frac{M}{2}\end{bmatrix}(Mz,M\tau)\\ &= \mathrm{e}^{-\mathrm{i}\,\pi j\left(1-\frac{j}{M}\right)}\,\mathcal{N}\mathrm{e}^{\mathrm{i}\,\pi Mz\frac{\mathrm{Im}\,z}{\mathrm{Im}\,\tau}}\,\vartheta\begin{bmatrix}\frac{j}{M}\\\frac{M}{2}\end{bmatrix}(Mz,M\tau)\,,\end{aligned} \tag{B.3.5}$$

where we used (B.1.7a) and (B.1.6b) in the second and third line, respectively. Defining $\widetilde{\mathcal{N}} := \mathrm{e}^{-\mathrm{i}\,\pi j\left(1-\frac{j}{M}\right)}\mathcal{N}$ we can thus write

$$\psi^{j,M}(z,\tau+1,0) = \widetilde{\mathcal{N}}\mathrm{e}^{\mathrm{i}\,\pi M z\frac{\mathrm{Im}\,z}{\mathrm{Im}\,\tau}}\vartheta\begin{bmatrix}\frac{j}{M}\\ \frac{M}{2}\end{bmatrix}(Mz,M\tau)\ . \tag{B.3.6}$$

Now we check that equation (B.3.6) satisfies boundary conditions given by equations (4.1.53a) and (4.1.53b). The first boundary condition is satisfied as shifting $z \to z+1$ in equation (B.3.6) gives

$$\begin{aligned}\psi^{j,M}(z+1,\tau+1,0) &= \widetilde{\mathcal{N}}\mathrm{e}^{\mathrm{i}\,\pi M(z+1)\frac{\mathrm{Im}\,z}{\mathrm{Im}\,\tau}}\vartheta\begin{bmatrix}\frac{j}{M}\\ \frac{M}{2}\end{bmatrix}(M(z+1),M\tau)\\ &= \exp\left(\mathrm{i}\,\frac{\pi M\,\mathrm{Im}\,z}{\mathrm{Im}\,\tau}\right)\widetilde{\mathcal{N}}\mathrm{e}^{\mathrm{i}\,\pi M(z+1)\frac{\mathrm{Im}\,z}{\mathrm{Im}\,\tau}}\mathrm{e}^{2\pi\mathrm{i}\,M\frac{j}{M}}\vartheta\begin{bmatrix}\frac{j}{M}\\ \frac{M}{2}\end{bmatrix}(Mz,M\tau)\\ &= \exp\left(\mathrm{i}\,\frac{\pi M\,\mathrm{Im}\,z}{\mathrm{Im}\,\tau}\right)\psi^{j,M}(z,\tau+1,0)\ ,\end{aligned} \tag{B.3.7}$$

where we used equation (B.1.5a) in the second line. For equation (4.1.53b) we have

$$\begin{aligned}\psi^{j,M}(z+\tau+1,\tau+1,0) &= \widetilde{\mathcal{N}}\mathrm{e}^{\frac{\mathrm{i}\,\pi M(z+\tau+1)}{\mathrm{Im}\,\tau}\mathrm{Im}(z+\tau+1)}\vartheta\begin{bmatrix}\frac{j}{M}\\ \frac{M}{2}\end{bmatrix}(M(z+\tau+1),M\tau)\\ &= \widetilde{\mathcal{N}}\mathrm{e}^{\frac{\mathrm{i}\,\pi M}{\mathrm{Im}\,\tau}[z\,\mathrm{Im}\,z+(\tau+1)\,\mathrm{Im}\,z+z\,\mathrm{Im}(\tau+1)+(\tau+1)\,\mathrm{Im}(\tau+1)}\,\mathrm{e}^{2\pi\mathrm{i}\,\frac{j}{M}M}\vartheta\begin{bmatrix}\frac{j}{M}\\ \frac{M}{2}\end{bmatrix}(M(z+\tau),M\tau)\\ &= \widetilde{\mathcal{N}}\mathrm{e}^{\frac{\mathrm{i}\,\pi M}{\mathrm{Im}\,\tau}[z\,\mathrm{Im}\,z+(\tau+1)\,\mathrm{Im}\,z+z\,\mathrm{Im}(\tau+1)+(\tau+1)\,\mathrm{Im}(\tau+1)}\,\mathrm{e}^{-\pi\mathrm{i}\,\tau M-2\pi\mathrm{i}\,(Mz+\frac{M}{2})}\vartheta\begin{bmatrix}\frac{j}{M}\\ \frac{M}{2}\end{bmatrix}(Mz,M\tau)\\ &= \mathrm{e}^{\frac{\mathrm{i}\,\pi M}{\mathrm{Im}\,\tau}[(\tau+1)\,\mathrm{Im}\,z+z\,\mathrm{Im}(\tau+1)+(\tau+1)\,\mathrm{Im}(\tau+1)-\tau\,\mathrm{Im}\,\tau-2z\,\mathrm{Im}\,\tau-\mathrm{Im}\,\tau]}\widetilde{\mathcal{N}}\mathrm{e}^{\frac{\mathrm{i}\,\pi M}{\mathrm{Im}\,\tau}z\,\mathrm{Im}\,z}\vartheta\begin{bmatrix}\frac{j}{M}\\ \frac{M}{2}\end{bmatrix}(Mz,M\tau)\\ &= \exp\left(\frac{\mathrm{i}\,\pi M}{\mathrm{Im}\,\tau}\,\mathrm{Im}(\bar{\tau}+1)z\right)\psi^{j,M}(z,\tau+1,0)\ ,\end{aligned} \tag{B.3.8}$$

where we have used equations (B.1.5a) and (B.1.5b) in the second and third line respectively. Therefore, the transformed modular wave function given by equation (B.3.6) follows the transformed boundary conditions of equations (4.1.53a) and (4.1.53b) for even and odd M.

Let us now tackle the problem of expressing the T transformed wave functions in terms of

the original ones. As noted in section (4.1.7), for odd values of M it is not possible to express the T transformed wave functions in terms of the original ones because of (4.1.55). At the level of the wave functions, one can refer to equation (B.3.6) and see that if M is even, then using (B.1.6b) confirms (4.1.56). However, if M is odd, in order to make use of (B.1.6b) we need to shift the z coordinate as $z \mapsto z + \Delta z$ with real Δz. Using equation (B.3.6) we have

$$\begin{aligned}\psi^{j,M}(z+\Delta z,\tau+1,0) &= \widetilde{\mathcal{N}}\mathrm{e}^{\mathrm{i}\,\pi M(z+\Delta z)\frac{\mathrm{Im}\,z}{\mathrm{Im}\,\tau}}\vartheta\begin{bmatrix}\frac{j}{M}\\ \frac{M}{2}\end{bmatrix}(M(z+\Delta z),M\tau)\\ &= \widetilde{\mathcal{N}}\mathrm{e}^{\mathrm{i}\,\pi M\Delta z\frac{\mathrm{Im}\,z}{\mathrm{Im}\,\tau}}\mathrm{e}^{\mathrm{i}\,\pi Mz\frac{\mathrm{Im}\,z}{\mathrm{Im}\,\tau}}\vartheta\begin{bmatrix}\frac{j}{M}\\ 0\end{bmatrix}(M(z+\Delta z+\tfrac{1}{2}),M\tau),\end{aligned} \tag{B.3.9}$$

where we have used (B.1.4) to rewrite the lower characteristic of the ϑ–function as a shift in the z coordinate. Therefore, if we assume that Δz is a half–integer number, we can use (B.1.5a) which gives

$$\begin{aligned}\psi^{j,M}(z+\Delta z,\tau+1,0) &= \widetilde{\mathcal{N}}\mathrm{e}^{\mathrm{i}\,\pi M\Delta z\frac{\mathrm{Im}\,z}{\mathrm{Im}\,\tau}}\mathrm{e}^{\mathrm{i}\,\pi Mz\frac{\mathrm{Im}\,z}{\mathrm{Im}\,\tau}}\mathrm{e}^{2\pi\mathrm{i}j(\frac{1}{2}+\Delta z)}\vartheta\begin{bmatrix}\frac{j}{M}\\ 0\end{bmatrix}(Mz,M\tau)\\ &= \mathrm{e}^{\mathrm{i}\,\pi M\Delta z\frac{\mathrm{Im}\,z}{\mathrm{Im}\,\tau}}\mathrm{e}^{\pi\mathrm{i}j\left(\frac{j}{M}+2\Delta z\right)}\psi^{j,M}(z,\tau,0).\end{aligned} \tag{B.3.10}$$

Note that in order to use (B.1.5a), $M\left(\frac{1}{2}+\Delta z\right)$ needs to be an integer. Therefore, for odd M, Δz needs to be half–integer, whereas for even M both integer and half–integer Δz are valid choices. After a redefinition of $z \to z - \Delta z$ with some half–integer Δz,

$$\psi^{j,M}(z,\tau,0) \overset{T}{\longmapsto} \mathrm{e}^{\mathrm{i}\pi M\Delta z\frac{\mathrm{Im}\,z}{\mathrm{Im}\,\tau}}\mathrm{e}^{\mathrm{i}\pi\frac{j^2}{|M|}+2\mathrm{i}\pi j\Delta z}\,\psi^{j,M}(z-\Delta z,\tau,0)\ , \tag{B.3.11}$$

and this is valid for both even and odd values of M.

B.4 Symmetries Between the Yukawa Couplings

In this appendix we identify additional relations between the Yukawa couplings given in equation (4.1.38). Yukawa entries with different i, j and/or k are equal if the upper characteristic,

$$\frac{\mathcal{I}'_{ca}\, i - \mathcal{I}'_{ab}\, j + \mathcal{I}'_{ca}\, (\mathcal{I}'_{ab})^{\phi\left(|\mathcal{I}'_{bc}|\right)}\, (k-i-j)}{\lambda} =: u_{ijk} \ , \tag{B.4.1}$$

with $\mathcal{I}'_{\alpha\beta} = \mathcal{I}_{\alpha\beta}/d$, is the same. For instance, suppose $i' = i + r$, $j' = j + s$ and $k' = k + r + s$, so that i', j' and k' also satisfy the selection rule (cf. equation (4.1.24)). Then, for values of r and s satisfying

$$\mathcal{I}_{ca}\, r - \mathcal{I}_{ab}\, s = 0 \ , \tag{B.4.2}$$

we find that $u_{ijk} = u_{i'\,j'\,k'}$, thus implying that $Y_{ijk} = Y_{i'\,j'\,k'}$. We know that $\mathcal{I}_{ca}$ and $\mathcal{I}_{ab}$ are divisible by $d = \gcd\big(|\mathcal{I}_{ab}|, |\mathcal{I}_{ca}|, |\mathcal{I}_{bc}|\big)$ (cf. equation (4.1.20)), u_{ijk} has the form

$$u_{ijk} = \frac{\widehat{\alpha}_{ijk}}{\lambda} \tag{B.4.3}$$

with some integer $\widehat{\alpha}_{ijk}$ given by

$$\widehat{\alpha}_{ijk} = \mathcal{I}'_{ca}\, i - \mathcal{I}'_{ab}\, j + \mathcal{I}'_{ca}\, (\mathcal{I}'_{ab})^{\phi(|\mathcal{I}'_{bc}|)}\, (k-i-j) \mod \lambda \ . \tag{B.4.4}$$

Further, as a shift of u_{ijk} by 1 leaves the ϑ–function in the Yukawa entry invariant (cf. equation (B.1.6a)), there are at most λ distinct entries, i.e.

$$u_{ijk} \in \{0, 1/\lambda, \ldots (\lambda-1)/\lambda\} \ . \tag{B.4.5}$$

Additionally, for vanishing Wilson lines, the ϑ–function takes the simple form (cf. equation (B.1.4))

$$\vartheta\begin{bmatrix}\frac{\widehat{\alpha}_{ijk}}{\lambda}\\ 0\end{bmatrix}(0,\lambda\,\tau) = \sum_{\ell=-\infty}^{\infty} \mathrm{e}^{\mathrm{i}\pi\,(\widehat{\alpha}_{ijk}/\lambda+\ell)^2\,\lambda\tau}\ , \tag{B.4.6}$$

which shows that

$$\vartheta\begin{bmatrix}-\frac{\widehat{\alpha}_{ijk}}{\lambda}\\ 0\end{bmatrix}(0,\lambda\,\tau) = \vartheta\begin{bmatrix}\frac{\widehat{\alpha}_{ijk}}{\lambda}\\ 0\end{bmatrix}(0,\lambda\,\tau)\ . \tag{B.4.7}$$

Therefore, there are $\lambda/2-1$ additional relations between the Yukawa couplings, and we have at most $\lambda/2+1$ distinct entries. These additional relations can manifest themselves in different ways. For instance, if $\mathcal{I}_{ab}=\mathcal{I}_{ca}$, the overlap integral (4.1.10) becomes

$$Y_{ijk} = g\,\sigma_{abc}\int\limits_{\mathbb{T}^2}\mathrm{d}^2z\,\psi^{i,\mathcal{I}_{ab}}(z,\tau,\zeta)\,\psi^{j,\mathcal{I}_{ab}}(z,\tau,\zeta)\left(\psi^{k,\mathcal{I}_{cb}}(z,\tau,\zeta)\right)^*\ . \tag{B.4.8}$$

This equation is symmetric under $i\leftrightarrow j$, which implies that

$$Y_{ijk} = Y_{jik}\ . \tag{B.4.9}$$

As we discuss around equation (4.1.85) in the main text, the $i\leftrightarrow j$ flip can entail an outer automorphism of the low–energy gauge symmetry.

B.5 Modular Transformations of the Yukawa Couplings

In this appendix we will show the different ways in which the Yukawa couplings obtained from the overlap integrals (4.1.10) transform under modular transformations and how that

they indeed are modular forms according to equation (1.30).

B.5.1 Transformation of the Overlap Integrals

Let us start by discussing how our dictionary (4.1.62b) between the wave functions with torus parameter τ and an equivalent torus with parameter $\tau+1$ allows us to infer how the three index Yukawa couplings Y_{ijk} transform. We start with the T transformation where we use (4.1.62b) for the 2D wave functions. As we have discussed around (4.1.59), our dictionary involves a shift of the z–coordinate, Δz. For definiteness we use $\Delta z = \frac{1}{2}$. Thus, from equation (4.1.10) we have

$$\begin{aligned} Y_{ijk}(\tau+1) &= \int_{\mathbb{T}^2} \mathrm{d}^2 z \left(\rho(T)^{\psi}_{i,i'} \mathrm{e}^{\mathrm{i}\pi\mathcal{I}_{ab}\frac{\mathrm{Im}\, z}{\mathrm{Im}\,\tau}} \psi^{i',\mathcal{I}_{ab}}\left(z-\tfrac{1}{2},\tau,0\right)\right)\left(\rho(T)^{\psi}_{j,j'} \mathrm{e}^{\mathrm{i}\pi\mathcal{I}_{ca}\frac{\mathrm{Im}\, z}{\mathrm{Im}\,\tau}} \psi^{j',\mathcal{I}_{ca}}\left(z-\tfrac{1}{2},\tau,0\right)\right) \\ &\quad \cdot \left(\rho(T)^{\psi}_{k,k'} \mathrm{e}^{\mathrm{i}\pi\mathcal{I}_{cb}\frac{\mathrm{Im}\, z}{\mathrm{Im}\,\tau}} \psi^{k',\mathcal{I}_{cb}}\left(z-\tfrac{1}{2},\tau,0\right)\right)^* \\ &= \int_{\mathbb{T}^2} \mathrm{d}^2 z\, \mathrm{e}^{\mathrm{i}\pi(\mathcal{I}_{ab}+\mathcal{I}_{ca}+\mathcal{I}_{bc})\frac{\mathrm{Im}\, z}{2\,\mathrm{Im}\,\tau}}\, \rho(T)^{\psi}_{i,i'}\rho(T)^{\psi}_{j,j'}\left(\rho(T)^{\psi}_{k,k'}\right)^* \\ &\quad \cdot \psi^{i',\mathcal{I}_{ab}}(z-\tfrac{1}{2},\tau,0)\, \psi^{j',\mathcal{I}_{ca}}(z-\tfrac{1}{2},\tau,0) \left(\psi^{k',\mathcal{I}_{cb}}(z-\tfrac{1}{2},\tau,0)\right)^* . \end{aligned} \tag{B.5.1}$$

Using equation (4.1.12), we find that,

$$\begin{aligned} Y_{ijk}(\tau+1) &= \rho(T)^{\psi}_{i,i'}\rho(T)^{\psi}_{j,j'}\left(\rho(T)^{\psi}_{k,k'}\right)^* \\ &\quad \cdot \int_{\mathbb{T}^2} \mathrm{d}^2 z\, \psi^{i',\mathcal{I}_{ab}}(z-\tfrac{1}{2},\tau,0)\, \psi^{j',\mathcal{I}_{ca}}(z-\tfrac{1}{2},\tau,0) \left(\psi^{k',\mathcal{I}_{cb}}(z-\tfrac{1}{2},\tau,0)\right)^* . \end{aligned} \tag{B.5.2}$$

We can now define $w := z - \frac{1}{2}$. Then $\mathrm{d}^2 z = \mathrm{d}^2 w$, i.e. the integration measure for torus coordinates and the domain of integration remains invariant. Thus we find that

$$Y_{ijk}(\tau+1) = \rho(T)^{\psi}_{i,i'}\rho(T)^{\psi}_{j,j'}\left(\rho(T)^{\psi}_{k,k'}\right)^* \int_{\mathbb{T}^2} \mathrm{d}^2 w\, \psi^{i',\mathcal{I}_{ab}}(w,\tau,0)\, \psi^{j',\mathcal{I}_{ca}}(w,\tau,0) \left(\psi^{k',\mathcal{I}_{cb}}(w,\tau,0)\right)^*$$

$$
\begin{aligned}
&= \rho(T)^{\psi}_{i,i'}\rho(T)^{\psi}_{j,j'}\left(\rho(T)^{\psi}_{k,k'}\right)^{*} Y_{ijk}(\tau) \\
&= \mathrm{e}^{\mathrm{i}\pi(i^2/\mathcal{I}_{ab}+j^2/\mathcal{I}_{ca}-k^2/\mathcal{I}_{cb}+i+j-k)}\, Y_{ijk}(\tau)\ . \qquad \text{(B.5.3)}
\end{aligned}
$$

Thus the z–dependent phase appearing in our dictionary for T transformation (4.1.61) cancels out due to the condition (4.1.12).

For the S transformation of Y_{ijk}, we use equation (4.1.62a), which gives

$$
\begin{aligned}
Y_{ijk}(-1/\tau) &= \int_{\mathbb{T}^2} \mathrm{d}^2 z \left(-\left(\frac{-\tau}{|\tau|}\right)^{1/2} \rho(S)^{\psi}_{i,i'}\psi^{i',\mathcal{I}_{ab}}(z,\tau,0)\right)\left(-\left(\frac{-\tau}{|\tau|}\right)^{1/2} \rho(S)^{\psi}_{j,j'}\psi^{j',\mathcal{I}_{ca}}(z,\tau,0)\right) \\
&\quad \cdot \left(-\left(\frac{-\tau}{|\tau|}\right)^{1/2} \rho(S)^{\psi}_{k,k'}\psi^{k',\mathcal{I}_{cb}}(z,\tau,0)\right)^{*} \\
&= -\left(\frac{-\tau}{|\tau|}\right)^{1/2} \rho(S)^{\psi}_{i,i'}\rho(S)^{\psi}_{j,j'}\left[\rho(S)^{\psi}_{k,k'}\right]^{*} Y_{i'j'k'} \\
&= -\left(\frac{-\tau}{|\tau|}\right)^{1/2} \frac{-\mathrm{e}^{\mathrm{i}\frac{\pi}{4}}}{\sqrt{|\mathcal{I}_{ab}\mathcal{I}_{bc}\mathcal{I}_{bc}|}} \sum_{i'=0}^{\mathcal{I}_{ab}-1}\sum_{j'=0}^{\mathcal{I}_{ca}-1}\sum_{k'=0}^{\mathcal{I}_{cb}-1} \mathrm{e}^{2\pi\mathrm{i}\left(\frac{ii'}{\mathcal{I}_{ab}}+\frac{jj'}{\mathcal{I}_{ca}}+\frac{kk'}{\mathcal{I}_{bc}}\right)} Y_{i'j'k'}\ , \qquad \text{(B.5.4)}
\end{aligned}
$$

where have used the fact that the automorphy factor and the $\rho(S)^{\psi}$ matrix do not depend in the z coordinate, and then, can be taken out of the integral.

Equations (B.5.3) and (B.5.4) give the modular transformations of Y_{ijk}. They can be used to infer the possible modular transformations of the 4D fields.

B.5.2 Modular Transformation of the $\boldsymbol{\lambda}$–plet of Yukawa Couplings

The λ–plet of holomorphic Yukawa couplings (4.1.66), $\mathcal{Y}_{ijk}(\tau) = \vartheta\begin{bmatrix}\widehat{\alpha}_{ijk}/\lambda \\ 0\end{bmatrix}(0,\lambda\,\tau)$, transforms as a modular form of weight $1/2$. To see this, let us first investigate how $\mathcal{Y}_{\widehat{\alpha}}(\tau)$, where $\widehat{\alpha} :=$

$\widehat{\alpha}_{ijk} \in \mathbb{Z}_\lambda$, behaves under T. Obviously,

$$\mathcal{Y}_{\widehat{\alpha}}(\tau) \stackrel{T}{\longmapsto} \mathcal{Y}_{\widehat{\alpha}}(\tau) = \sum_{\ell=-\infty}^{\infty} \exp\left[\mathrm{i}\pi\left(\frac{\widehat{\alpha}}{\lambda}+\ell\right)^2 \lambda\,(\tau+1)\right] \ . \tag{B.5.5}$$

The phase can be manipulated to give

$$\mathrm{i}\pi\left(\frac{\widehat{\alpha}}{\lambda}+\ell\right)^2 \lambda\,(\tau+1) = \mathrm{i}\pi\left(\frac{\widehat{\alpha}}{\lambda}+\ell\right)^2 \lambda\,\tau + \mathrm{i}\pi\frac{(\widehat{\alpha}+\lambda\,\ell)^2}{\lambda} \ . \tag{B.5.6}$$

The second term can be rewritten as

$$\mathrm{i}\pi\frac{(\widehat{\alpha}+\lambda\,\ell)^2}{\lambda} = \mathrm{i}\pi\frac{\widehat{\alpha}^2}{\lambda} + 2\pi\mathrm{i}\,\ell + \mathrm{i}\pi\,\lambda\,\ell^2 \ . \tag{B.5.7}$$

Only the first term on the right–hand side yields a nontrivial phase. The two others are integer multiples of $2\pi\mathrm{i}$ because λ is even. Therefore,

$$\mathcal{Y}_{\widehat{\alpha}}(\tau+1) = \mathrm{e}^{\mathrm{i}\pi\frac{\widehat{\alpha}^2}{\lambda}}\,\mathcal{Y}_{\widehat{\alpha}}(\tau) \ . \tag{B.5.8}$$

Likewise, under S

$$\mathcal{Y}_{\widehat{\alpha}}(\tau) \stackrel{S}{\longmapsto} \mathcal{Y}_{\widehat{\alpha}}(-1/\tau) = \vartheta\left[\begin{smallmatrix}\widehat{\alpha}/\lambda\\ 0\end{smallmatrix}\right]\!\big(0,-\lambda/\tau\big) =: \vartheta\left[\begin{smallmatrix}\widehat{\alpha}/\lambda\\ 0\end{smallmatrix}\right]\!\big(0,-1/t\big) \tag{B.5.9}$$

where $t := \tau/\lambda$. Then

$$\begin{aligned}\mathcal{Y}_{\widehat{\alpha}}(-1/\tau) &= \sqrt{-\mathrm{i}\,t}\,\vartheta\left[\begin{smallmatrix}0\\ \widehat{\alpha}/\lambda\end{smallmatrix}\right]\!\big(0,t\big) = \frac{\sqrt{-\mathrm{i}\,\tau}}{\sqrt{\lambda}}\sum_{\widehat{\beta}=0}^{\lambda-1}\mathrm{e}^{\frac{2\pi\mathrm{i}\,\widehat{\alpha}\,\widehat{\beta}}{\lambda}}\,\vartheta\left[\begin{smallmatrix}\widehat{\beta}/\lambda\\ 0\end{smallmatrix}\right]\!\big(0,\lambda\,\tau\big)\\ &= (-\tau)^{1/2}\sum_{\widehat{\beta}=0}^{\lambda-1}\frac{\mathrm{e}^{\frac{\pi\mathrm{i}}{4}}}{\sqrt{\lambda}}\mathrm{e}^{\frac{2\pi\mathrm{i}\,\widehat{\alpha}\,\widehat{\beta}}{\lambda}}\,\vartheta\left[\begin{smallmatrix}\widehat{\beta}/\lambda\\ 0\end{smallmatrix}\right]\!\big(0,\lambda\,\tau\big) = -(-\tau)^{1/2}\sum_{\widehat{\beta}=0}^{\lambda-1}\left(-\frac{\mathrm{e}^{\frac{\pi\mathrm{i}}{4}}}{\sqrt{\lambda}}\right)\mathrm{e}^{\frac{2\pi\mathrm{i}\,\widehat{\alpha}\,\widehat{\beta}}{\lambda}}\mathcal{Y}_{\widehat{\beta}}(\tau) \ .\end{aligned} \tag{B.5.10}$$

Here we used equations (B.1.8) and (B.1.7b). This shows that the λ–plet of $\mathcal{Y}_{\widehat{\alpha}}(\tau)$ picks up the correct automorphy factors to be a modular form of weight $1/2$. Note that we choose the minus sign in equation (B.5.10), anticipating that these transformations comply with equation (1.30), for $\varphi(S,\tau) = -\sqrt{-\tau}$, and thus with equation (1.31). Therefore, from equations (B.5.8) and (B.5.10) we get the representations of the λ–plet of Yukawa couplings (4.1.68b), which we recast here

$$\rho_{\boldsymbol{\lambda}}(\widetilde{S})_{\widehat{\alpha}\widehat{\beta}} = -\frac{\mathrm{e}^{\mathrm{i}\pi/4}}{\sqrt{\lambda}}\,\exp\left(\frac{2\pi\mathrm{i}\,\widehat{\alpha}\,\widehat{\beta}}{\lambda}\right)\,, \tag{B.5.11a}$$

$$\rho_{\boldsymbol{\lambda}}(\widetilde{T})_{\widehat{\alpha}\widehat{\beta}} = \exp\left(\frac{\mathrm{i}\pi\,\widehat{\alpha}^2}{\lambda}\right)\delta_{\widehat{\alpha}\widehat{\beta}}\,. \tag{B.5.11b}$$

Finally, although these matrices may be not be irreducible for some choice of $\mathcal{I}_{\alpha\beta}$, in section 4.1.8 we get the irreducible representation matrix in each case (cf. e.g. equations (4.1.82) and (4.1.84)). Therefore, equation (1.30) is satisfied and the Yukawa couplings given by equation (4.1.10) are modular forms of weight $k_Y = 1/2$. Furthermore, as discussed in section 4.1.8, the representation matrix will correspond to a representation of the metaplectic group $\widetilde{\Gamma}_{2\lambda}$, which implies that the Yukawa couplings have level 2λ.

Appendix C

(This appendix first appeared in the publication with Mu-Chun Chen, Victor Knapp-Perez, Mario Ramos-Hamud, Saul Ramos-Sanchez and Michael Ratz) [24]

C.1 Flavon VEV alignment*

We use the flavon VEVs (5.2.3) and (5.2.5) (cf. Section 5.2.3), which in the so–called real basis (cf. [49, Appendix C]) are given by

$$\langle \chi_i^a \rangle = v_1 \begin{pmatrix} 1 & 0 & 0 \\ 0 & 1 & 0 \\ 0 & 0 & 1 \end{pmatrix} \quad \text{and} \quad \langle \varphi_i \rangle = \frac{v_2}{\sqrt{3}} \begin{pmatrix} 1 \\ 1 \\ 1 \end{pmatrix} . \quad \text{(C.1.1)}$$

We assume that the $A_4^{\text{traditional}}$ representation matrices act from the left, and the Γ_3 matrices act from the right. Then the VEV $\langle \chi_i^a \rangle$ is the unique VEV which is invariant simul-

field	χ	φ	S_χ	S_φ
$A_4^{\text{traditional}}$	$\mathbf{3}$	$\mathbf{3}$	$\mathbf{1}_0$	$\mathbf{1}_0$
Γ_3	$\mathbf{3}$	$\mathbf{1}_0$	$\mathbf{1}_0$	$\mathbf{1}_0$
$\mathbb{Z}_3^\chi$	1	0	1	0
$\mathbb{Z}_3^\varphi$	0	1	0	1

Table C.1.1: Flavon sector.

*The computations of this Appendix can be checked in the attached supplementary Mathematica notebook which makes use of the `Discrete` package.

taneous S and T transformations from both groups,

$$S\,\langle\chi\rangle\,S^T = T\,\langle\chi\rangle\,T^T = \langle\chi\rangle\ . \tag{C.1.2}$$

So it is a symmetry–enhanced point, which suggests that it should not be too difficult to obtain such VEVs [80].

One can make this more explicit. Let us consider the most general renormalizable superpotentials involving the flavons χ, φ, S_χ and S_φ (see Table C.1.1 for their charges),

$$\mathscr{W} = \mathscr{W}_\chi + \mathscr{W}_\varphi\ , \tag{C.1.3}$$

where

$$\mathscr{W}_\chi = \frac{\kappa_\chi}{2} S_\chi\,(\chi\chi)_{\mathbf{1}_0} - \frac{\lambda_1}{3}(\chi\chi\chi)^{(1)}_{\mathbf{1}_0} - \frac{\lambda_2}{3}(\chi\chi\chi)^{(2)}_{\mathbf{1}_0} + \kappa_1 S_\chi^3\ , \tag{C.1.4a}$$

$$\mathscr{W}_\varphi = \frac{\kappa_\varphi}{2} S_\varphi(\varphi\varphi)_{\mathbf{1}_0} - \frac{\lambda_3}{3}(\varphi\varphi\varphi)_{\mathbf{1}_0} + \kappa_2 S_\varphi^3\ . \tag{C.1.4b}$$

Here, the subscript "$\mathbf{1}_0$" indicates the contraction to a singlet. There are two independent such contractions of three χ fields,

$$(\chi\chi\chi)^{(1)}_{\mathbf{1}_0} = \chi_1^1\chi_3^2\chi_2^3 + \chi_2^1\chi_1^2\chi_3^3 + \chi_3^1\chi_2^2\chi_1^3\ , \tag{C.1.5a}$$

$$(\chi\chi\chi)^{(2)}_{\mathbf{1}_0} = \chi_1^1\chi_2^2\chi_3^3 + \chi_2^1\chi_3^2\chi_1^3 + \chi_3^1\chi_1^2\chi_2^3\ . \tag{C.1.5b}$$

We assume that S_χ and S_φ acquire VEVs $\langle S_\chi\rangle \ll \Lambda$ and $\langle S_\varphi\rangle \ll \Lambda$. This is plausible since in string–derived models often the VEVs get fixed by D–terms [17, 18]. In fact, in the heterotic orbifold models, which underlie the eclectic scheme, the Fayet–Iliopoulos (FI) D–terms drive the flavons to nonzero VEVs [9], which has been verified in many explicitly constructed models (cf. e.g. [81]). One can verify that there is a nontrivial solution to the

F–term equations[†], where the VEVs are given by Equation (C.1.1) with

$$v_1 = \frac{\kappa_\chi \langle S_\chi \rangle}{\lambda_2} \quad \text{and} \quad v_2 = \frac{\kappa_\varphi \langle S_\varphi \rangle}{\lambda_3} \ . \tag{C.1.6}$$

Of course, there is another solution at which all VEVs vanish, and there are solutions in which only one of the VEVs vanishes. Technically, in supergravity, the above solution is the deepest minimum of the scalar potential, but addressing the vacuum energy is beyond the scope of this study. Furthermore, Equation (C.1.4) exhibits two accidental R symmetries which get spontaneously broken by the flavons. As a consequence, there are, at this level, two flat directions. However, these flat directions parametrize the overall magnitudes of the VEVs but do not alter their shapes given by Equations (C.1.1) and (C.1.6). The stabilization of the flat directions is beyond the scope of this study as the magnitudes of the VEVs are input parameters and only the shapes of the VEVs are important for our scenario. We also note that at higher orders there are additional terms that can alter the above solution slightly. Especially cross terms between χ and φ can shift the VEVs. However, these terms appear at much higher order, and are thus suppressed against the Kähler corrections which we discuss and tame in the main text. Altogether we find that, in a bottom–up EFT theory approach we can successfully align the VEVs to provide us with a scenario of diagonal breaking $A_4^{\text{traditional}} \times \Gamma_3 \to \Gamma_3^{\text{diagonal}}$.

[†]Note that, since we have assumed that S_χ and S_φ acquire VEVs by a different mechanism, their dynamics is not relevant in the F–term equations.

C.2 Basis Change Matrices

Considering the three-dimensional representation of A_4, the group generators can be expressed in the *complex basis*,

$$S_{\mathbf{3}}^C = \frac{1}{3}\begin{pmatrix} -1 & 2 & 2 \\ 2 & -1 & 2 \\ 2 & 2 & -1 \end{pmatrix}, \qquad T_{\mathbf{3}}^C = \begin{pmatrix} 1 & 0 & 0 \\ 0 & \omega & 0 \\ 0 & 0 & \omega^2 \end{pmatrix}, \tag{C.2.1}$$

where $\omega = \exp(2\pi\mathrm{i}/3)$. However, one might find it useful to express these generators in the *real basis*, where they adopt the form

$$S_{\mathbf{3}}^R = \begin{pmatrix} 1 & 0 & 0 \\ 0 & -1 & 0 \\ 0 & 0 & -1 \end{pmatrix}, \qquad T_{\mathbf{3}}^R = \begin{pmatrix} 0 & 1 & 0 \\ 0 & 0 & 1 \\ 1 & 0 & 0 \end{pmatrix}. \tag{C.2.2}$$

These bases are related by the unitary transformation

$$S_{\mathbf{3}}^R = U S_{\mathbf{3}}^C U^\dagger \quad \text{and} \quad T_{\mathbf{3}}^R = U T_{\mathbf{3}}^C U^\dagger , \tag{C.2.3}$$

where U is a unitary matrix, given by

$$U = \frac{1}{\sqrt{3}}\begin{pmatrix} 1 & 1 & 1 \\ 1 & \omega & \omega^2 \\ 1 & \omega^2 & \omega \end{pmatrix}. \tag{C.2.4}$$